EUROPEAN AVIATION SAFETY AGENCY
AGENCE EUROPÉENNE DE LA SÉCURITÉ AÉRIENNE
EUROPÄISCHE AGENTUR FÜR FLUGSICHERHEIT

Research Project EASA.2011/4

HighIWC - Ice Water Content of clouds at high altitude

easa.europa.eu

EASA.2011.C30
HighIWC — Ice Water Content of clouds at High altitude

Final report December 2012

Authors:

Alfons Schwarzenboeck, CNRS-LaMP
Fabien Dezitter, Alice Grandin, AIRBUS
Alain Protat, BOM

Contact person:

Alfons Schwarzenboeck, CNRS-LaMP

Date: 17 December 2012

Table of Contents

Figures

Tables

List of acronyms / abbreviations used in this document

Acronyms / abbreviations

2D	Two Dimensional
2D-C	Two Dimensional Cloud particle probe
2D-Grey	Two Dimensional Grey scale cloud particle probe
2D-P	Two Dimensional Precipitation particle probe
2D-S	Two Dimensional Stereo imaging probe
3D	Three Dimensional
A	Area
A340 MSN1	Airbus 340 MSN1
AIMMS-20	Aircraft–Integrated Meteorological Measurement System 20
BOM	Bureau Of Meteorology
CAS-DPOL	Cloud Aerosol Spectrometer with Depolarization
CCD	Charge-Coupled Device
CDP	Cloud Droplet Probe
CIP	Cloud Imaging Probe
CIRA	Centro Italiano Ricerche Aerospaziali
CPI	Cloud Particle Imager
CNRS-LaMP	Centre National de Recherche Scientifique – Laboratoire de Météorologie Physique
CPSD	Cloud Particle Spectrometer with Depolarization
CSI	Cloud Spectrometer and Impactor
CVI	Counterflow Virtual Impactor
CWC	Condensed Water Content* *which would be a more precise term for often used TWC (without water vapour phase)
dBZ	Decibel relative to Z (reflectivity)
D	Diameter
D_{eq}	Area equivalent diameter
D_{max}	Maximum diameter
DFRC	Dryden Flight Research Centre, NASA
DGAC	Direction Générale de l'Aviation Civile
DMT	Droplet Measurement Technologies
EASA	European Aviation Safety Agency

EHWG	Engine Harmonization Working Group
F-20	Falcon 20 research aircraft
F/T	Flight Tests
FTA	Flight Test Associates
EASA HighIWC	This proposal : EASA High Ice Water Content
FSSP-100	Forward Scattering Spectrometer Probe (Model 100)
FAA	Federal Aviation Administration
G-II	Gulfstream-II research aircraft
HAIC	High Altitude Ice Crystals
HIWC	High Ice Water Content
HSI	High Speed Imager
HYMEX	HYdrological cycle in Mediterranean EXperiment
ICCP	International Conference on Clouds and Precipitation
IKP	IsoKinetic evaporator Probe
IMC	Instrument Meteorological Conditions
IWC	Ice Water Content
LaMP	Laboratoire de Météorologie Physique
LWC	Liquid Water Content
m	Mass
MCS	Mesoscale Convective System
MMD	Median Mass Diameter
MT	Megha-Tropiques
MT1	Megha-Tropiques 1st field campaign
MT2	Megha-Tropiques 2nd field campaign
NASA	National Aeronautics and Space Administration
NCAR	National Centre for Atmospheric Research
N(D)	Number size distribution
NRC	National Research Council, Canada
OAP	Optical Array Probe
p	Pressure
PCASP	Passive Cavity Aerosol Spectrometer Probe
PIP	Precipitation Imaging Probe
PMS	Particle Measurement Systems
PSD	Particle Size Distribution

RASTA	RAdar SysTem Airborne
RICE	Rosemount Ice Detector
S	Size
SAFIRE	Service des Avions Français Instrumentés pour la Recherche en Environnement
SAT	Static Air Temperature
SID	Small Ice Detector
SEA	Science Engineering Associates
SPEC	Stratton Park Engineering Company
SPP-100	SPP-100 (FSSP, Forward Scattering Spectrometer Probe)
T	Temperature
TAT	Total Air Temperature
TWC	Total Water Content
V	Sampling volume
V1423	A340 flight number 1423
WP	Work Package
Z	Reflectivity

Comment

This final report presents the final status of all tasks as defined in EASA-HighIWC project with a summary of the main results for each task.

This document corresponds to the deliverable 3.3 of EASA-HighIWC project.

Background

Commercial aircraft have been experiencing in-service events while flying in the vicinity of deep convective clouds since at least the early 1990s. Heated probes and engines are the areas of aircraft most prone to mixed phase and glaciated icing threat.

In anticipation of regulation changes according to mixed phase and glaciated icing conditions, the European HAIC (High Altitude Ice Crystals) project will provide Acceptable Means of Compliance (numerical and test capabilities) and appropriate ice particle detection/awareness technologies for use on-board of commercial aircraft in order to enhance safety when an aircraft is flying in such weather conditions.

The EASA-HighIWC is aimed to be a preparatory project to the European integrated HAIC project. In particular, EASA-HighIWC will contribute in funding the scientific and technical preparatory work of HAIC atmosphere characterization work package, that aims to complement international measurement field campaign HIWC (High Ice Water Content) led by NASA by the addition of a second flight test aircraft, the SAFIRE Falcon 20.

This international measurement campaign will address for the first time with a comprehensive set of measurements the engineering and scientific issues related to the in-service events in convective clouds, and a variety of fundamental scientific issues related to the microphysical properties and structure of deep convective cloud systems over land and over the warm tropical ocean.

Aims and Objectives of the EASA HighIWC project within the international context

In the overall objective to improve our understanding of the phenomenon and to reproduce the microphysical properties of ice in an icing wind tunnel, Airbus has performed preliminary flight tests in high altitude icing conditions in 2010. These flights will allow proposing first characterizations of the corresponding atmospheric conditions (particles size / water concentrations) and preliminary assessment of proposed new regulations.

To characterize in a (statistically) much more reliable manner the above mentioned atmospheric conditions, an international team (NASA, FAA, Environment Canada, Transport Canada, Boeing, Airbus, NCAR, and the Australian Bureau of Meteorology) is leading an international flight test campaign called HIWC (High Ice Water Content) that is to be conducted in Darwin in January-March 2014. NASA is currently deploying all the instrumentation tailored for this project on a Gulfstream-II aircraft.
The European Union integrated project HAIC (High Altitude Ice Crystals) is joining the HIWC project, bringing the French SAFIRE Falcon 20 research aircraft to Darwin to complement the HIWC measurements.

EASA recognized as a high priority the validation of the new icing envelopes as defined in the proposed regulation, which are based on a theoretical approach. The EASA-HighIWC project discussed here is the starting point at the European level. EASA-HighIWC study is designed to support all the preparatory work for the Falcon 20 deployment to Darwin.

The main objectives of the EASA HighIWC proposal are:

- To analyse existing measurements of high ice water content (IWC) occurrence in the atmosphere that had been collected by Airbus during their flight test campaigns in 2010
- To evaluate the adequacy of airworthiness authorities proposed appendix envelopes for mixed phase and glaciated icing conditions based on these preliminary measurements in the atmosphere, and thus, to assess the proposed Appendix D and P in light of the analysis of the Airbus F/T campaigns. The analysis of existing data, associated with evaluation of proposed regulation will allow the pursuing of rulemaking activities that are on-going for Aircraft systems certification (navigation systems, propulsion systems).
- To define and integrate the payload of the French Falcon 20 research aircraft in order to contribute to the International high IWC field campaign (HIWC project from NASA and partners and HAIC project) over Darwin, Australia.

Methodology & implementation

The project is implemented through the straightforward execution of the 3 work packages of the proposal as there are:

- WP1: Preliminary analysis of the microphysical properties of the high IWC regions using existing airborne in-situ observations started to conduct a preliminary analysis of flights performed by Airbus over Darwin and Cayenne in 2010 in order to assess the proposed mixed phase and glaciated icing environment as defined in Appendix D and P and perform a gap analysis.
- WP2: Elaboration of Falcon 20 Flight Tests Development Plan that will provide the detailed action plan and will define a suitable instrumental payload for the French Falcon 20 in order to participate to the HIWC / HAIC international measurement field campaign.
- WP3: Monitoring of the project, administration and reporting, and provision of final recommendations to EASA with regards to on-going rulemaking activities.

The work plan timing of the specific tasks within the corresponding work packages is recalled in the subsequent figure 0-1. The accomplished work within each task is detailed in the chapter of results and outcomes.

EASA-HighIWC Workbreakdown Structure	2011	2012										Start	End
	M1	M2	M3	M4	M5	M6	M7	M8	M9	M10	M11	Month	Month
WP1: Preliminary analysis of the microphysical properties of the HighIWC												M1	M6
Task 1.1: Literature survey & Data acquisition												M1	M3
Task 1.2: Analysis of the microphysical properties of the HighIWC regions												M1	M6
WP2: Falcon 20 Flight Tests Development Plan												M1	M10
Task 2.1: Recommendation & Development plan for research activities and F/T												M1	M7
Task 2.2: Feasibility study & Demonstration												M1	M10
WP3: Management, Reporting & Recommendations												M1	M11
Task 3.1: Management & Reporting												M1	M11
Task 3.2: Recommendations												M8	M11

1st Interim report

2nd Interim report

Final report & Presentation

Figure 0-1: Work plan timing of work packages

Results & Outcomes

I. Literature survey and availability of microphysical data of deep convection clouds to be used for this study

Recall from proposal:

The objective of this task is to perform a literature survey of existing reports and publications dealing with the variety of fundamental scientific issues related to the microphysical properties and structure of deep convective cloud systems over land and over the warm tropical ocean. To do so, the consortium (LaMP and AIRBUS, subcontractor BOM) collect supporting data underlying these papers - gathered during flight trials - publicly accessible, available for the purpose of this study, and / or operational data covering the issues of this study which was recorded in the context of a similar or any other related exercise.

Accordingly, Airbus provided flight test data measurements and results from Darwin and Cayenne Flight test campaigns conducted in 2010. LAMP made data from 2010 and 2011 Megha-Tropiques measurement campaigns available for the objectives of the EASA HighIWC project as well.

I.1. Literature survey

The first description of the meteorological conditions suspected in these jet engine power loss events was reported by Lawson et al. (1998) after a series of events on a commuter-class aircraft.

In 2004 the Engine Harmonization Working Group (EHWG), an international committee composed of airframe manufacturers, engine manufacturers, regulating authorities, and other government agencies was assembled to study the effect of a proposed extension of icing envelopes for supercooled large droplets on engine icing certification. In the process of their investigations, approximately 100 engine events thought to be related to meteorological conditions were investigated. Many of these events were in the vicinity of deep convection. The EHWG concluded that the engine power loss events were caused by a previously unrecognized form of icing inside the engine that did not require the presence of atmospheric supercooled liquid water, and was largely due to ingestion of high mass concentration of ice particles. The EHWG identified flight test research of high IWC environments as a first-order priority, and specifically, to collect accurate information on the threat of high IWC in and around deep convective clouds, as well as information on the characteristic size of the particles in these clouds. Figure I-1 presents a very simple schematic figure of an organised propagating deep convection clouds system (often denoted as mesoscale convective system).

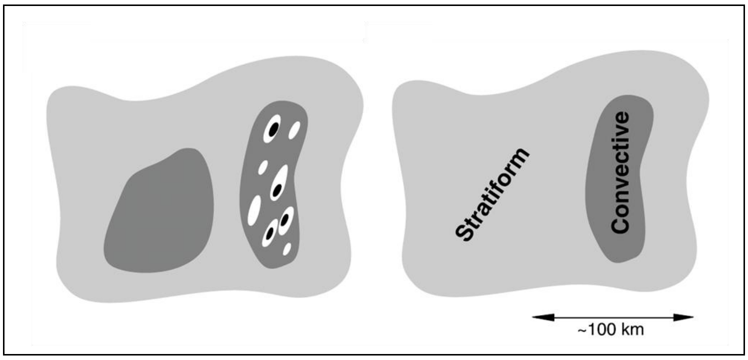

Figure I-1: Idealized horizontal map of radar reflectivities (left), leading to the scheme of convective and stratiform regions (right) in the convective meso-scale system. From Houze et al. (1997, 2004).

Radar echoes show that the precipitation divides distinctly into a convective and a stratiform region. The convective region consists of intense, vertically extending cores (figure I-1, left), while the stratiform region is of a more uniform texture of lighter precipitation. The stratiform precipitation is partly produced by the dissipation of older convective cells and partly produced by broader-sloping mesoscale layer ascent (Houze, 1997). The vertical cross section of a more conceptual model of the kinematic, microphysical, and radar echo structure is given in figure I-2. Intermediate and strong radar reflectivity is indicated by medium and dark shading, respectively. H and L indicate centres of positive and negative pressure perturbations, respectively.

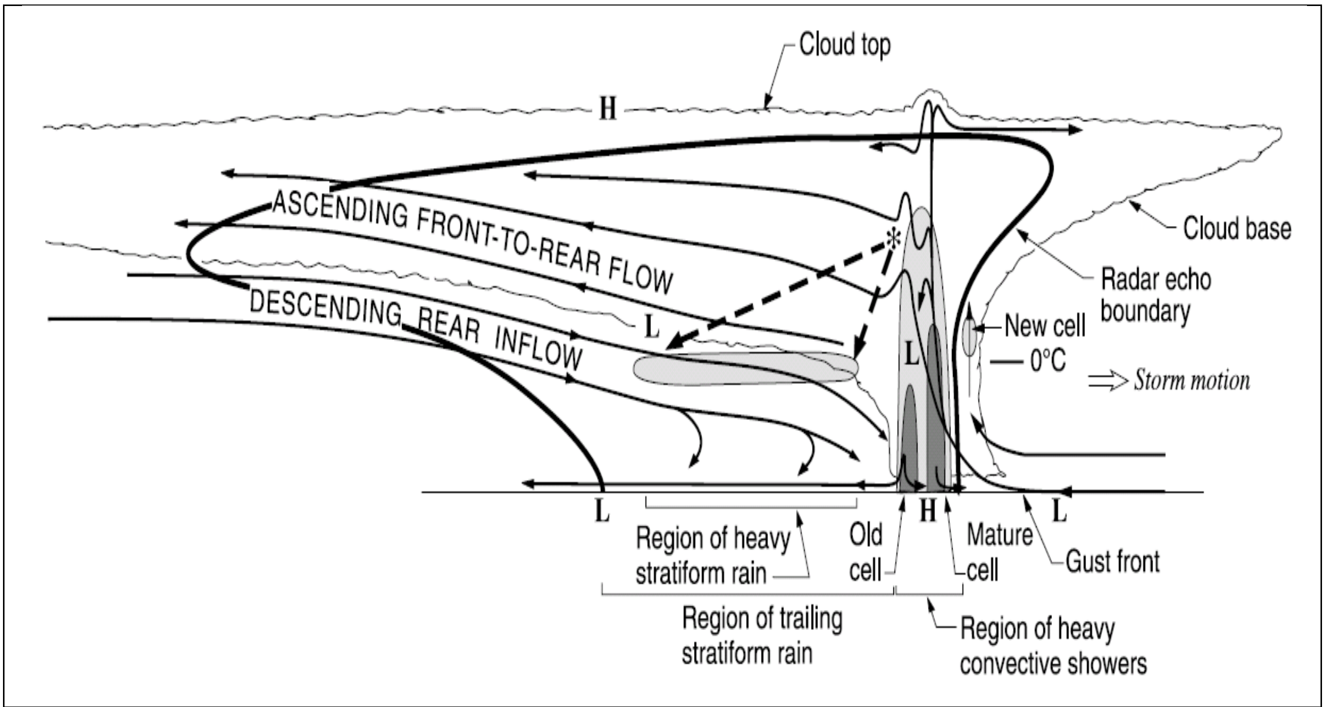

Figure I-2: Conceptual model of kinematic, microphysical, and radar echo structure of a propagating organized convective system. From Houze et al. (1989, 2004).

Mason et al. (2006) have provided the following information on the common observations from commercial aircraft Flight Data Recorder (FDR) data and pilots' reports associated with engine power loss events:

- High altitude, cold temperature :
  Commuter: 28,000- 31,000 ft, median 29,000 ft, –20 to –37 °C, median -32 °C
  Transport: 11,500-39,000 ft, median 25,800 ft, -10 to –55 °C, median –21 °C,
- Aircraft in the vicinity of convective clouds/ thunderstorms,
- Environment significantly warmer than standard atmosphere,
- Visible moisture / Instrument Meteorological Conditions (IMC) / In cloud,
- Light to moderate turbulence,
- Aircraft total air temperature probe (TAT) anomaly,
- Lack of observations of significant airframe icing,
- No flight-radar echoes at the location and altitude of the engine event.

In general, most engine power loss events have been reported near active deep convection, and in a warm tropical environment. Power loss events are observed in the vicinity of both oceanic and continental convection. There are almost no observations of ice build-up on the aircraft, and there was generally no indication of icing activity. The pilot's radar almost always measures reflectivity below 30 dBZ, and often below 20 dBZ, at the location and altitude of the aircraft, although in some cases the aircraft has been diverted around a high-reflectivity region at altitude. The simultaneous occurrence of high IWC and relatively low radar reflectivity implies that the ice particles are smaller than usual (to produce relatively small radar reflectivity) but in very high concentration (to produce significant ice water content). The aircraft TAT probe anomaly is very frequently observed, and is known to occur when high mass concentrations of ice crystals are present.

More than any other cloud type, a deep convective cloud has the potential to create areas of very high condensed total water content TWC (TWC = liquid water content LWC + ice water content IWC) at high altitude. Near the core area of the cloud are updraft regions that can transport moist boundary layer air, with water vapour mixing ratios that can reach 30 g kg^{-1} or more in a tropical environment, high into the atmosphere where most of that vapour is forced to condense. In theory this can create total water contents as high as 9 gm^{-3} at intermediate altitudes in undiluted 'adiabatic' updrafts.

Initially the condensed water is in the form of water droplets, but ice formation mechanisms and mixing at temperatures below 0°C can lead to mixed phase conditions (liquid + ice), and as the updraft passes up through approximately the -38°C level, homogenous nucleation quickly freezes any remaining liquid particle.

The availability of such large local concentrations of hydrometeors results in production of heavy precipitation that falls through the freezing level, melts, and forms cells of heavy rain. Deep convective clouds also have a high-altitude cloud outflow region, or anvil, where cloud hydrometeors are advected downwind out of the core area, sometimes for hundreds of kilometres. In fact, the core area of the cloud may be a very small fraction of the cloudy area as seen from above. Anvil regions may also contain relatively large IWC values, although there is evidence that in general the IWC drops off with distance from the core of the storm.

Commercial aircraft routinely penetrate these anvils. However, there is clearly insufficient evidence to determine specifically where relative to a core updraft area a power loss event has occurred. Some events have occurred in anvils, others have occurred while diverting around high reflectivity regions at altitude, and may therefore be closer to cores. It is suspected that in many cases the aircraft has been flying above an area of heavy rain, although radar reflectivity at flight-altitude was quite low. Therefore the flight strategy employed during HIWC/HAIC will consist in flying through updraft cores (at least for oceanic convection) of convective cells and progressively fly out of these cores to document the variation of IWC as a function of distance to the convective cores (probably up to 50 km away from the cores).

With regards to the potential role of supercooled liquid water content in these power loss events, it appears that LWC is apparently not required (and not present). The fractional distribution of LWC and IWC in deep convective clouds is not well understood, and probably depends on factors such as altitude, temperature, location in the storm, period in the storm's lifecycle, and other more subtle factors such as aerosol concentration and composition. However the literature on the subject seems to indicate that supercooled liquid water is essentially found where there is significant updraft velocities, and that stratiform anvil regions are glaciated (Stith et al. 2002, Black and Hallett 1986; Lawson et al. 1998). Finally it is suspected that high IWC regions will be located near convective cores, with more moderate updrafts (weaker continental convection, oceanic convection), in the anvils, in the remnants of vigorous convection, and in tropical storms.

There are significant fundamental cloud physics questions raised by the observations of clouds with high IWC. The formation of high concentrations of small ice crystals and the associated absence of supercooled water droplets within convective clouds is clearly not well understood. The occurrence of these conditions and the stage in a cloud system lifecycle at which these extreme characteristics occur are completely open questions at this stage.

The use of satellite imagery and active ground- and air-based remote sensing (radar, lidar) along with the aircraft in-situ data will put the sample in appropriate spatial and life cycle context. The combination of observations will allow the study of the microphysical evolution of cloud systems including both within growing convective cores as well as subsequent evolution of the anvil clouds. The observations extending in-situ measurements to cloud regions with very high water content will be a unique resource.

The sampling strategy to address the engine issues will also be effective for addressing a number of science questions. The measurement of core regions, and possibly quasi-adiabatic updrafts, will improve the understanding of a number of fundamental cloud physics problems, such as the initiation of ice particles and the evolution of the mixed-phase. Statistics of cloud updraft and associated microphysical structure will be generated.

The available data sets with this kind of information are very limited. In particular the in situ measurement data are often limited to 2D particle imagery, since so far bulk TWC measurement devices have not been capable to measure reliably beyond 1-2 g/m3 on aircraft. Estimating TWC from 2D cloud particle imagery is tricky, since we have to make assumptions first about how the 2D image translates into the 3D shape of a cloud particle and second about the variable ice density (Lawson and Baker, 2006; Baker and Lawson, 2006; Brown and Francis, 1994; Heymsfield et al., 2007, 2008, 2010).

The HAIC data will be of fundamental importance for the development of parameterizations of convection as well as providing unique data for the validation of models and remotely sensed data (from all kinds of platforms from ground to space). Validation of remote sensing will include but not be limited to an examination of the ground-based polarimetric radar and airborne Doppler cloud radar data on the Falcon 20. There are several features to be validated. The radar retrievals include the cloud microphysical type as well as ice water contents and in cases below the freezing level estimation of rain drop size distributions.

If in fact convective cores have regions of high IWC characterized by relatively low radar reflectivity and unusually small ice particles, the accuracy of existing relationships to derive IWC from reflectivity may not be accurate for these regions. This type of relationship is for instance the cornerstone of the space borne CloudSat cloud radar retrievals at global scale. Flights crossing from active convection into stratiform rain areas and anvil cloud will provide detailed cloud observations for testing retrievals from a range of radars operating at various frequencies including cloud radars as well as satellite remote sensing.

I.2. References related to the scientific discussion of the high IWC phenomenon on the one hand and to in situ and remote sensing measurement techniques on the other hand

I.2.1. References related to the high IWC in convective tropical clouds

Black, R. and J. Hallett, 1986: Observations of the ice distributions in hurricanes, *J. Atmos. Sci.,* 43, 802-822.

Bouniol, D., J. Delanoë, C. Duroure, A. Protat, V. Giraud, and G. Penide, 2009 : The microphysical characterisation of West African mesoscale convective anvils. *Quart. J. Roy. Meteor. Soc..,* 136(S1), 323-344, 2010, doi: 10.1002/qj.557.

Houze, R. A., Jr., 1989: Observed structure of mesoscale convective systems and implications for large-scale heating. *Quart. J. Roy. Meteor. Soc*., 115, 425-461.

Houze, R. A., Jr., 1997: Stratiform precipitation in regions of convection: A meteorological paradox? *Bull. Amer. Meteor. Soc.,* 78, 2179-2196.

Houze, R. A., Jr., 2004: Mesoscale convective systems. *Rev. Geophys.*, 42, 10.1029/2004RG000150, 43 pp.

Jensen, E. J., P. Lawson, B. Baker, B. Pilson, Q. Mo, A. Heymsfield, A. Bansemer, T.-P. Bui, M. McGill, D. Hlavka, G. Heymsfield, S. Platnick, T. Arnold, and S. Tanelli, 2009: On the importance of small ice crystals in tropical anvil cirrus, *Atmos. Chem. Phys.,* 9, 5519–5537.

Keenan, T., S. Rutledge, R. Carbone, J. Wilson, T. Takahashi, P. May, N. Tapper, M. Platt, J. Hacker, S. Sekelsky, M. Moncrieff, K. Saito, G. Holland, A. Crook and K. Gage, 1999: The Maritime Continent Thunderstorm Experiment (MCTEX): Overview and some results, *Bull. Amer. Meteor. Soc*., **81**, 2433-2455.

Lawson R.P., E. Jensen, D.L. Mitchell, B. Baker, Q. Mo and B. Pilson, 2010: Microphysical and radiative properties of tropical clouds. *J. Geophys. Res.*, submitted, 2010.

Lawson, R.P., Angus, L.J., and Heymsfield, A..J., 1998: Cloud particle measurements in thunderstorm anvils and possible threat to aviation. *J. Aircraft*, **35(1)**, 113-121.

Mason, J.G., J.W. Strapp, and P. Chow, 2006: The ice particle threat to engines in flight. *44th AIAA Aerospace Sciences Meeting, Reno, Nevada,* 9-12 January 2006, AIAA-2006-206.

May, P. T., J.H. Mather, G. Vaughan, C. Jakob, G.M. McFarquhar, K.N. Bower, and G. G. Mace, 2008: The Tropical Warm Pool International Cloud Experiment. *Bull. Amer. Meteor. Soc., 89*, 629–645.

McFarquhar, G. M., J. Um, M. Freer, D. Baumgardner, G. L. Kok, and G. Mace, 2007: The importance of small crystals to cirrus properties: Observations from the Tropical Western Pacific International Cloud Experiment (TWP-ICE). *Geophys. Res. Lett.*, *34*, L13803, doi:10.1029/2007GL029865.

Mech, M., S. Crewell, I. Meirold-Mautner, C. Prigent, and J.-P. Chaboureau (2007). Information content of millimeter observations for hydrometeor properties in mid-latitudes, IEEE Trans. Geosci. Remote Sens., 45, 2287 – 2299.

Protat, A., G. McFarquhar, J. Um, and J. Delanoë, 2010: Obtaining best estimates for the microphysical and radiative properties of tropical ice clouds from TWP-ICE in-situ microphysical observations. *J. Appl. Meteor. Clim.*, Accepted, March 2010.

Protat, A., J. Delanoë, A. Plana-Fattori, P. T. May, and E. O'Connor, 2009: The statistical properties of tropical ice clouds generated by the West-African and Australian monsoons from ground-based radar-lidar observations. *Quart. J. Roy. Meteor. Soc.*, 136(S1), 345-363, 2010, doi: 10.1002/qj.490.

Protat, A., J. Delanoë, D. Bouniol, A.J. Heymsfield, A. Bansemer, and P. Brown 2007: Evaluation of ice water content retrievals from cloud radar reflectivity and temperature using a large airborne in situ microphysical database. *J. Appl. Meteor. Clim*, 46, 557-572, 2007.

Stith, J. L., J. E. Dye, A. Bansemer, A. Heymsfield, C. Grainger, W.W. Petersen, and R. Berticelli, 2002: Microphysical observations of tropical clouds. *J. Appl. Meteor.,***41**, 97-117.

Webster, P.J., and R.A. Houze Jr, 1991: The Equatorial Mesoscale Experiment (EMEX): An overview*, Bull. Amer. Meteor. Soc*., **72**, 1481-1505.

I.2.2. References related to the in situ and remote sensing measurement techniques (for discussion of potential F-20 in situ and remote sensing instrumental payload) in the high IWC context of convective tropical clouds

Baker, B. A., and R. P. Lawson, 2006: Improvement in determination of ice water content from two-dimensional particle imagery: Part I: Image to mass relationships. *J. of Appl. Meteor.*: Vol. 45, No. 9, pp. 1282-1290.

Lawson, R. P., and B. A. Baker, 2006: Improvement in determination of ice water content from two-dimensional particle imagery. Part II: Applications to collected data. *J. of Appl. Meteor.*:Vol. 45, No. 9, pp. 1291-1303.

Brown, P. R. A., and P. N. Francis, 1995: Improved measurements of the ice water content in cirrus using a total-water probe. *J. Atmos. Oceanic Technol.,* **12,** 410–414.

Delanoë J. and Hogan R., 2010: Combined CloudSat-CALIPSO-MODIS retrievals of the properties of ice clouds. J. Geophys. Res., 115, D00H29, doi:10.1029/2009JD012346.

Delanoë , J. and R. J. Hogan, 2008: A variational scheme for retrieving ice cloud properties from combined radar, lidar, and infrared radiometer, *J. Geophys. Res. 113,* D07204.

Delanoë, J., A. Protat, D. Bouniol, A. Heymsfield, A. Bansemer and P. Brown, 2007: The characterization of ice clouds properties from Doppler radar measurements, *J. Appl. Meteor. Climatol. 46*, 1682–1698.

Delanoë, J., A. Protat, J. Testud, D. Bouniol, A.J. Heymsfield, A. Bansemer, P.R.A. Brown and R.M. Forbes, 2005: Statistical properties of the normalized ice particle size distribution, *J. Geophys. Res. 110*, D10201.

Field, P.R., A.J. Heymsfield, and A. Bansemer, 2006: Shattering and interarrival times measured by optical array probes in ice clouds, *Journal of Atmospheric and Oceanic Technology, 23*, 1357-1371.

Heymsfield, A.J., 2007: On measurements of small ice particles in clouds, *Geophysical Research Letters, 34*, L23812, doi:10.1029/2007GL030951.

Heymsfield, A.J., A. Protat, D. Bouniol, R. T. Austin, R. J. Hogan, J. Delanoë, H. Okamoto, K. Sato, G.-J. van Zadelhoff, D. P. Donovan A.., Z. Wang. (2008) Testing IWC Retrieval Methods Using Radar and Ancillary Measurements with In Situ Data. *Journal of Applied Meteorology and Climatology* **47**:1, 135-163

Heymsfield, A.J.,, A. Bansemer, and C. H. Twohy, 2007: Refinements to ice particle mass dimensional and terminal velocity relationships for ice clouds. Part I: Temperature dependence. J. Atmos. Sci., 64, 1047–1067.

Heymsfield A. J., C. Schmitt, A. Bansemer, C. H. Twohy. Improved Representation of Ice Particle Masses Based on Observations in Natural Clouds. *Journal of The Atmospheric Sciences* - J ATMOS SCI , 2010.

Heymsfield, A.J. 2003: Properties of tropical and midlatitude ice cloud particle ensembles. Part I: Median mass diameters and terminal velocities. *J. Atmos. Sci.,* **60,** 2592–2611.

Heymsfield, A.J., and J. Iaquinta, 2000: Cirrus crystal terminal velocities. *J.Atmos. Sci.,* **57,** 916–938.

Heymsfield, A.J., and L. M. Miloshevich, 2003: Parameterizations for the cross-sectional area and extinction of cirrus and stratiform ice cloud particles. *J. Atmos. Sci.,* **60,** 936–956.

Hogan, R. J., M. P. Mittermaier, and A. J. Illingworth, 2006a: The retrieval of ice water content from radar reflectivity factor and temperature and its use in evaluating a mesoscale model. *J. Appl. Meteor.,* **45,** 301–317.

Keenan, T., K. Glasson, F. Cummings, T.S. Bird, J. Keeler, and J. Lutz, 1998: The BMRC/NCAR C-Band Polarimetric (CPol) radar system. *J. Atmos. Oceanic Tech.*, **15**, 871-886.

Korolev, A.V., J.W. Strapp, G.A. Isaac, and A.N. Nevzorov, 1998a: The Nevzorov airborne hot-wire LWC-TWC probe: Principle of operation and performance characteristics, *J. Atmos. Oceanic Technol.*, **15**, 1495-1510.

Liu, C. L., and A. J. Illingworth, 2000: Toward more accurate retrievals of ice water content from radar measurements of clouds. *J. Appl. Meteor.,* **39,** 1130–1146.

Mitchell, D. L., 1996: Use of mass- and area-dimensional power laws for determining precipitation particle terminal velocities. *J. Atmos. Sci.,* **53,** 1710–1723.

Plana-Fattori A., A. Protat, and J. Delanoë, 2010: Observing ice clouds with a Doppler cloud radar, *Comptes Rendus Physique,* ***11**, 1, 96-103, doi:10.1016/j.crhy.2009.11.004*.

Prigent, C., E. Defer, J. R. Pardo, C. Pearl, W. B. Rossow, and J.-P. Pinty (2005), Relations of polarized scattering signatures observed by TRMM microwave instrument with electrical processes in cloud systems, Geophys. Res. Lett., 32, L04810, doi:10.1029/2004GL022225.

Protat, A., and I. Zawadzki, 1999: A variational method for real-time retrieval of three-dimensional wind field from multiple-doppler bistatic radar network data. *J. Atmos. Oceanic Technol.*, 16 (4), 432-449.

Schwarzenboeck A., G. Mioche, A. Armetta, A. Herber and J.-F.Gayet, 2009: Response of the Nevzorov hot wire probe in Artcic clouds dominated by very large droplet sizes, *Atmospheric Measurement Techniques, 2*, 779-788.

Shcherbakov V., J.-F. Gayet, G. Febvre, A. J. Heymsfield and G. Mioche, 2010: Probabilistic model of shattering effects on in-cloud measurements. *Atmos. Chem. Phys. Discuss*., submitted, 2010.

Tinel, C., J. Testud, J. Pelon, R. J. Hogan, A. Protat, J. Delanoë, and D. Bouniol, 2005: The Retrieval of Ice-Cloud Properties from Cloud Radar and Lidar Synergy, Journal of Applied Meteorology, 44, 860-865.

I.3. Microphysical data of deep convection clouds available for this study

Many aircraft measurement programs in the tropical field have already been performed. Decades of observations have permitted the collection of preliminary information on these atmospheric conditions and contributed to our knowledge-base of tropical oceanic convection.

Nevertheless and despite ample industry evidence that deep convective clouds over tropical oceans can be safely penetrated by research aircraft with appropriate caution, the research programs have not resulted in a large sample of data from penetration of suspected high IWC regions of Mesoscale Convective System (MCS), either because such data were not the highest priority and/or there was instrumentation on the aircraft that could be compromised by penetrating high IWC regions, or because fitted instrumentation was not capable of providing accurate measurements. As a result, scientific knowledge is very limited (or almost non-existent) regarding the frequency of occurrence, conditions of formation, and microphysical and dynamical processes involved in the HighIWC regions encountered by commercial aircraft during the reported in-service events.

Thus, for the EASA-HighIWC project Airbus provided flight test data measurements from their flight test campaigns conducted in 2010. The analysis of these measurements will be presented in detail in the subsequent chapter II. The flight tests were conducted in high altitude icing conditions in order to preliminary characterise these atmospheric conditions (particles size / water concentrations). The campaigns were conducted in Darwin (Australia) in February 2010 and in Cayenne (French Guyana) in May 2010. A total of fourteen flights were performed during the campaigns with an A340 test aircraft in both oceanic and continental convective conditions. The A340 has been equipped with the Airbus Nephelometer, a high resolution cloud particle imager and the SEA Robust probe, a new bulk condensed total water content probe (TWC).

In addition, CNRS-LaMP provided for the EASA-HighIWC study in situ cloud microphysics measurements from Megha-Tropiques measurement campaigns in 2010 (MT1 in the following) and 2011 (MT2 in the following). The work on the retrieval of information on the properties of ice phase hydrometeors (crystal density and size) from these data is presented likewise in the subsequent chapter II. Two measurement campaigns have been performed to improve the existing parameterization in order to capture correctly the properties of these particles. The ice microphysics study will primarily result in an overview of the microphysical cloud data (PSD, density, vertical & horizontal gradients in cloud microphysical properties, etc…) from state of the art instrumentation (2D-S, CPI, PIP, Nevzorov, etc.) mounted during two campaigns on the French Falcon 20 research aircraft. The study covers cases of continental (2010 over West Africa) and oceanic convection (2011 over the Indian Ocean) over the Tropical belt, in order to demonstrate most eminent differences in continental and oceanic ice cloud microphysics. The IWC values estimated using microphysical characteristics constrained by the in-situ observations (see further explanations later) seem to reach several times 5-6 g/m3 particularly during the 2010 campaign over West Africa.

II. Analysis of the microphysical properties of the HighIWC regions using existing airborne in-situ observations

Recall from proposal:
The objective of this task is to analyse the gathered/available data in order to preliminary characterize glaciated and mixed phase icing conditions in term of particle size and total water concentrations. The result of this task will allow validating or identifying the necessary changes of the environment proposed in the NPA 2011-03(Appendix P) defining mixed phase and glaciated icing conditions.

II.1. Analysis of A340 measurement data from 2010 campaigns (Cayenne & Darwin) in glaciated icing conditions

In 2010, Airbus performed two flight test (F/T) campaigns in Darwin and Cayenne with the objective to preliminary characterise glaciated icing conditions in term of particles size and total water concentrations. The aircraft selected for these campaigns was the A340 MSN1 (figure II-1) with adequate instrumentation (Airbus nephelometer for non-intrusive imagery and SEA ROBUST probe for IWC measurement based on phase change of particles). Fourteen flights were performed in both oceanic and continental convection.
These data constitute a unique set of measurements which have to be further post-processed and analysed in order to produce a first characterization of the high IWC environment. Furthermore, the experience gained during these flights could be of great interest for the high IWC project in term of preparation of the 2013 Darwin flight test campaign.

Figure II-1: Airbus flight test aircraft & Airbus nephelometer probe

II.1.1. Airbus Nephelometer general measurement principle

The Airbus Nephelometer imaging probe (e.g. S. Roques, 2007) has been developed to measure particle sizes between 10 to 1500 microns, adapted to operational requirements. The imager is based on an optical principle called "coherent shadowgraphy" (see below), where droplets and crystals going through the measurement area of the probe are lightened by a low coherency punctual source. The number and the size of the particles are measured from their shadows on a CCD camera. Images are processed in real time to provide TWC, histograms of diameter, MVD, etc…

Because of the very wide range of diameters to be sized (10–1500 μm), two channels are used in parallel; one is adapted to the smallest droplets with a pixel resolution of 3 μm and the second one to larger particles, with a pixel resolution of 15 μm.

II.1.2. Image processing and derived microphysical parameters

By means of the above point illumination, the contrast of the shadow of the particles located in the measuring region is increased. This increase in contrast leads to an improvement in single cloud particle observability (S. Roques, 2007) at the expense of the focus, and thus, a considerable increase in the depth of field results from that, since the image remains observable for higher defocused values.
This increase in depth of field itself leads to an increase in the measuring (or sampling) volume which, as indicated above, depends on the size of the sensor and on the depth of field.

To sum up, the above mentioned point source provides a broadened depth of field. This increase in the depth of field itself leads to an increase in the measuring volume which depends in a known manner both on the size of the CCD sensor, and on the depth of field. Thereby, instead of a more or less clear image of the particle, the cloud particle shadow is a figure of the Fresnel diffraction pattern (=coherent shadowgraphy) of the particle due to the chosen coherent laser source.
The diffraction pattern of the cloud particle then allows deriving particle size and distance to the focal point. The size recovery procedure is described in the image processing section below.

II.1.2.1. Airbus Nephelometer data in 2nd channel (large particles): Image processing

Nephelometer camera delivers 262 frames per second. Images are processed in real time and recorded for post-processing. The post-processing includes a more sophisticated processing for crystals, where crystals can be differentiated from droplets while estimate their surfaces and numbers.
The principle used by this instrument is ‘shadowgraphy’. This means that the shadows of particles are cast on a CCD. Because of the very wide range of diameters to be sized (10–1500 μm), the instrument uses two channels in parallel; one is adapted to the smallest droplets with a pixel resolution of 3 μm and the second one to larger particles, with a pixel resolution of 15 μm. Each channel is imaged on the same CCD alternately and is illuminated by its own laser.
The camera delivers 512 × 512 pixels. So far the only parameters derived from the 2nd channel (large particles) are surface and surface equivalent diameter equivalent to the diameter of a disc corresponding to the crystal surface from ‘shadowgraphy’, as well as geometric sampling volume. For larger particles, sampling volume is rather well determined from geometric considerations. In addition, the sampling volume (particularly the depth of field!) has been calibrated for the second channel with synthetic particles. However, for the smaller objects of the 1st channel the sampling volume is less well defined. The impact of sampling volume uncertainty on the 1st channel is not impacting the IWC calculation which is solely deduced from the 2nd channel of larger particles. Habit classification has not yet been implemented. Likewise, in near future, further geometric parameters (maximum diameter, diameter perpendicular to maximum diameter,

and perimeter) will be added to the data extraction. Airbus will accomplish this further study with the support of a subcontractor.

The remaining task then is to define ice density to deduce IWC from PSD and sampling volume of the 2nd channel. For processing of the Airbus nephelometer data the ice density has been chosen according to the Brown and Francis (1994) and Baker and Lawson (2006) parameterizations. From the measured area of individual ice crystals the related mass can be derived from the relation presented in figure II-2 (Baker and Lawson, 2006), or as proposed in Brown and Francis (1995) from a mass-diameter relationship $m(D) = a \cdot D^b$ with m the particle mass in gram and diameter D in µm (D taken as the mean of the maximum chord lengths), a= 7.38 * 10^{-11} and b=1.9. Precisely, Airbus data processing uses the Brown and Francis (1995) approach, however using the area equivalent diameter D_{eq}, instead of the mean of the maximum chord lengths. Therefore, it has been demonstrated by Airbus that this latter approach yields IWC values that are very close to the Baker and Lawson (2006) calculations. We would like to state here that the Baker and Lawson area-mass relationship has been established for

The dataset for the Baker and Lawson (2006) area-mass relation was originally obtained by collecting ice particles falling from winter storms onto Petri dishes positioned near the surface in the Sierra Nevada of California in 1987. The ice particles were photographed under a microscope, melted, and the resulting drops were photographed. Later, the photographic slides were analyzed to categorize the ice particles, and to measure their maximum length and the mean diameter of the melted drops. The mass was calculated assuming a hemispherical drop shape. The three main sources of error, applying the Baker and Lawson (2006) approach to the Airbus data may be (i) that crystal orientation on the Petri dishes may not be arbitrary, thus overestimating the surface, (ii) that ice density of falling snow may be smaller than ice density in Airbus datasets, and (iii) that the assumption of hemispheric drops after melting may be slightly false. Thus, arguments (i) and (ii) may lead to an underestimation of calculated IWC for the Airbus data, whereas (iii) should have, if any, the opposite effect.

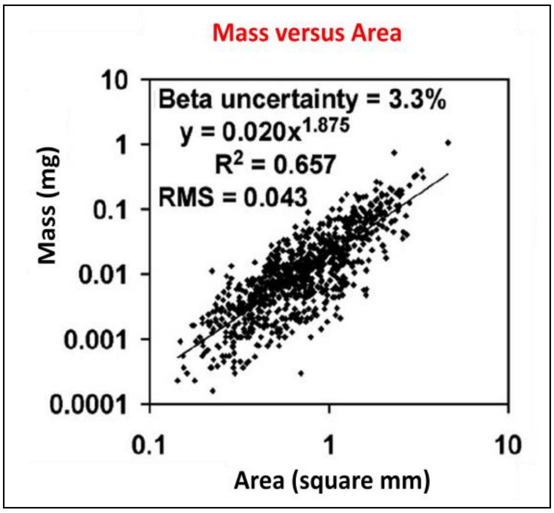

Figure II-2: Area-mass relationship taken for TWC calculations from Airbus nephelometer data (figure from Baker and Lawson, 2006).

The area is related to the area equivalent diameter plotted in the particle size distributions (PSD) of the Airbus nephelometer data. Integration of the PSD data, takes into account the above area-mass relationship, thus yielding TWC (or ice water content IWC). The variability of the PSD spectra is presented while averaging all PSD data for Cayenne, Darwin and Chile flights for distinct temperature bins of 5°C. The results are presented in figure II-3.

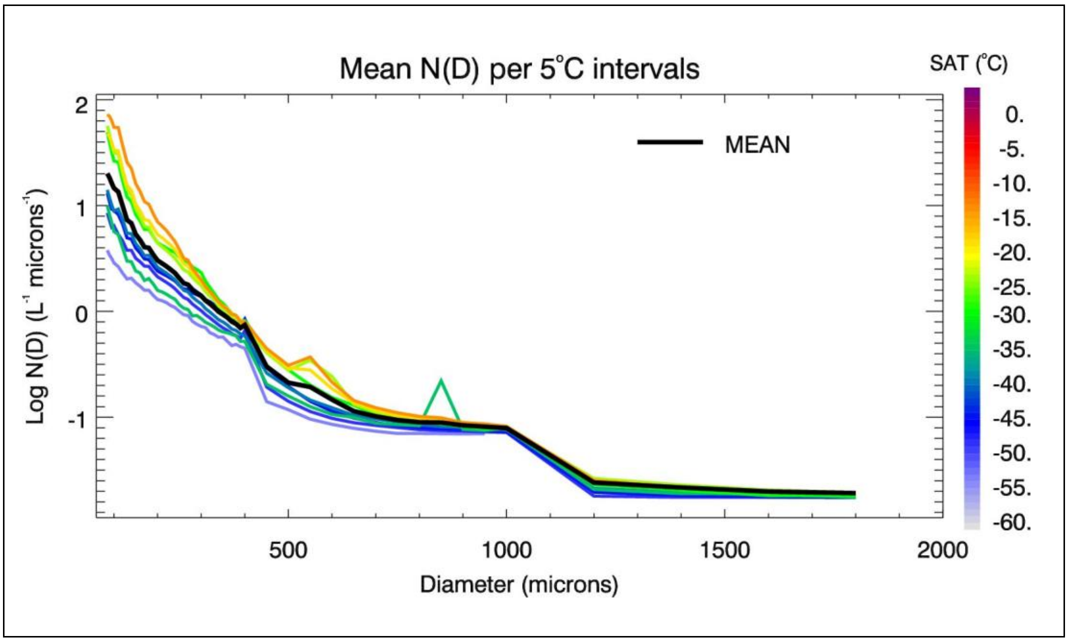

Figure II-3: Variability of particle size distributions PSD for all Airbus nephelometer data averaged for 5°C temperature domains (flight nr. 1423).

The chosen statistical relationship between the ice particle mass and its diameter (from Brown and Francis (1994)) reveals a rather good correlation coefficient, when comparing respective IWC calculations with calculations from the direct IWC measurements of the ROBUST probe. The ROBUST probe, however, is still lacking accurate calibration. Wind tunnel calibrations in the Ottawa wind tunnel suggest a collection efficiency of approximately 0.4 for ice particles produced in the tunnel (W. Strapp, personal communication, 2010). Comparing the ROBUST probe data to the Airbus nephelometer retrieved IWC values yield a ROBUST probe factor of 0.73*0.4 = 0.29 in natural conditions for Flight # 1423, which includes high IWC. The efficiency factor of 0.4 had been preset before the experiments, thus corresponding to the performed wind tunnel measurements (conditions not entirely applicable for ROBUST probe use on aircraft). In addition, as mentioned previously, this factor is derived, assuming that the Nephelometer estimates are the absolute truth, which is not the case since a mass-size relationship has been assumed. Figure II-4 shows time series of Airbus nephelometer PSD spectra, calculated IWC from ROBUST probe and Airbus nephelometer, including IWC correlation charts for one flight (flight nr. 1423) with measured high IWC (up to 6-7 gm^{-3}).

A statistical analysis of all Darwin and Cayenne flights together has also been performed and is presented in Fig. II-5. The ROBUST factor is found to be 0.27. The same values are obtained if the Darwin and Cayenne flights are processed separately. Regarding the mass-size relationship used to estimate IWC from the nephelometer data, Heymsfield et al. (2010) clearly showed that it was consistently producing an overestimation of the IWC for the six field experiments considered in that study. The authors also reported that the use of a single mass-size relationship such as that of Brown and Francis (1994) could not represent accurately the dependence of the mass-size relationship as a function of particle mean diameter and temperature (a conclusion also reached by Protat and Williams 2011 for the fall speed – diameter relationship). That could explain the differences between the wind tunnel estimates of 0.4 and our estimate of 0.27. This result clearly highlights the crucial need for a true IWC reference in those comparisons, such as that which will be provided by the isokinetic probe during the HIWC / HAIC project. Each data point of

Figure II-5 is colour coded by the respective static air temperature (SAT). No obvious variability of the ROBUST factor as a function of temperature (or number concentration, not shown) is found.

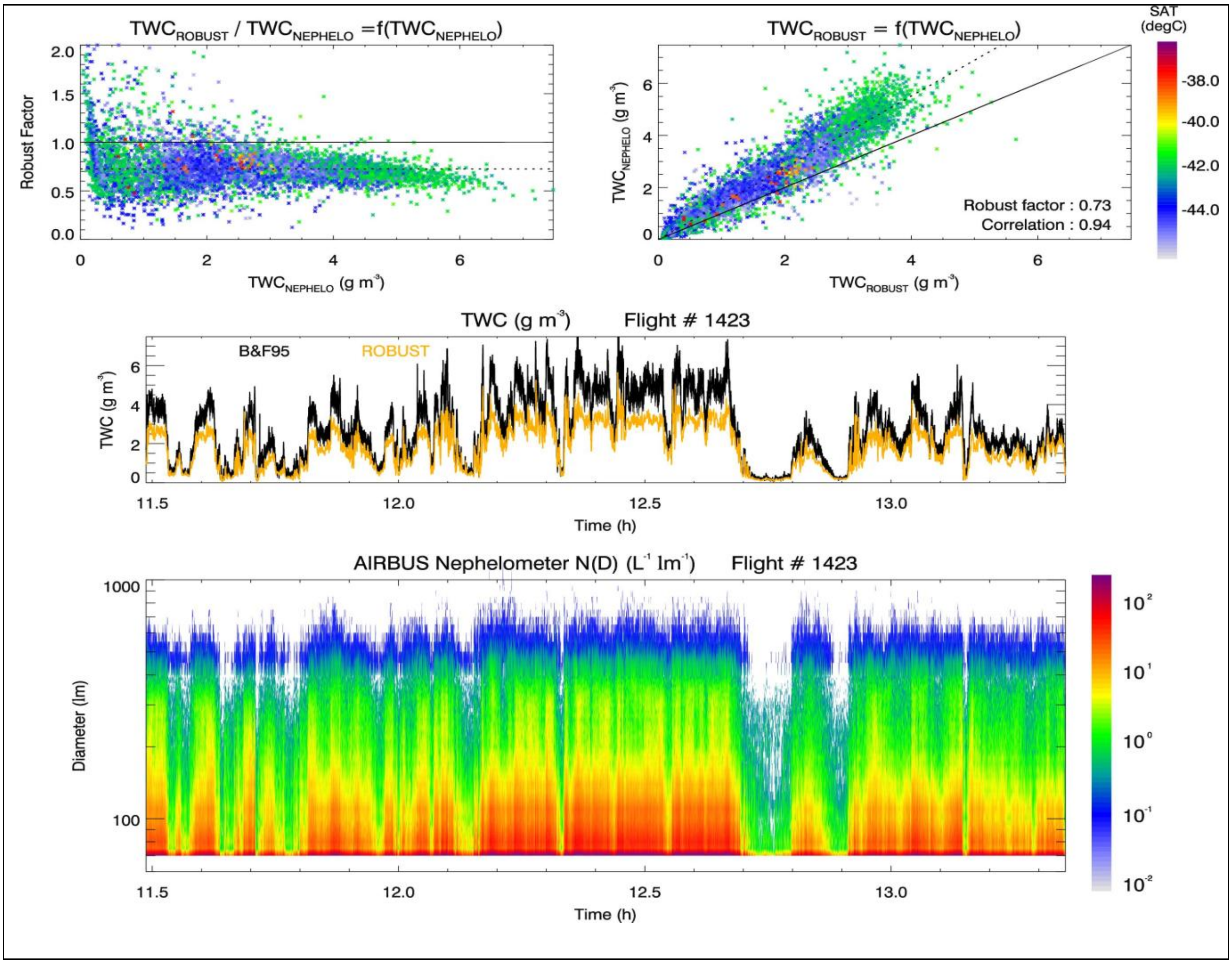

Figure II-4: Time series of Airbus nephelometer PSD spectrum (bottom panel), calculated IWC from ROBUST (with 0.4 efficiency factor) probe (orange) and Airbus nephelometer (black) for flight # 1423 in the Cayenne area (middle panel), and IWC correlation charts : Robust factor as a function of the Nephelometer TWC (upper-left panel), and TWC from the Robust as a function of TWC from the Nephelometer (upper-right panel), with the static air temperature of each comparison point in colour.

The use of other mass-size relationships found in the literature has been explored to evaluate the variability of the nephelometer estimates. As shown in Figure II-6, quite different TWC estimates are obtained when considering that all particles are bullet rosettes (red), aggregates of plates (green) and hexagonal columns (blue). The use of these three ice crystal habits which are commonly found in ice clouds results in a large underestimation when compared to the Brown and Francis mass-size results (black).

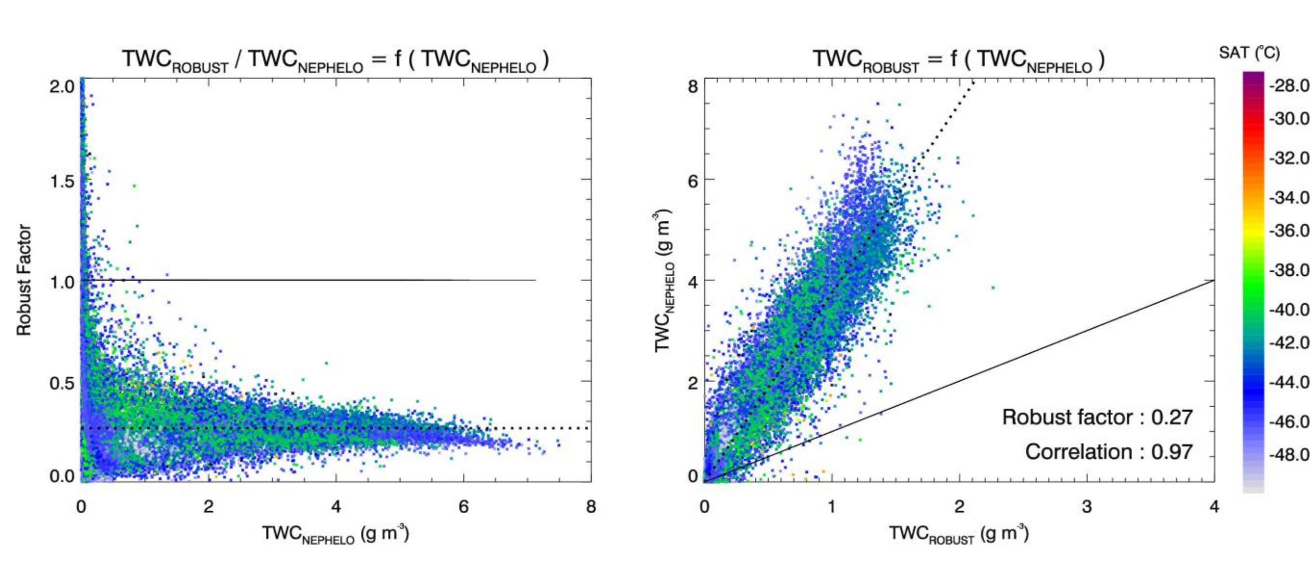

Figure II-5: Robust factor as a function of the Nephelometer TWC (left), and TWC from the Robust as a function of TWC from the Nephelometer (right), with the static air temperature of each comparison point in colour. This plot has been derived using all observations from Darwin and Cayenne.

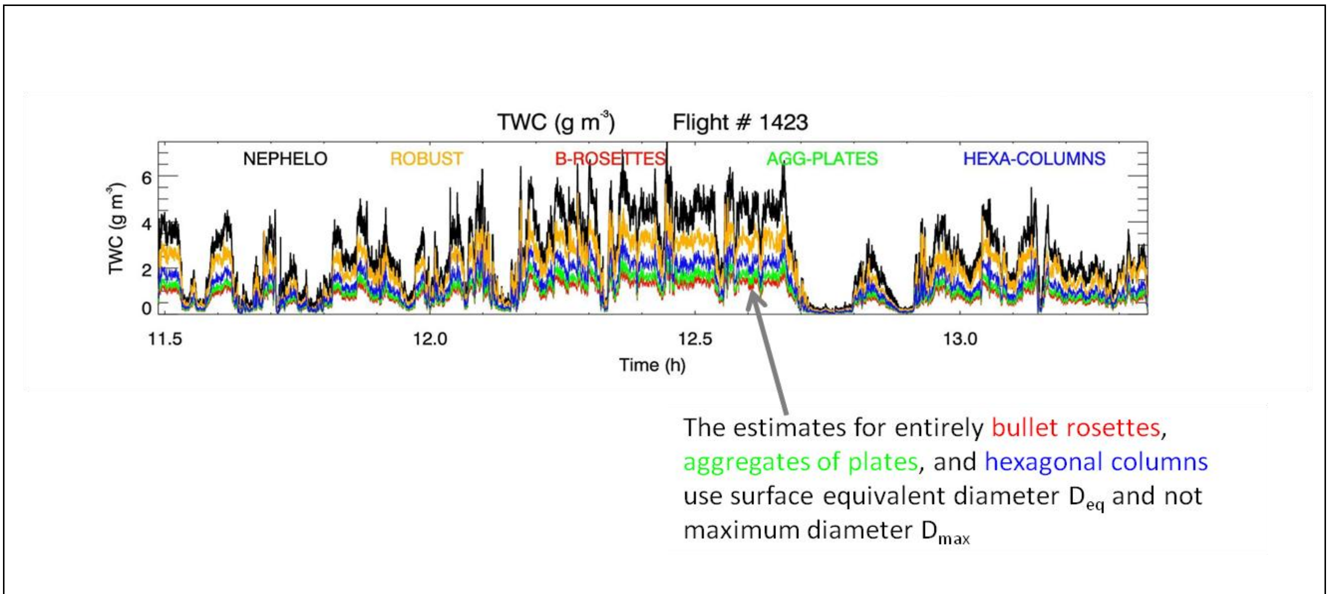

Figure II-6: Time series of TWC estimated from the Robust probe (orange) and from the nephelometer with different mass-size assumptions : Brown and Francis (1994) aggregates (black), Mitchell et al (1990) bullet rosettes (red), aggregates of plates (green) and hexagonal columns (blue).

This is however due to the fact that the mass-size relationships in the literature are actually given as a function of the maximum diameter D_{max} of the ice crystals (which is not the case of the Brown and Francis relationship, given as a function of the mean of the maximum chord lengths measured parallel and perpendicular to the 2DC and 2DP photodiode array axis), while we apply here the relationships using a median volume diameter as provided by the image processing software of the nephelometer. Further studies are therefore planned to derive more parameters from each single nephelometer image, so that we can really apply these relationships and estimate the variability of TWC estimates as a function of the mass-size relationship.

II.1.2.2. Airbus Nephelometer images in 1st channel (particles smaller than 50 µm in diameter)

The sampling volume has to be most adequately defined, since the sampling volume is one of the most important sources of measurement uncertainty of particle number concentrations (per cloud volume) and particle size distribution (PSD), and consequently of condensed water content TWC (ice and water).

Airbus processing tools seem to be best adapted to detect numerous out of focus particles (presence of diffraction pattern), including even interaction of out-of-focus particles with neighbouring particles. However, the processing tools may not entirely ensure the correct calculation of the sampling volume as a function of the image defocusing.

In order to partially validate the measurements of the Airbus Nephelometer, including in particular a most precise retrieval of the particle concentrations from the instrumental data, CNRS-LaMP worked out a statistical method, comparing the homogeneity of particle distributions in different photographic cross sections of the measurement volume. We started the implementation on the measurement data of one test flight.

Therein, the images from shadowgraphy are used to estimate local concentration fluctuations (figure II-7) and to compare those to perfectly homogeneous distributions from a theoretical model. The test represents a new method to quantitatively estimate the sampling volume. Moreover the method is independent of the optical measurement of the depth of field (z-axis of the sampling volume) used by Airbus and therefore allows to validate independently the sampling volume.

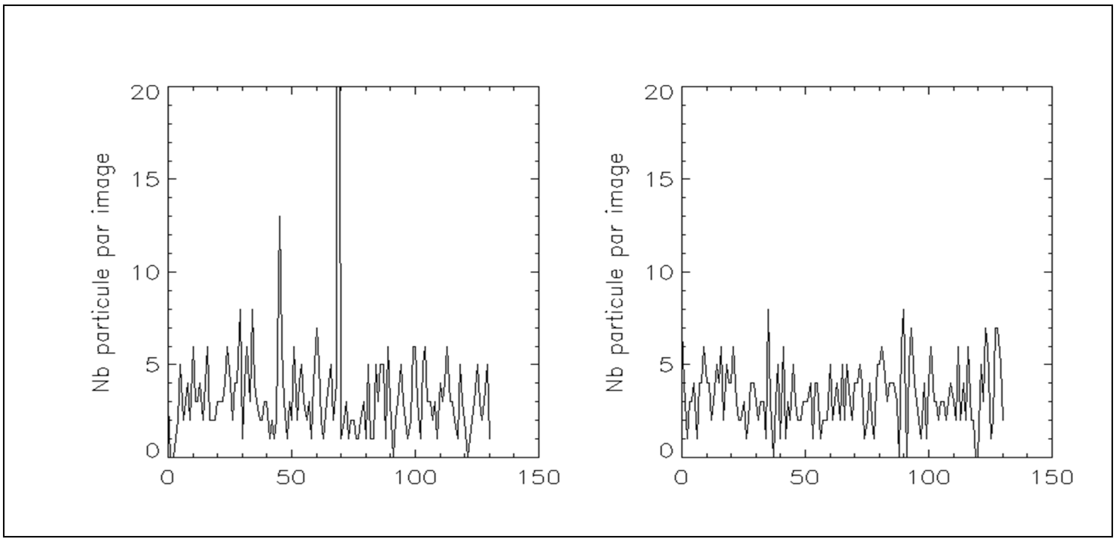

Figure II-7: Measured fluctuations of particle numbers in an area of high concentrations of small natural ice crystals (left). Theoretical fluctuations of particle numbers in a simulated area of perfectly uniform high concentrations of small natural ice crystals (right).

Deviations from the theoretical fluctuation can be artefacts (seems to be the case here), or natural (which would mean intermittent occurrence of increased concentrations of small crystals).

The following work has been performed for this validation method:

(i) detection of areas of uniform distribution of particles (Poisson distribution) in the x-y photographical plane,

(ii) analysis of defocusing measurements with subsequent correction of the optical measurements as a function of the depth of field (z-axis),

(iii) analysis of spatial fluctuations of image (particle) numbers and intercomparison with mean concentrations.

As a preliminary result we can state uniformity in the photographical plane (figure II-8) and partially non uniformity in the z-axis (analogue to the depth of field), with a possible overestimation of small particles and underestimation of large particles close to the focal plane (figure II-9). This will however not impact IWC calculations performed from channel 2 data. The 1st channel data are not yet used by Airbus, but give exciting insights in spatial structure of the convective cell variations.

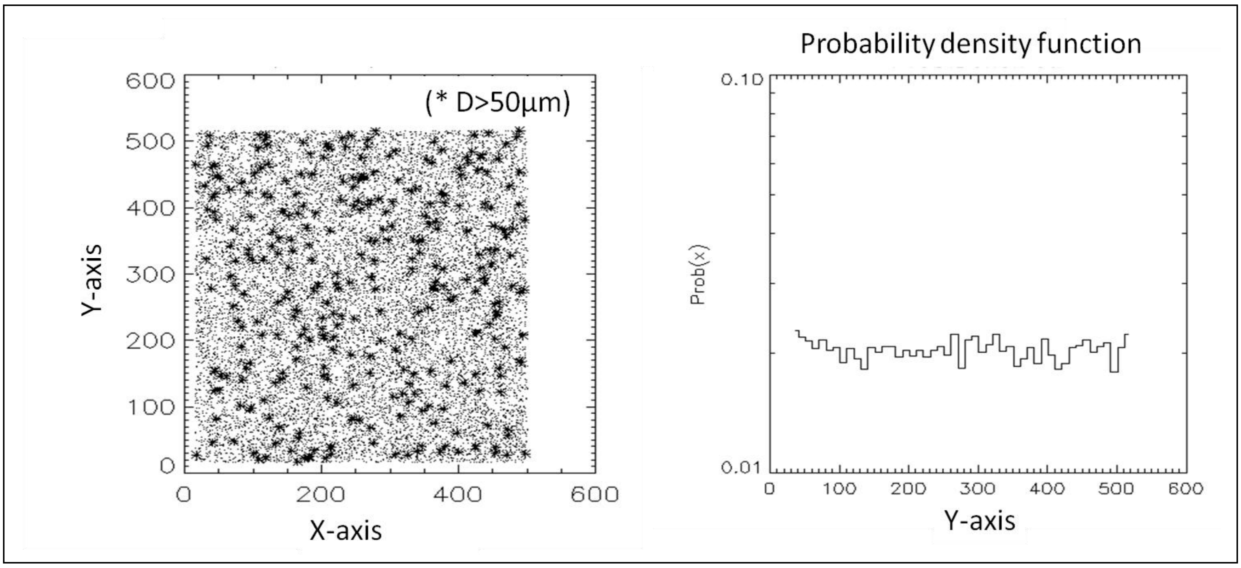

Figure II-8: Test of particle uniformity in photographic x-y plane. Large symbols: particles larger 50 µm left). Histogram of particle positions in y-axis (right).

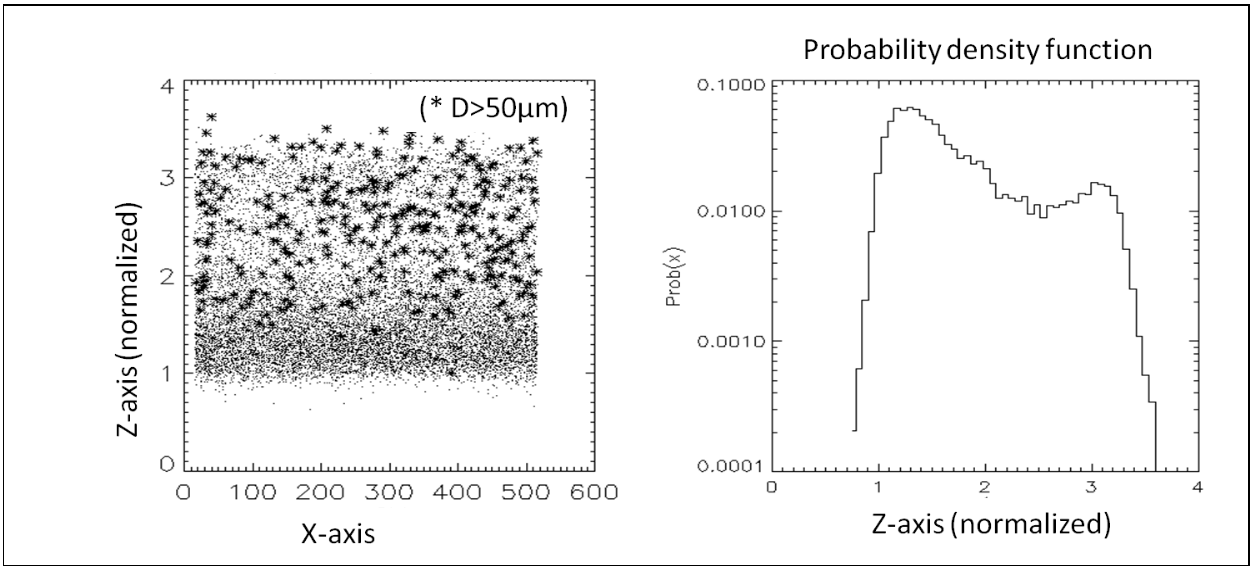

Figure II-9: Test of particle uniformity in photographic y-z plane (left). z is a variable corresponding to the depth of field, defined here as the ratio between measured (out focus) particle size and derived real particle size (from diffraction pattern). Large symbols: particles larger 50 µm. Histogram of particle positions in z-axis (right).

Figure II-10 shows a simple analysis of the number of cloud particles detected per image on the 1st channel of the Airbus nephelometer. The figure shows time series of the number of particles per image as we zoom in from 150 km to 30 km to 1.5 km, and then 200 m. This result is clearly indicating that within 17.4 nautical miles (Appendix D charts) the convective cloud systems are not at all homogeneous.

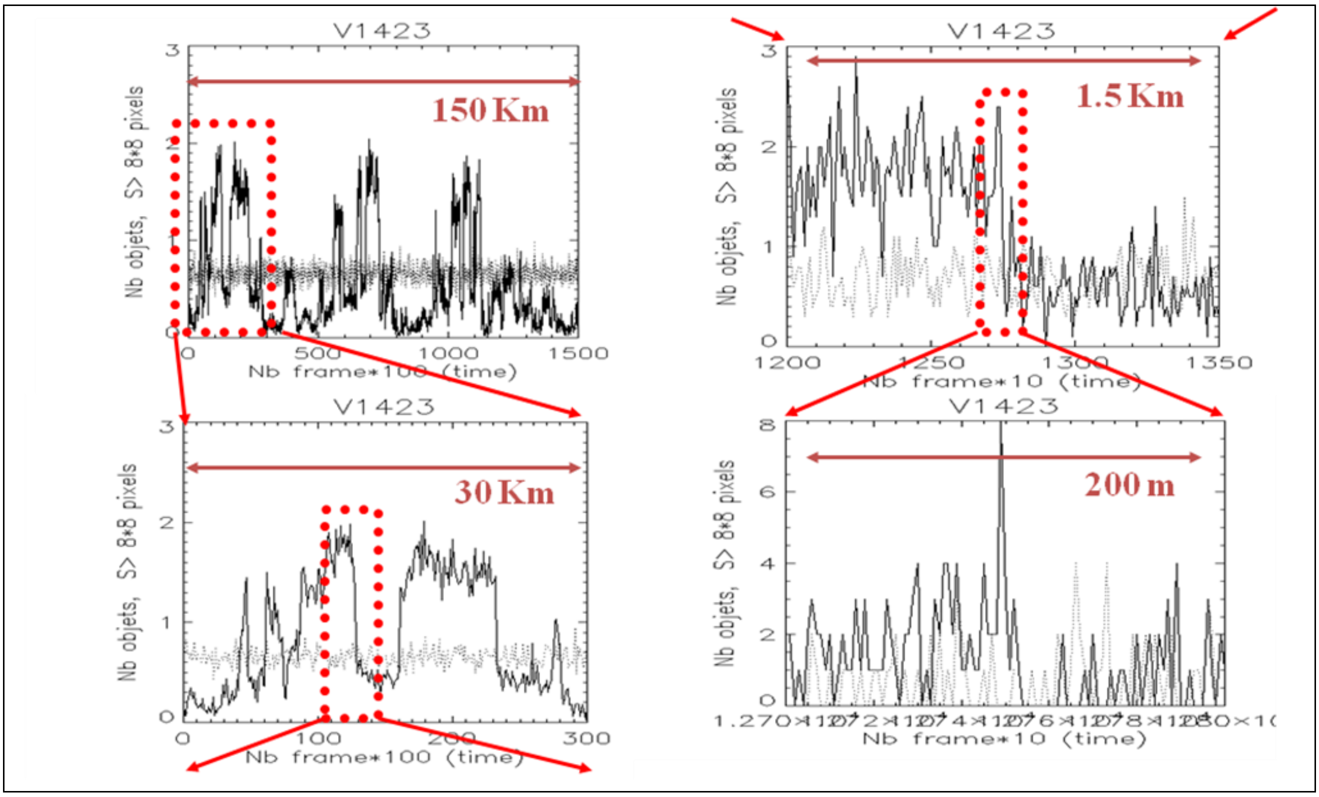

Figure II-10: Zoom on a small region with large concentration of ice particles allows statistical transition analysis. Shown on the y-axis is the number of objects larger 8*8 pixels.

II.2. Analysis of Megha-Tropiques microphysical data from 2010 and 2011 campaigns in glaciated icing conditions

The dataset presented here have been acquired within the Megha-Tropiques (MT) project. Megha-Tropiques is a French-Indian satellite devoted to improve our understanding of the processes linked to tropical convection. Two aircraft measurement campaigns (MT1 over West Africa in 2010 and MT2 over the Indian Ocean in 2011) have been performed using the French F-20 research aircraft. The instrumental F-20 payload relevant for this study consisted of the Doppler radar RASTA (Radar Aéroporté et Sol de Télédétection des *propriétés nuageuses*; with a frequency of 95GHz: Protat & Al, 2009), the Cloud Imaging Probe (CIP), the Precipitation Imaging Probe (PIP), and the 2D Stereo Probe (2DS).

Particles recorded by the particle imagers were classified both as a function of their maximum length (D_{max}) and as a function of the equivalent diameter of a disc corresponding to the crystal surface (D_{eq}). From the individual PSD of different probes used during all flights of the two Megha-Tropiques campaigns, 1Hz composite PSD spectra (as a function of D_{max} and D_{eq}) have been built (figure II-11).

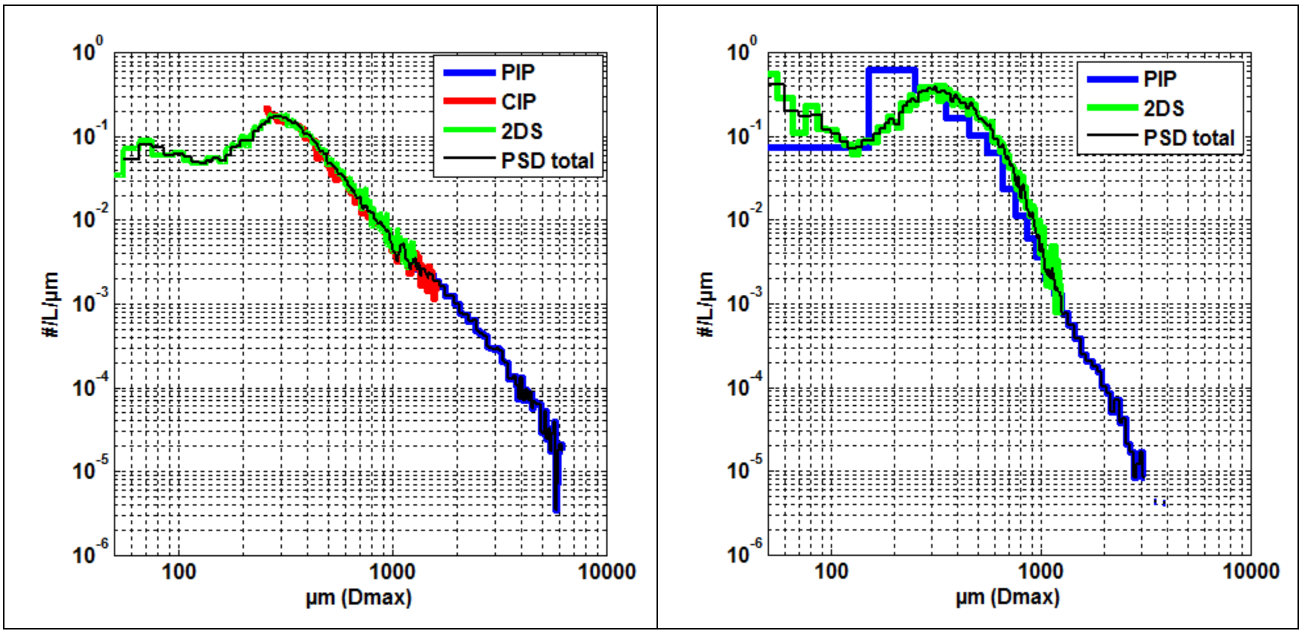

Figure II-11: PSD averaged over 10 seconds for MT1 (left) and MT2 (right) data. In blue the PSD for PIP, in red PSD for the CIP, and in green the PSD for the 2DS probe. In black the PSD composed from the individual PSDs from 2DS, CIP and PIP.

II.2.1. Investigation of mass-diameter m(D) relationships and impact on IWC

Particles recorded by the particle imagers were classified, both as a function of their maximum length (D_{max}) and as a function of the surface equivalent diameter of a disc corresponding to the crystal surface (D_{eq}) in order to perform sensitivity studies about the definition of ice crystal diameter. A 1Hz cloud particle number size distribution then is derived for each individual imaging probe. Finally, a composite particle size distribution (PSD) has been derived, combining PSD (in D_{max} or D_{eq}) of individual probes used during each flight.

Determining the mass of a cloud particle is very difficult when its habit and related ice density is not known. Baker and Lawson, (2006) presented a statistical relationship between particle mass and geometric parameters derived from 2D particle images. Schmitt and Heymsfield (2010) showed that the fractal dimension of aggregates was related with their mass.

The CNRS-LaMP estimation of IWC in MCS systems over West Africa presented in this chapter is based on two slightly different approaches of IWC retrievals from simultaneous analysis of in situ cloud particle imagery and radar reflectivity measured at 95GHz with the Doppler cloud radar RASTA.

The reflectivity at 95 GHz is usually calculated assuming the mass of the ice particles. Thus, the purpose is to estimate the mass-diameter relationship which produces the smallest deviations (equation 2) between the measured radar reflectivity *(Z_{95GHz})* and the simulated equivalent reflectivity *($Z_{T\text{-}matrix}$)* calculated from T-matrix theory from the mass-diameter power law (equation 1). The diameter D stands either for D_{eq} or D_{max}. In the present study the maximum error (cf. equation 2) has been set to 5%.

$$m(D) = \alpha \cdot D^{\beta} \qquad \text{(eqn. 1)}$$

$$error(\%) = 100\left|\frac{Z_{95GHz} - Z_{T-matrix}}{Z_{95GHz}}\right| \qquad \text{(eqn. 2)}$$

The problem cannot be solved with only the reflectivity as a constraint, since there are two unknowns (α and β). So we need to make an additional assumption on one of the coefficients (or state a relationship between the two) or use an additional observational constraint (such as the terminal fall velocity retrieved using the Doppler cloud radar RASTA observations, see below). In the present study we have mostly investigated the use of an additional assumption. Two different possible assumptions are evaluated in this work: either the β exponent is considered equal to 2.1 (as suggested in Heymsfield et al. 2010) or the β exponent is calculated as a function of the exponent of an area-diameter relationship derived from particle images of the crystals. Thus, either β is a constant, or it is a function of the 2D images recorded by the in situ imagers (2DS, CIP, PIP).

In order to characterize a falling particle in the atmosphere, Heymsfield and Miloshevich, (2003) and Mitchell (1996) use the area $S_{\perp}$ and the aspect ratio A_r (which is the area of the particle projected normal to the flow ($S_{\perp}$) divided by the area of a circumscribing disc).

$$A_r = \frac{S_{\perp}}{\frac{\pi}{4} D_{\max}^2} \qquad \text{(eqn. 3)}$$

$$S_{\perp} = \gamma \cdot D_{\max}^{\sigma} \qquad \text{(eqn. 4)}$$

In a first approximation the diameter-area law is considered equal to ($S_{\perp}$). The diameter-area law could be explained as the expected area (or mean area) for a given maximum length (D_{max}*)*. An example of a diameter-area law is given in the figure II-12 and has been calculated using all particle images in a time interval of 10 seconds for one arbitrary flight of the MT1 campaign. The relationship between the mean area and the maximum length is well fitted with a power law.

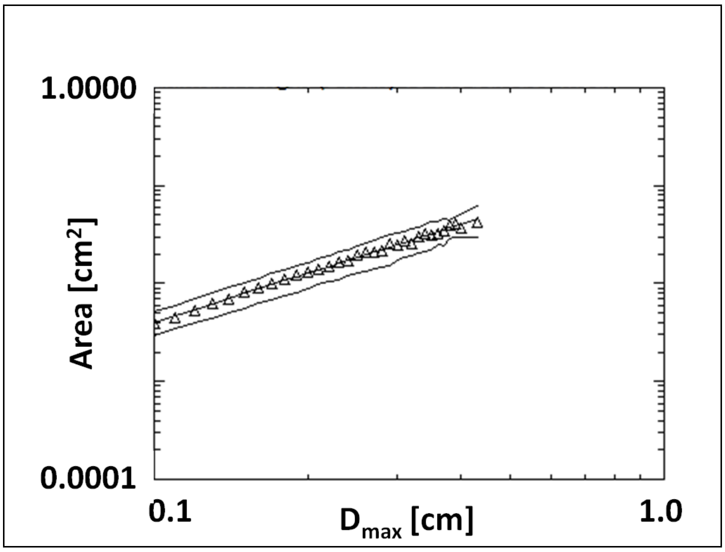

Figure II-12: Example of relationship for crystal mean area as a function of the maximum length for an ice crystal population of more than 200 analyzed crystals within a time period of 10 seconds. The particles have been recorded by the PIP probe.

A reason to study area-diameter relationships from particle imagery is also to compare in a future work the in situ estimates of the terminal velocity of the hydrometeors deduced from the Doppler measured by the radar RASTA. Since the area-diameter relationship is varying during a flight and since the area-diameter law of the particles is strongly influenced by the specific ice microphysics, relationships between the β exponent of the mass-diameter law and the σ exponent from the area-diameter (figure II-13) law have been established by theoretical simulations of statistical projections of 3D synthetic crystal images (figure II-14) on a 2D-plane.

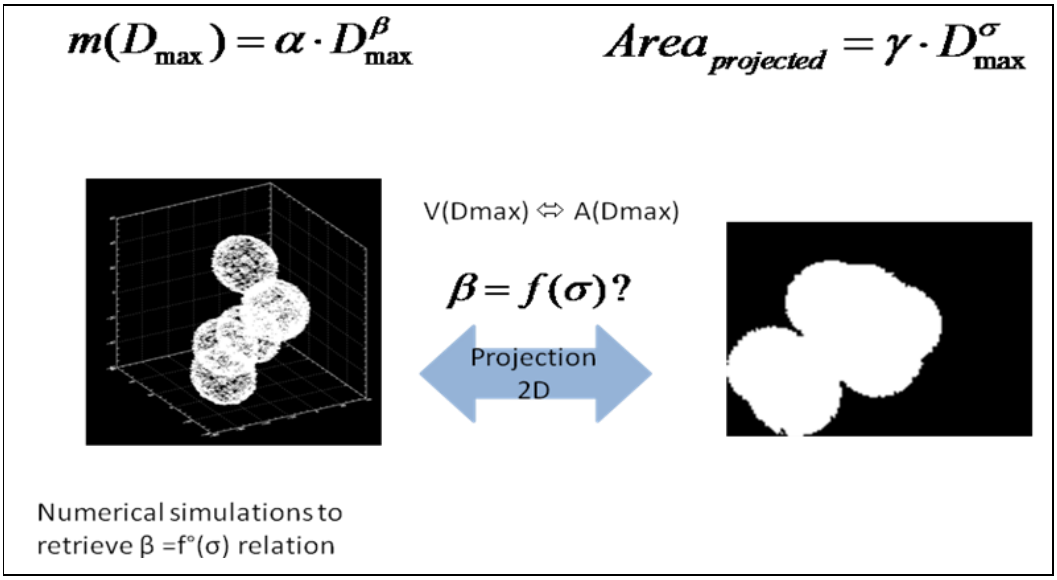

Figure II-13: Method of projecting 3D crystal structure on a 2D plane in order to relate statistically the β exponent of the mass-diameter law with the σ exponent of the surface diameter relation.

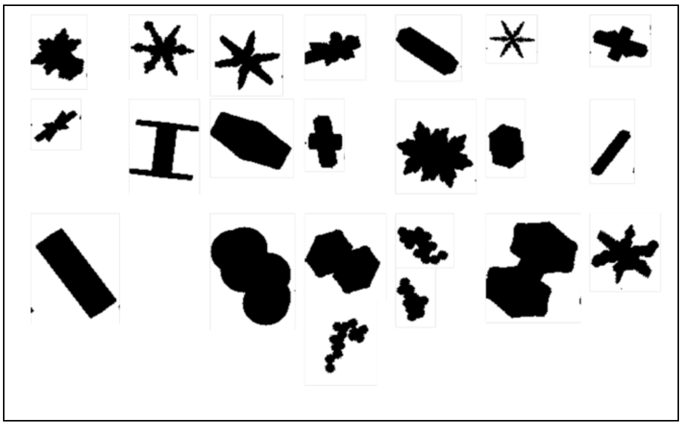

Figure II-14: Example of 2D projections of simulated 3D ice crystals of different shapes in order to relate β exponent of the m(D_{max}) power law with the σ exponent of A(D_{max}) power law.

The results of these theoretical studies are presented as the relation of the β exponent of the mass-diameter law with the σ exponent of the surface diameter relation in figure II-15.

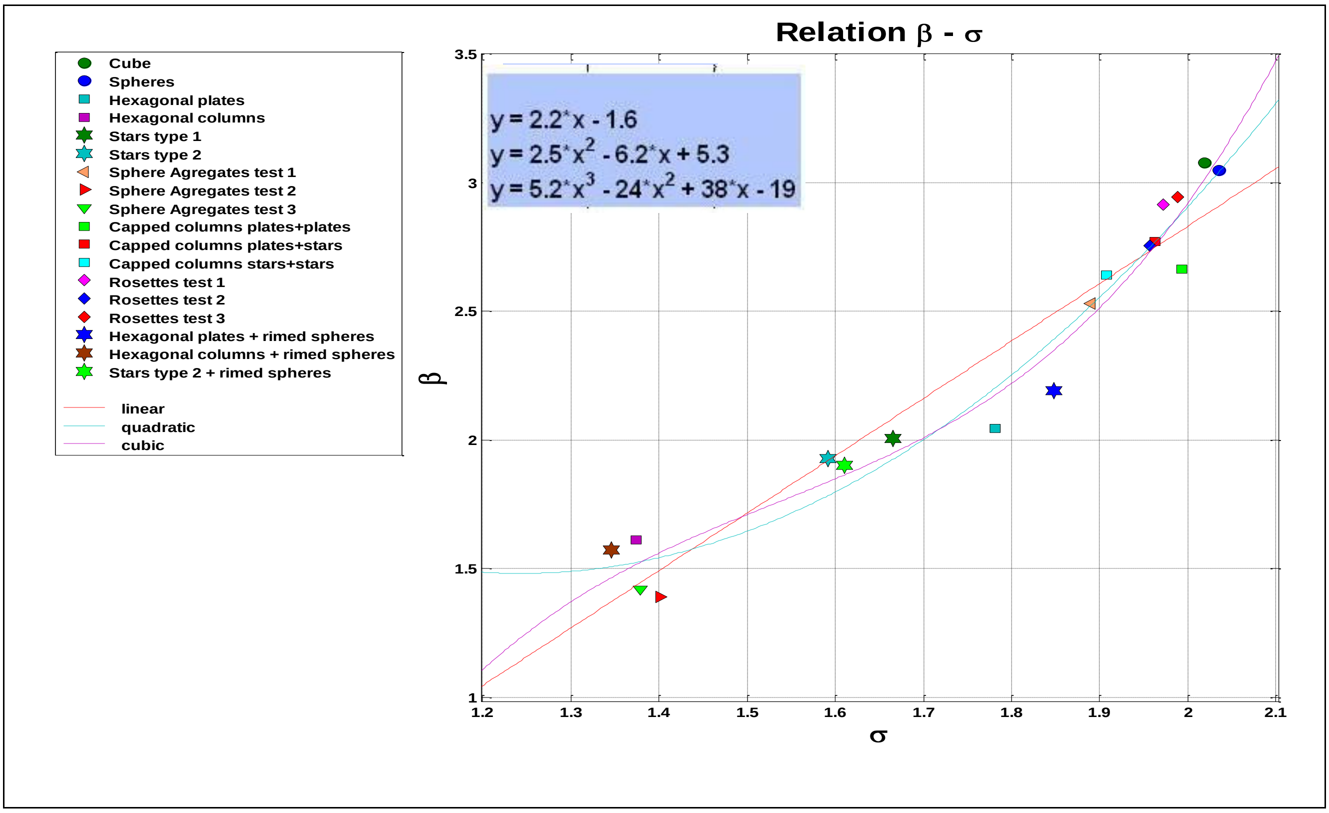

Figure II-15: Relation of â exponent of the mass-diameter law and the ó exponent from the area-diameter law established by theoretical simulations (statistical projections of 3D synthetic crystal images on a 2D-plane).

Figures II-16 and II-17 present the results obtained with the dataset from the MT1 campaign, where the mass-diameter laws are calculated for the flights 15, 17, 18, 19, 20 with a time integration of 10 seconds. The PSD have been calculated as a function of the surface equivalent diameter D_{eq} and the area-diameter law has been calculated using the 2D images monitored with the PIP probe. In figure II-16 we can see the relationship between the condensed water content (equation 5; TWC) and the measured reflectivity *(Z_{95GHz})*. The data points are colour coded with measured temperature. The resulting relationship is a power law which is influenced by the temperature (equation 6). For a given reflectivity, TWC increases with decreasing temperature, in agreement with earlier work using radar data and assuming Brown and Francis mass-size relationships (Hogan et al. 2006; Protat et al. 2007). A given TWC produces lowest reflectivity for lowest temperatures.

$$TWC = \sum_D n(D) \cdot m(D) \qquad \text{(eqn. 5)}$$

$$TWC = C_{CWC}(T) \cdot Z_{95GHz}{}^{A_{CWC}(T)} \qquad \text{(eqn. 6)}$$

The subsequent relation in equation 7 resumes what is presented in figure II-17, where α is written as a power law of β and with C_m and A_m both depending upon temperature. Overall, β increases (for a given α) with increasing temperature T, whereas α increases with decreasing T (for given β).

$$\alpha = C_m(T) \cdot \beta^{A_m(T)} \qquad \text{(eqn. 7)}$$

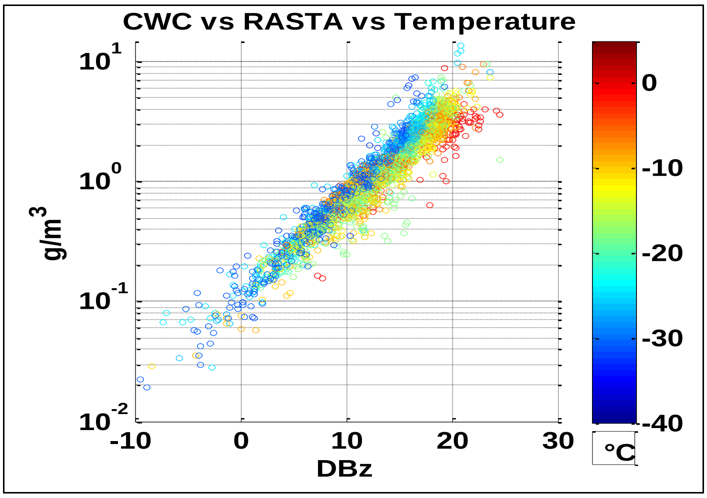

Figure II-16: Scatter plot of the CWC versus the reflectivity at 95 GHz measured by RASTA. Each point corresponds to 10 seconds of measurement data of flights 15, 17, 18, 19, 20 of MT1 and its colour shows the in-situ temperature.

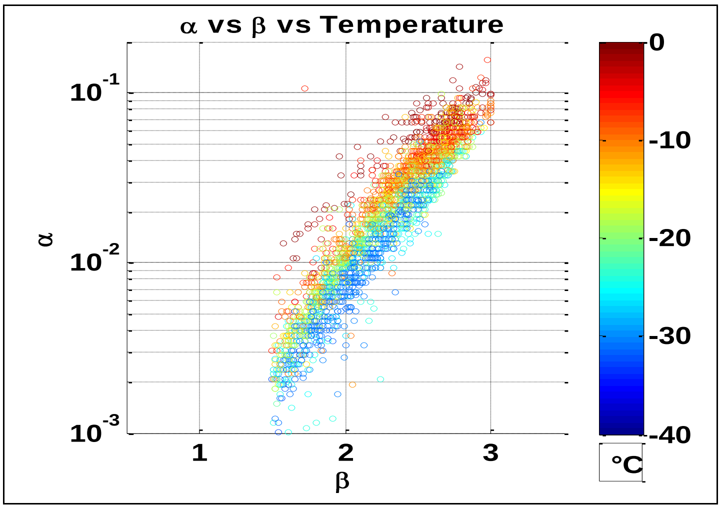

Figure II-17: Scatter plot of α versus β from the mass-diameter law $m=\alpha D^{\beta}$. Each point corresponds to 10 seconds of measurement data of flights 15, 17, 18, 19, 20 of MT1 and its colour shows the temperature in-situ.

II.2.2. Calculation of mass of total condensed water (total water content TWC)

Finally, figure II-18 shows the impact on TWC retrievals when applying 6 different parameterizations of the β exponent of the mass-diameter relationship. For these different parameterizations of the β exponent the pre-factor α is constrained, respectively, using the described T-matrix method. The figure is a zoom of 15 minutes of calculations for one exemplary flight (flight number 19). It shows results obtained with 4 different relationships between σ (from the area-diameter law) and β (from the mass-diameter law) calculated for PSD expressed in terms of the maximum length D_{max} and the area-diameter law calculated from the PIP probe (maximal length between 1000µm to 6400µm). To these four curves are added following two curves: In one of these two curves TWC is calculated for PSDs expressed in terms of the equivalent diameter D_{eq} with data from the PIP probe, whereas in the other curve TWC is calculated for D_{max}, however for CIP data only (maximal length between 500µm to 1600µm) derived area-diameter relationships. The reason for doing this is that the area-diameter relationship has been found to vary with probe resolution in the course of this work, so the variability of the IWC estimates with respect to this needed to be assessed.
The calculated TWC time series of these 6 parameterizations are rather similar and somewhat independent of the relationship between σ and β, independent of the probe used for the area-diameter relationship and thus, the range of the particles used to calculate that relationship, and independently of the parameters (D_{max} or D_{eq}) of 2D images used to classified the particles to build up the PSD.

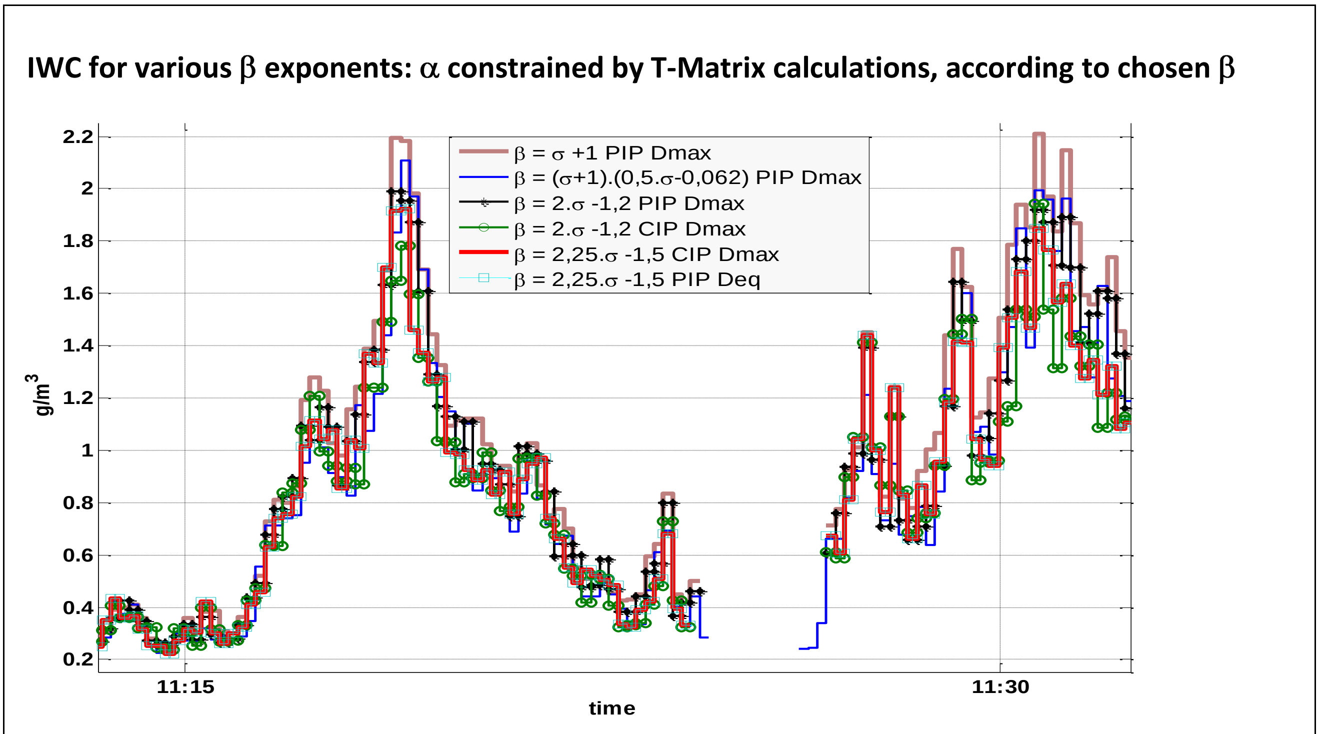

Figure II-18: TWC calculations for 6 different parameterizations of the exponent of the mass-diameter relationship. All laws have been constrained by the radar reflectivity.

Subsequently the above described strategy of computing IWC constrained by measured radar reflectivities is compared with two other methods: Firstly, the method described by Lawson and Baker (2006), and secondly a constant mass-diameter law as proposed by Heymsfield (2010).

The Baker and Lawson method calculates first the geometric parameter $X = 2 \cdot A \cdot W(L+W) \ / P$, from which then the ice water content IWC is derived: $IWC = \left[0.135 \cdot \sum_i X_i^{0.793}\right] / V$, where A is crystal area, W is crystal width, L is crystal length, P the perimeter , and V the sampling volume.

The constant mass-diameter relationship in the immediate vicinity of deep convection as proposed by Heymsfield (2010, personal communication 2012) is of the following type: $m = 0,010 \cdot D_{\max}^{2.1}$.

The results (figure II-19) suggest that the method implemented within Megha-Tropiques is estimating TWC values somewhat below the methods of Baker & Lawson and Heymsfield.

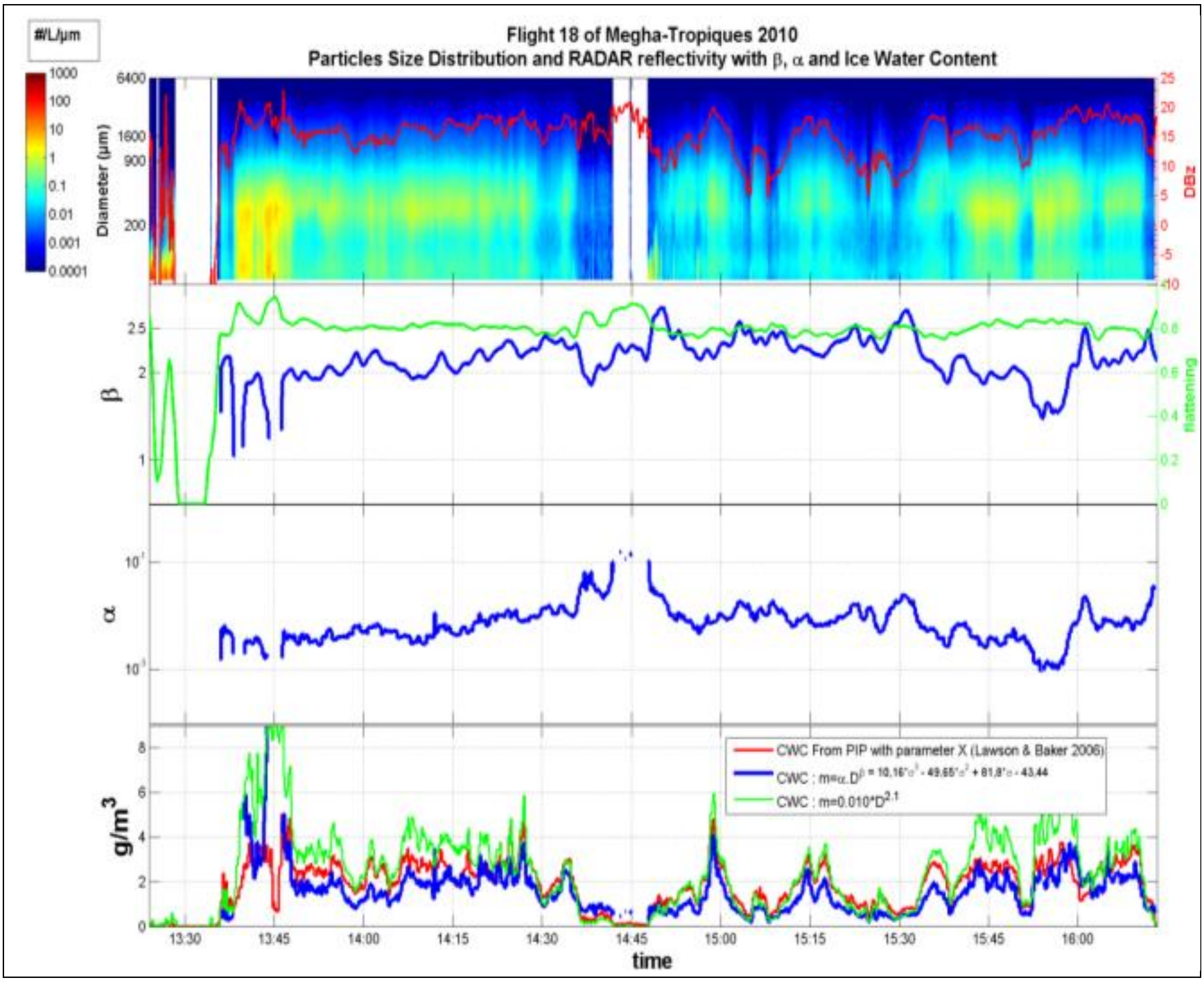

Figure II-19: Time series of PSD contour plot and radar reflectivities, β mass-diameter exponent derived from area-diameter relation, image derived flattening parameter for T-matrix simulations of radar reflectivities, α prefactor constrained while matching simulated and measured reflectivities, and finally IWC calculations comparing Baker & Lawson method and constant mass-diameter law with our method presented here for Megha-Tropiques data.

This is particularly true for largest IWC when the calculated IWC might be more dominated by larger, less dense, and less spherical ice particles (at least for the MT data set). In this case the Heymsfield method (which may be more adapted to the convective cores than to the more stratiform regions of mesoscale convective systems) of a constant mass-diameter relationship is producing larger IWC than the method of calculating m(D) while matching measured RASTA reflectivities. This seems to be consistent with the fact that for largest aggregates (large in maximum dimension) a mass-diameter relationship exponent of 2.1 may be too high, likewise the α prefactor might be overestimated leading to higher IWC as compared to our method. Hence the Heymsfield calculation seems to be an upper limit for IWC.

Regarding the Baker and Lawson approach, it has been found to overestimate the IWC as measured by the CSI bulk IWC probe in tropical cirrus clouds by about 40% (Protat et al. 2011) but there has been no evaluation using observations in stratiform ice clouds to our knowledge. If one trusts our MT IWC estimates, then the Baker & Lawson technique does seem to overestimate IWC as well in stratiform systems.

As mentioned above, particles recorded by the particle imagers were classified, both as a function of their maximum length (D_{max}) and as a function of the equivalent diameter of a disc corresponding to the crystal surface (D_{eq}). The 1Hz composite particle size distribution (PSD) has been derived, combining PSD (in D_{max} or D_{eq}) of individual probes used during each flight. For this study, composite PSD were built for flights 15,17,18,19, 20 of MT1 from the size-restricted individual PSD of 2DS, CIP and PIP. For MT2 the composite PSD for flights 45, 46, 49 and 50 were build from the individual PSD of 2DS and PIP probes.

The averaged composite PSD have been calculated separately for each flight and subsequently averaged over all flights of the same category of cloud systems. Therefore the available microphysical data from F-20 flights have been grouped in three different categories corresponding to different synoptic features as there are: (i) MCS (Mesoscale Convective System) above African continent, (ii) MCS above Indian Ocean, and (iii) isolated convection above the Indian Ocean (figure II-20).

Averaged PSD for the two types of MCS (category (i) and (ii)) are similar in shape, however with higher total concentrations of sub-millimetre crystals and larger sizes of super-millimetre crystals for the continental PSD as compared to the oceanic PSD.

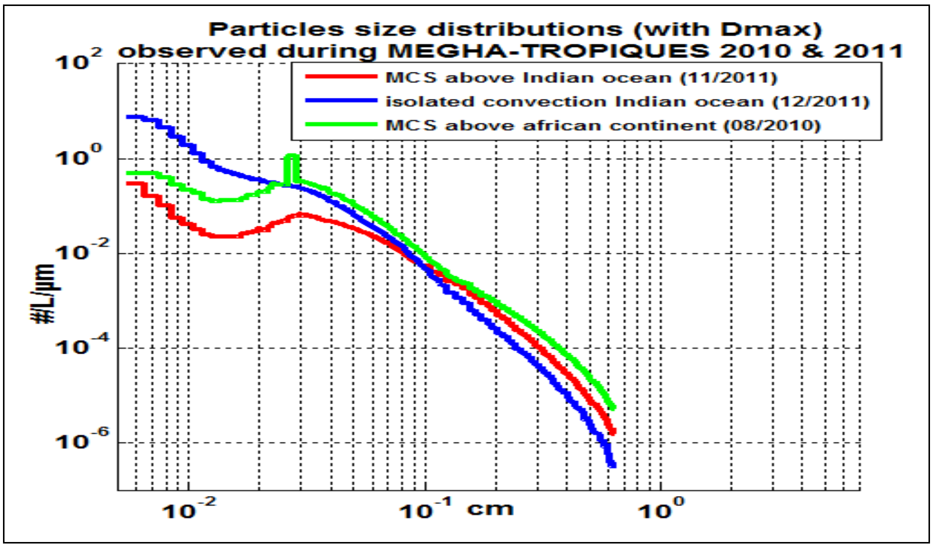

Figure II-20: Trends of particles size distributions as a function of D_{max} of the particles measured during the two measurement campaigns of Megha-Tropiques. Flights included in the category "MCS above African continent" are flight numbers 15, 17, 18, 19, and 20 of MT1. The category "isolated convection above the Indian Ocean" averages PSD from flight numbers 49 and 50 of MT2 (December 2011). Finally flight numbers 45 and 46 are included in the category "MCS above Indian Ocean" (November 2011).

Compared to both MCS type PSD, the averaged PSD of isolated oceanic convection reveals much higher concentrations of smallest ice particles and also significantly smaller sizes of the entire crystal population.

It appears (figure II-21), that the mean mass-diameter relationship deduced by constraining simulated reflectivity from particle size distributions with measured reflectivities from the Doppler radar RASTA (95 GHz), is greater for MCS observed above the African continent ($m=0.015D_{max}^{2.09}$) than for oceanic MCS systems and isolated convection ($m=0.009D_{max}^{1.80}$ and $m=0.0055D_{max}^{1.78}$), respectively. Figures II-21 also illustrate that, on average, super-millimetre particles (with D_{max} beyond 1mm) correspond to a mass fraction of 55% in the continental MCS compared to 67% and 46% in oceanic MCS and isolated convection systems, respectively.

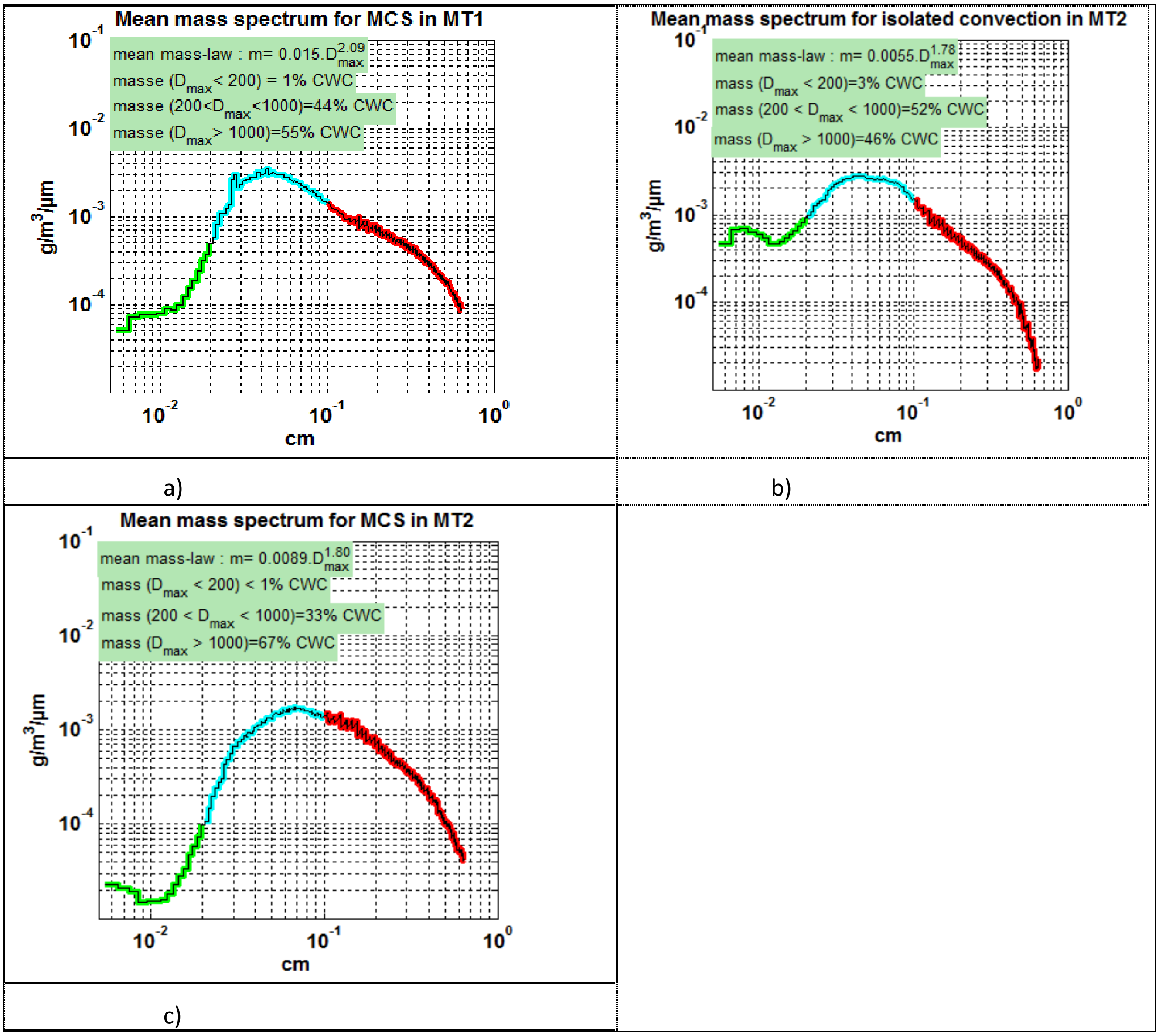

Figure II-21: Mean mass spectrum calculated with the mass-diameter relationships constrained by the reflectivity measured by RASTA and the simulated reflectivity from the composite PSD and area-diameter relationships. The fraction of the mass size distribution of particles with diameters smaller than 200µm is underlined in green, the range between 200µm and 1000µm in blue the super-millimetre particles in red.

In general, the mean density of the cloud particles is larger in continental MCS (MT1) than in oceanic MCS (MT2). Whereas it is not possible to clearly classify the particle shapes in the continental MCS (shapes somewhere between graupel and aggregates), in the oceanic MCS much more pristine (rosettes, columns, sideplanes, etc…) ice can be found.
An important conclusion is that for observed oceanic convection the growth of the cloud particles is much more dominated by vapour diffusion, as compared to the more violent continental convection. Thus, cloud particle aggregation that leads to very large particles in the continental convection is somewhat limited in oceanic convection.

II.3. Synthesis and conclusions of the retrievals of microphysical properties of HighIWC regions using existing airborne in-situ observations

1. The absolute need of a most reliable TWC reference measurement has been demonstrated by both, the A340 and the Megha-Tropiques datasets. This bulk measurement will be provided by the ROBUST probe and in particular the isokinetic evaporator probe (IKP) during the HIWC / HAIC project. The ROBUST probe is still lacking accurate calibration (see A340 dataset) and has to be calibrated absolutely by the use the isokinetic evaporator probe (IKP).
2. Concerning the best suited mass-diameter relationship m(D) to be used for best guess of ice density in HIWC regions, we illustrated that the use of a single mass-size relationship such as that of Brown and Francis (1994) used for the A340 data may not represent accurately the dependence of the mass-size relationship as a function of particle mean diameter and temperature. The presented study for the Megha-Tropiques dataset demonstrates that the mass-diameter relationship is significantly influenced by the temperature. This result is consistent with the observation in Heymsfield et al. (2010) that the use of a single mass-size relationship is not appropriate to represent the variability of ice mass as a function of temperature, growth regime (vapour diffusion plus aggregation and/or riming). More studies need to be performed in order to understand how the area-diameter law varies in natural clouds, and what are the most significant physical parameters controlling the calculation of the mass-diameter law. In general, the mean density of the cloud particles is larger in continental MCS (MT1) than in oceanic MCS (MT2). Whereas it is not possible to clearly classify the particle shapes in the continental MCS (shapes somewhere between graupel and aggregates), in the oceanic MCS much more pristine (rosettes, columns, sideplanes, etc…) ice can be found. An important conclusion is that for observed oceanic convection the growth of the cloud particles is much more dominated by vapour diffusion, as compared to the more violent continental convection showing predominant aggregation and riming processes.
3. A study is actually performed to derive more parameters from each single Airbus nephelometer image, so that we can apply other relationships (for example Lawson and Baker, 2006) and estimate the variability of TWC estimates as a function of different mass-size relationships, as has been performed for imaging probes used during MT. Further geometric parameters in addition o the crystal area and area equivalent diameter are maximum diameter, diameter perpendicular to maximum diameter, and perimeter. Those parameters will be extracted for each individual ice crystal.
4. Concerning the A340 datasets we demonstrated that Airbus nephelometer and ROBUST probe data are correlated, despite a scale factor between those two probes. The two sources of uncertainty are

that (i) the ROBUST efficiency is not yet calibrated for use on individual aircraft and will be a function of aircraft velocity, ice water content IWC, median mass diameter MMD, temperature T, pressure p, etc...), and (ii) the uncertainty in crystal image use for diameter to mass conversion cannot be constrained just with the measured surface of each crystal.

5. The presented T-matrix calculations for IWC retrieval from crystal imagery seems to be very promising. We will conduct further studies of factors influencing the relation between α and β: continental influence, oceanic influence, synoptic conditions, etc… Within the recently collected HYMEX dataset (Megha-Tropiques instrumental setup plus ROBUST probe) we will try a closure of ROBUST TWC with T-matrix retrievals. We will try a very preliminary characterization of the ROBUST probe performance for flight conditions on the Falcon 20.

III. Proposed envelope and encountered glaciated icing conditions during A340 Cayenne and Darwin flights and Megha-Tropiques measurements

III.1. Recall of proposed envelope

NPRM10-10 and NPA 2011-03 propose, among other things, new icing envelopes to cover mixed phase and glaciated icing conditions (figure III-1). This is the CS25 future Appendix P, as provided in NPA 2011-03.

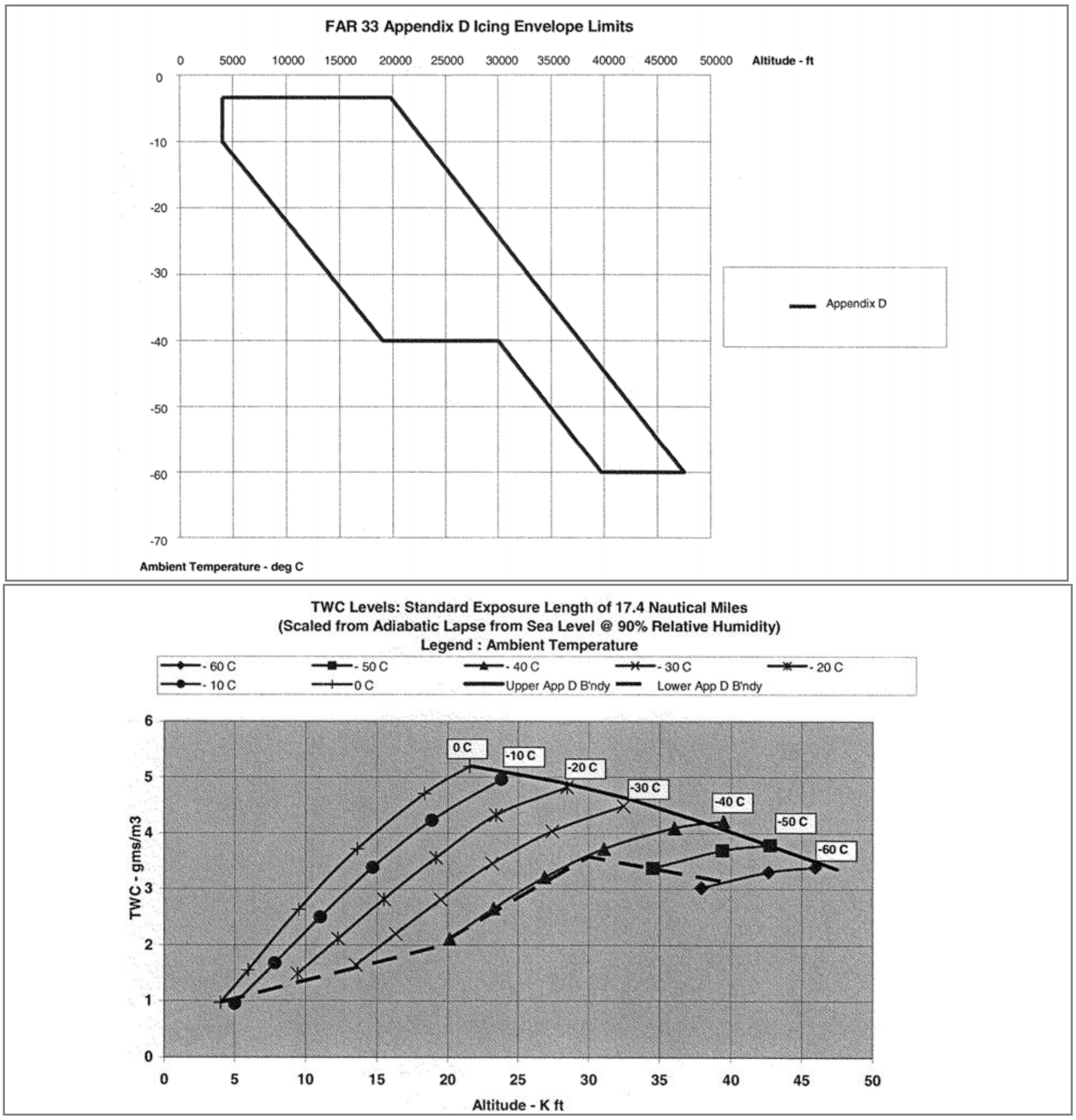

Figure III-1: CS25 future appendix P mixed phase and glaciated icing envelope factor / Extract from NPA 2011-03 – figures 1 (upper) & 2 (lower)

Figure 1 of NPA 2011-03 provides the icing envelope for mixed phase and glaciated icing conditions. For every point of this envelope, the TWC to be considered is provided in figure 2 of NPA 2011-003.

If TWC values are given in the above chart for a standard exposure length of 17.4Nm, other sizes of clouds can be considered by using f factor provided on following graph.

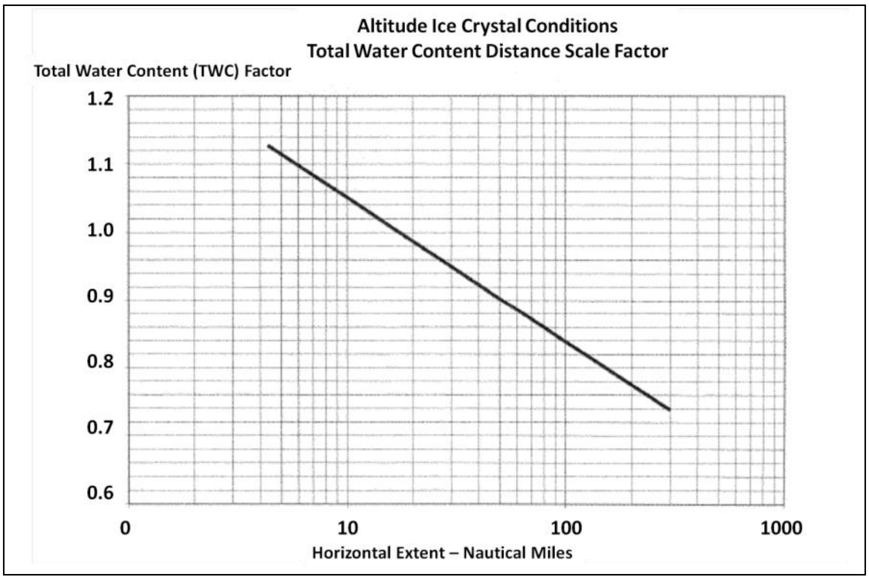

Figure III-2: CS25 future appendix P f factor / Extract from NPA 2011-03 – figure 3

The LWC to consider for liquid part of mixed phase conditions is provided in next table.

Table 1 – Supercooled Liquid Portion of TWC		
Temperature range [°C]	Horizontal cloud length	LWC [g/m³]
0°C to -20°C......................	≤ 50 miles.........................	≤ 1 g/m³............................
0°C to -20°C......................	Indefinite..........................	≤ 0.5 g/m³........................
≤ 20 C................................	....	0...

Table III-1: CS25 future appendix P supercooled liquid portion of TWC.

Ice crystals are various macroscopic crystalline formations, with a basic hexagonal symmetry, which depends on the conditions of temperature and vapour pressure. Their creation is induced by the formation of a crystalline structure on microscopic nuclei or by the freezing of very small supercooled droplets. Ice particles may be in the form of individual ice crystals, aggregates of crystals such as snowflakes, or crystals that have collided with supercooled water droplets to form more dense and spherical particles such as graupel and hail. Ice particles can span a very large size range, from microns to centimetres.

Future regulation considers that ice crystals median mass dimension (MMD) range is 50-200µm (equivalent spherical size) based upon measurements near convective storm cores.

III.2. Proposed envelope and encountered glaciated icing conditions during A340 Cayenne and Darwin flights

A preliminary assessment of the encountered glaciated icing conditions has been performed to compare flight test results with the proposed regulations appendix envelope for mixed phase and glaciated icing conditions.

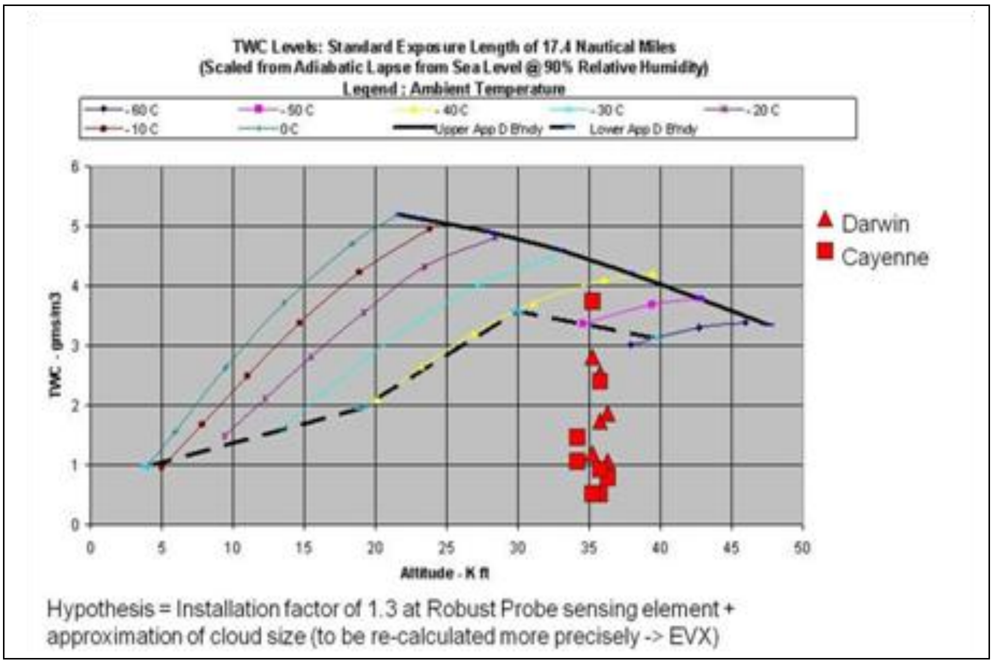

Figure III-3: Airbus Flight Tests Results versus proposed regulations envelope (altitude versus TWC)

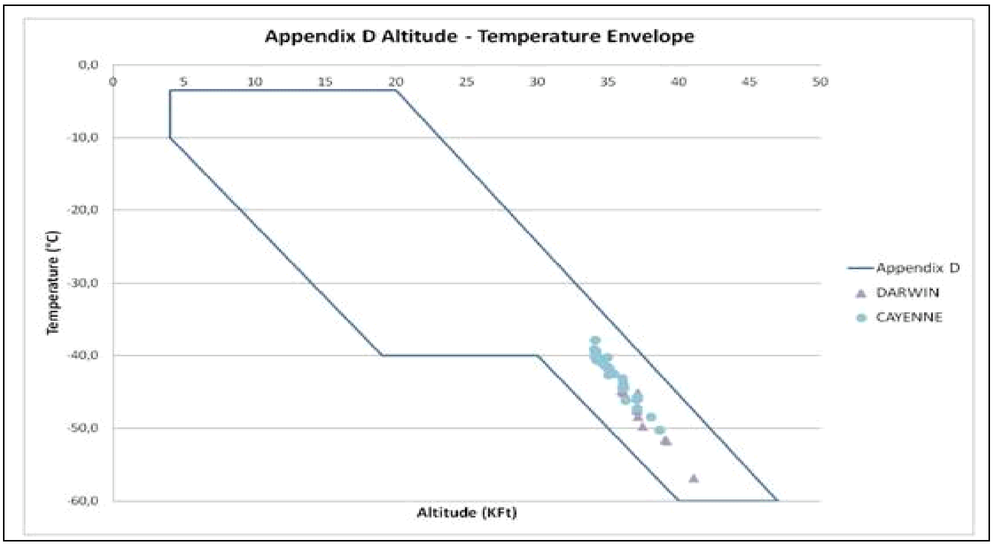

Figure III-4: Aircraft flight test results plotted on proposed regulations envelope (altitude versus temperature)

As a reminder, the preliminary nature of this assessment comes from the fact that the accuracy of the TWC estimates used are still with a largely unknown scaling factor between the two probes (ROBUST and Airbus nephelometer), due to the lack of a reference measurement (which will be provided in HIWC / HAIC by the isokinetic evaporator probe, IKP) and the difficulty in estimating an error bar due to the mass-size relationship, as the theoretical relations for single ice crystal habits available in the literature, and other retrieval techniques relying on ice crystal morphology, such as Baker and Lawson (2006), or particle habit classification, such as Protat et al. (2001), cannot be used because only the median volume diameter has been computed so far from the nephelometer images (the maximum diameter would be needed). This latter point is an ongoing study just launched by Airbus and CNRS-Lamp.

These figures show the Airbus flight test results plotted on the proposed regulations envelope. It illustrates that despite the fact that the encounters were inside the envelope, the TWC was lower than the one specified by future proposed regulations except for one flight test point, considering that temperatures during flight tests where close to -40°C.

III.3. Proposed envelope and encountered glaciated icing conditions during F-20 Megha-Tropiques flights

An assessment of the encountered glaciated icing conditions during Megha-Tropiques has been performed to compare flight test results with the proposed regulations appendix envelope for mixed phase and glaciated icing conditions. These figures show the Megha-Tropiques flight campaign results plotted on the proposed regulations envelope. The TWC values are taken from our T-Matrix calculations (figure III-5 and III-6). It illustrates that despite the fact that the encounters were inside the envelope the corresponding TWC values (17.4 nm averages) did not exceed the proposed envelope.

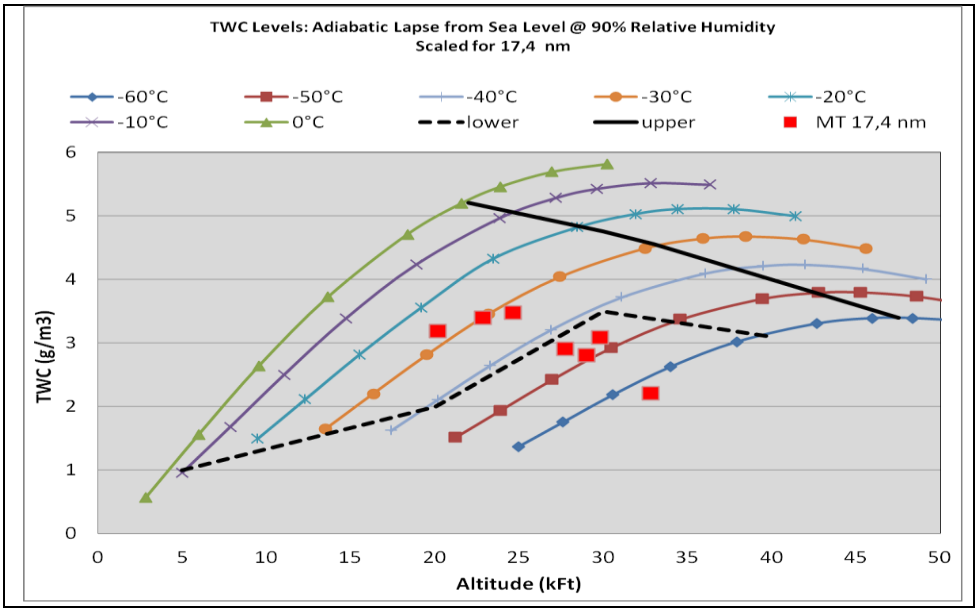

Figure III-5: Megha-Tropiques results versus proposed regulations envelope (altitude versus TWC).

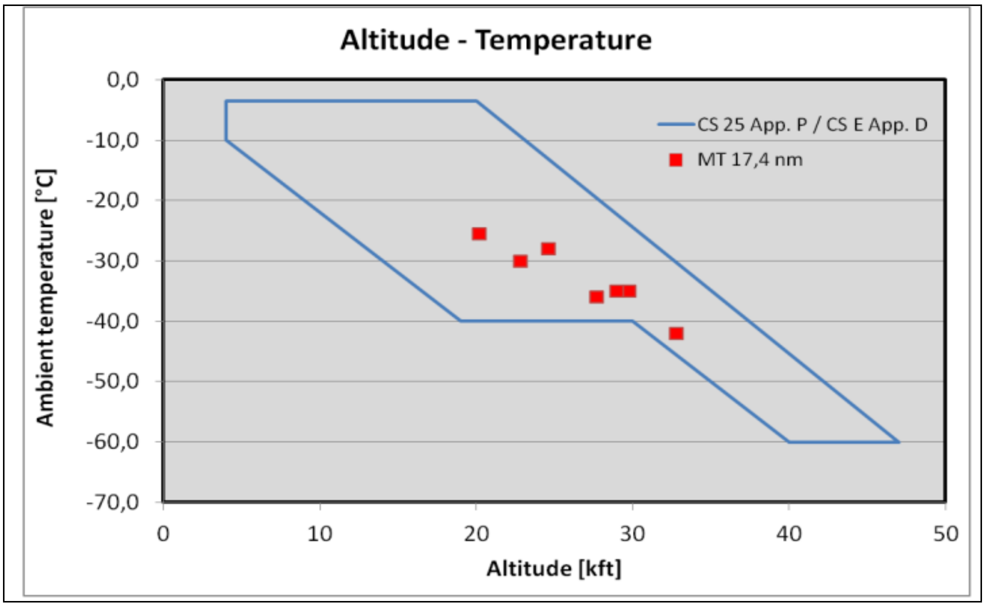

Figure III-6: Megha-Tropiques results versus proposed regulations envelope (altitude versus temperature).

IV. Comparison study between existing in-service events and proposed envelope

IV.1. Engine in-service events

In response to National Transportation Safety Board recommendations A-96-54, A-96-56, and A-96-58, the joint Engine Harmonization Working Group (EHWG) and Power Plant Installation Harmonization Working Group (PPIHWG) was assembled by the Ice Protection Harmonization Working Group (IPHWG) for the purpose of reviewing requirements for engine and engine installation certification under supercooled large drops (SLD) and mixed-phase/glaciated icing conditions.

The EHWG was tasked to review all icing-related engine service difficulty experience and flight test icing-related difficulty experience that may be related to SLD or mixed-phase icing and to determine possible SLD and mixed-phase threats to engine operation. The EHWG initially assessed the extent of engine problems in SLD or mixed-phase/glaciated environments based upon service history provided by the manufacturers participating in the EHWG. Information on engine icing events were compiled into a database with events categorized according to a number of variables, including the nature of problems encountered.

This work is described in the *Technical Compendium from meetings of the Engine Harmonization Working Group* **DOT/FAA/AR-09/13.**

The database of commercial service engine icing events detailed in section 2 of the EHWG technical compendium in the mixed phase/glaciated environment established that the current 14 CFR Part 25 Appendix C icing envelope with supercooled large drops does not cover the range of altitude and ambient temperature established by these events.

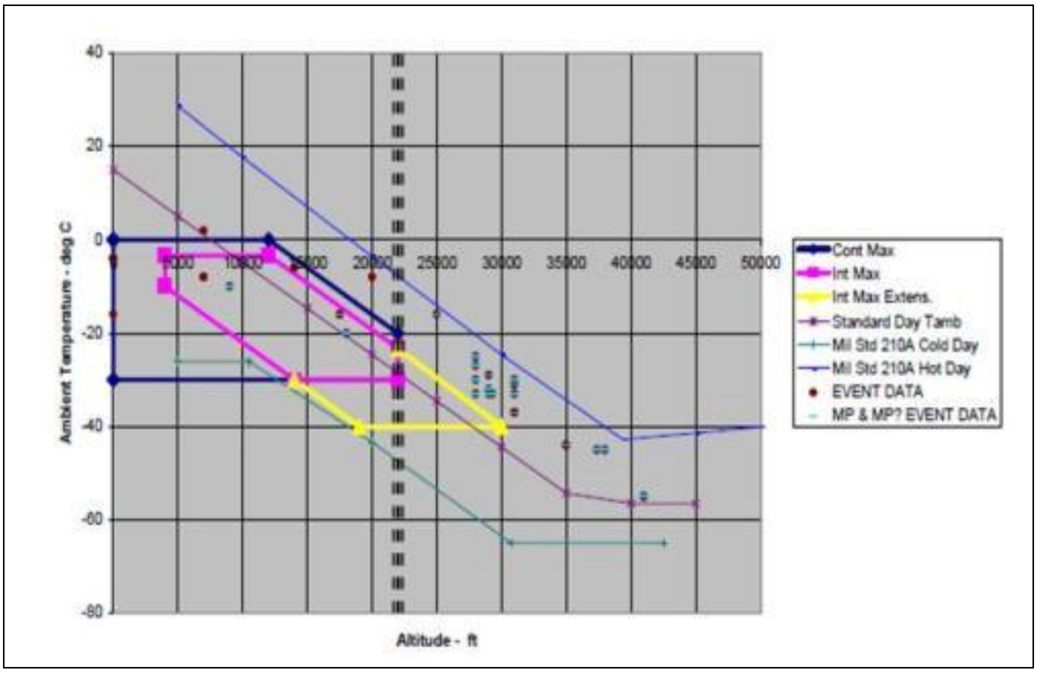

Figure IV-1 : CS25 Appendix C envelope compared to EHWG in-service events database. Extract of Technical Compendium from meetings of the Engine Harmonization Working Group DOT/FAA/AR-09/13.

Analysis made by the EHWG of the international database of engine in-service events led to the recommendations at the basis of proposed envelope.

No engine in-service event had been reported outside of the proposed envelope (altitude – SAT envelope). Due to lack of information available on the concentration of water during the in-service events, no evaluation of proposed envelope for TWC values can be made.

International field campaign should fill this gap and provide the necessary data for rulemaking activities and evaluation of proposed envelopes.

IV.2. Air Data Probes in-service events

Airbus has observed 6 in-service events of Pitot icing in Ice Crystals conditions that were outside of the Appendix D Altitude versus Temperature SAT domain.

These 6 events were in the 2 different regions represented by the 2 ellipses in blue dotted line on figure below. The first region is between the Appendix D upper limit (which is on ISA+20°C) and the ISA+30°C line, the second region is between the Appendix D lower limit and the ISA line.

The figure also presents examples of 3 in-service events of Pitot icing in Ice Crystals conditions that were inside the Appendix D domain.

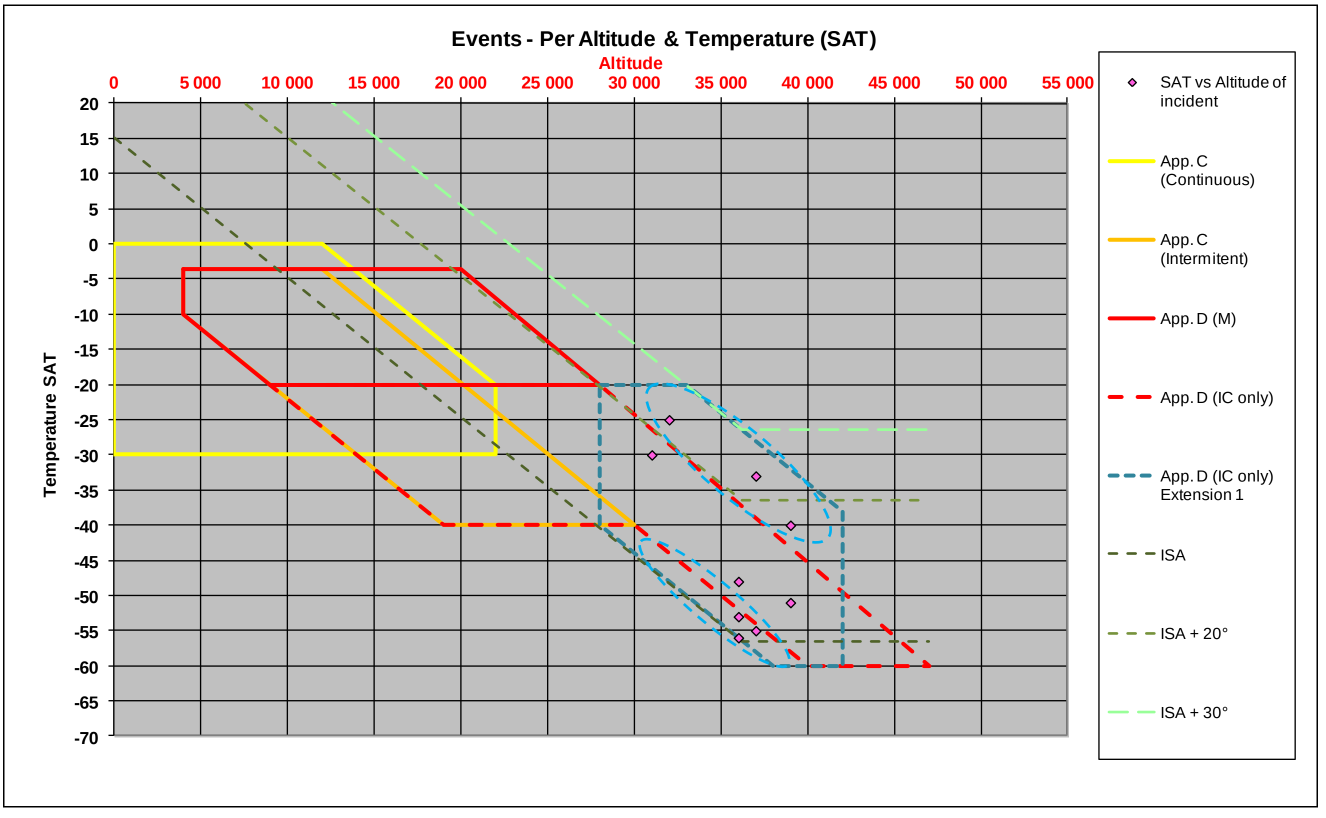

Figure IV-2: Airbus in-service experience in ice crystal conditions.

Thus, based on its experience, Airbus proposes the following extension of the Appendix D Altitude versus Temperature domain for Air Data Probes for ice crystals (**blue dotted line**):

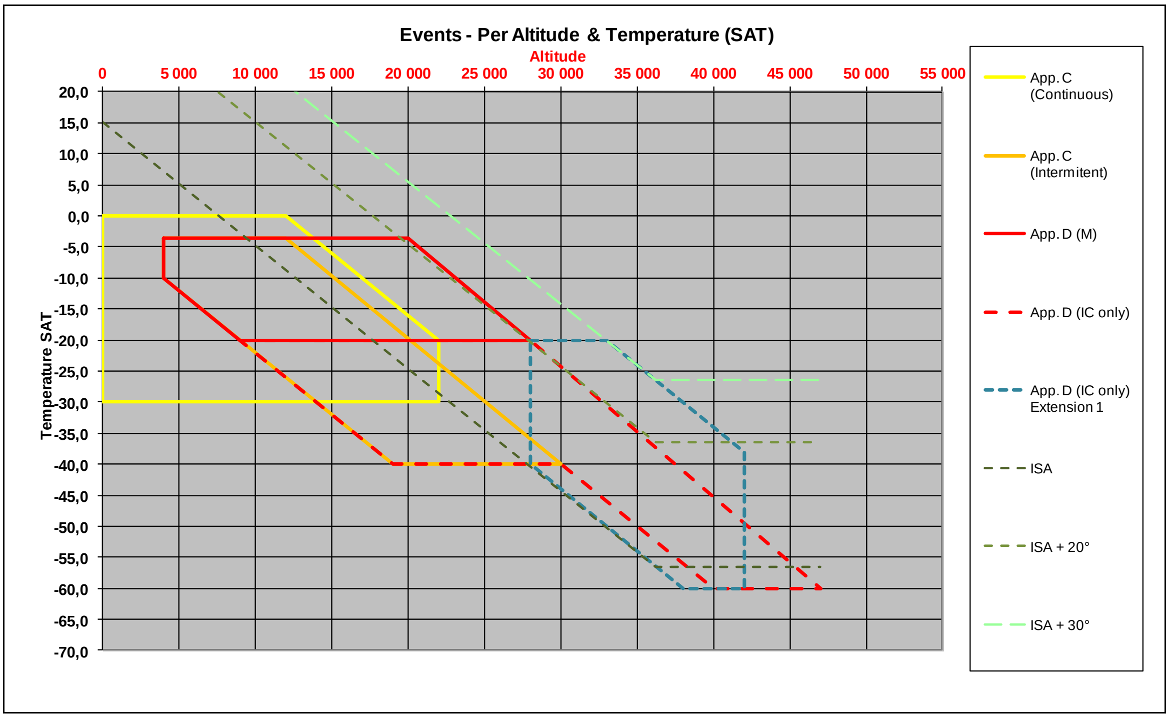

Figure IV-3: Airbus proposal for Alt. versus Temp. Domain for ice crystals

Based on its experience, Airbus proposes the following extension of the Appendix D TWC concentration for Air Data Probes:

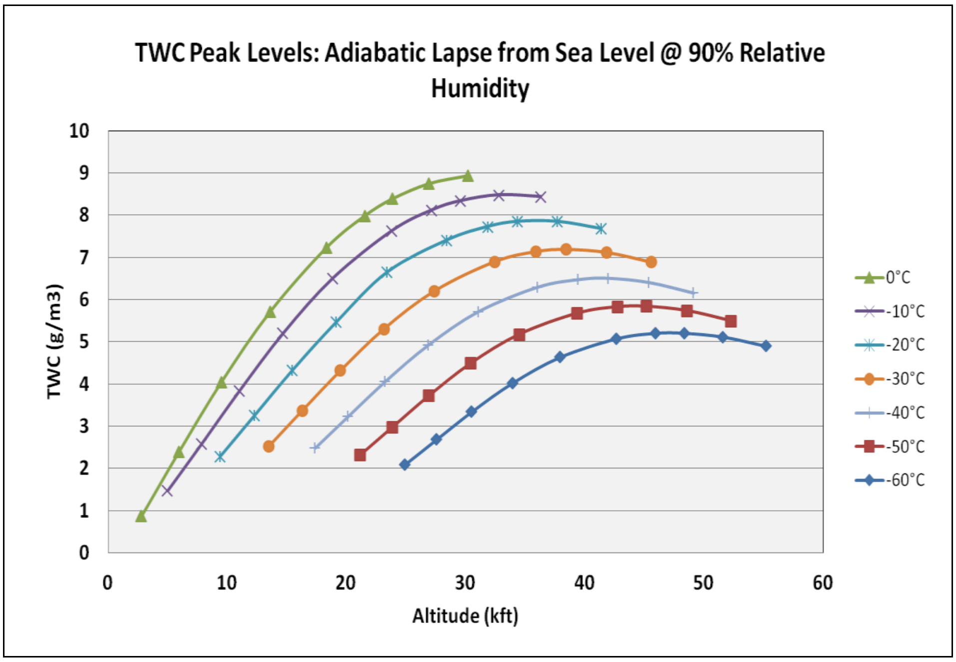

Figure IV-4: Airbus proposal for TWC concentration for ice crystal conditions.

These TWC curves are given in the **FAA document DOT/FAA/AR-09/13, in § 4.5 figure 23**. They correspond to the **max or peak** TWC concentration values that can be encountered in clouds.

The peak values correspond to the 17.4 NM scaled values multiplied by a factor of **1.538** (1/0.65). The peak concentration values are provided on the above figure.

The Appendix D provides TWC concentration values scaled for a **17.4 NM** cloud. Airbus considers that these 17.4 NM scaled values are not adequate for Air Data Probes qualification. For Air Data Probes, Airbus believes that the **peak** TWC concentration values have to be considered instead of the 17.4 NM values.

This position is substantiated by the 3 following rationales:

IV.2.1. Rationale #1: Air Data Probe reaction time (Physics of phenomenon)

Due to its size, a probe has a low reaction time and rapidly freezes (in less than 10 seconds) as soon as the IWC concentration reaches exceeds value above the threshold limit of the probe (no inertia phenomenon).
Airbus conclusion is then that a probe is affected by **peak** values in clouds and not by average values over 17.4 NM.
Airbus observed this phenomenon during both flight tests and wind tunnel tests.
On contrary, an engine needs a certain exposure time (corresponding to a distance in icing conditions i.e. cloud size) before being affected as there is a minimum size for accreted ice block that can lead to engine adverse issues.
The Appendix D was specifically defined to deal with engine icing issues. That is why the Appendix D provides concentration values for a typical horizontal extent of 17.4 NM.

The Appendix D also provides a TWC correction law (TWC factor), allowing correcting the 17.4 NM typical values for horizontal extensions from 300 NM down to 4.5 NM. From this correction law, the correction factor is about 1.13 for the minimum horizontal extent of 4.5 NM provided by the law. But the correction law does not allow accounting horizontal extensions that are shorter than 4.5 NM. For horizontal extensions shorter than 4.5 NM we must use the peak values provided by the FAA document DOT/FAA/AR-09/13, in § 4.5 figure 23.

III.2.2. Rationale #2: Concentrations measured during Airbus flight tests

During flight tests in Guyana, Airbus has been able to freeze a Pitot probe (during flight #1423) in the following conditions:

- Altitude: 35 000 ft
- Temperature SAT: -42°C
- Temperature TAT: -14°C
- Mach: 0.78
- CAS: 260 kt
- TAS: 460 kt
- **IWC upstream concentration (1s measure / peak value): 5.9 g/m^3**
- **IWC upstream concentration (mean value for a 17.4Nm distance): 3.8 g/m^3**

By applying the local overconcentration factor (1.7 factor for A340 fuselage), the IWC local concentration for this flight test event was: **10.1 g/m^3** (5.94 x 1.7).

During wind tunnel tests in NRC, Airbus determined that the freezing concentration limit (concentration level from which the Pitot probe freezes) of the current Airbus Pitot probes in ice crystals was around **10 g/m^3** (more exactly between 8,5 and 12 g/m3 pending on atmospheric conditions (altitude / speed / temperature).

During icing wind tunnel tests, Airbus validated these measures of IWC and reproduced flight tests conditions.

Then, when applying the captation coefficient F1 on the probe and testing to this level (IWC*F1), the following had been observed:

- Pitot probe did not freeze at [3.8*F1] g/m^3
- Pitot probe froze at [5.9*F1] g/m^3 in less than 10 seconds

Consequently, Airbus considers that the peak values are the ones to consider for Air Data probes sizing (the 17.4 Nm value does not lead to the freezing of probe).

IV.2.3. Rationale #3: Concentrations computed for Airbus in-service events

Airbus analyzed 9 examples of in-service Pitot probe icing events. Detailed DFDR data are available for each of these 9 events. For all events, pilots reported poor weather conditions.
Altitude versus Temperature of these 9 events was as follows:

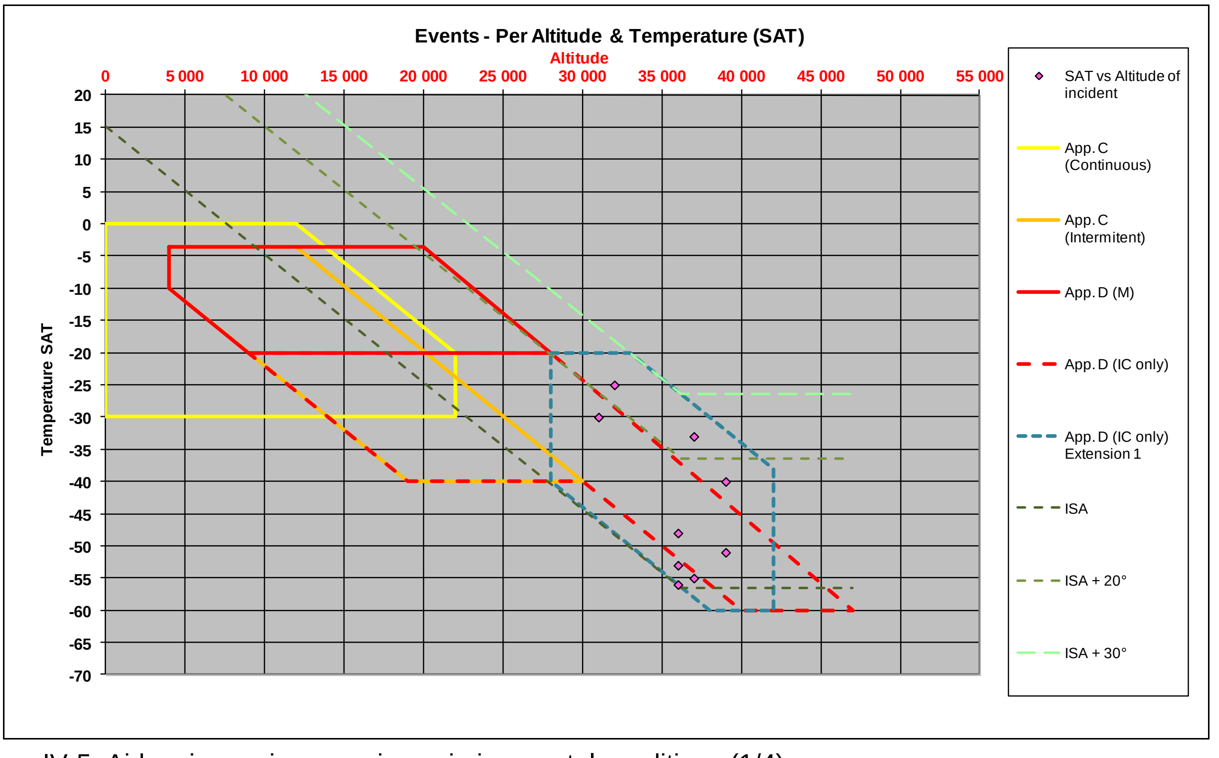

Figure IV-5: Airbus in-service experience in ice crystal conditions (1/4)

If Appendix D scaled at 17.4 NM is considered, the IWC upstream concentrations for each event would have been:

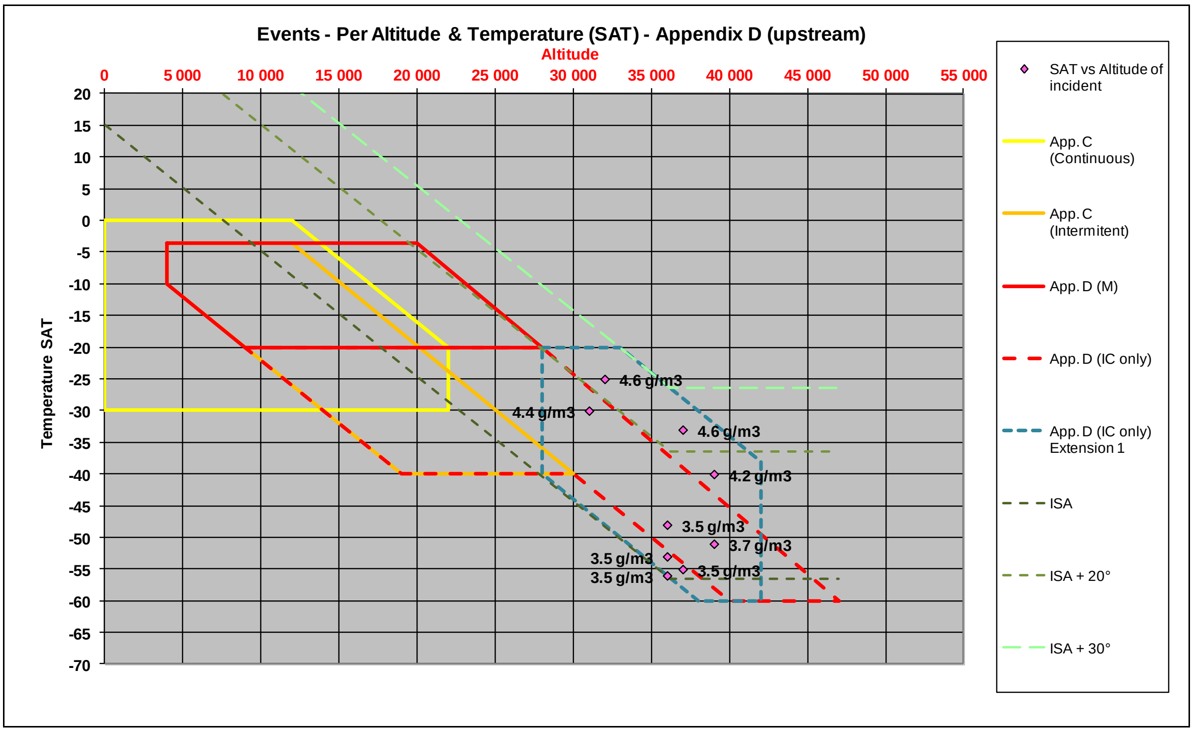

Figure IV-6: Airbus in-service experience in ice crystal conditions (2/4)

When applying the local overconcentration factor (F1) due to fuselage installation on IWC values given by Appendix D for a 17.4Nm (see figure III-3 providing associated figures), all cases are below the threshold of Pitot probes (determined thanks to icing wind tunnel tests), which means that no freezing should have been observed.

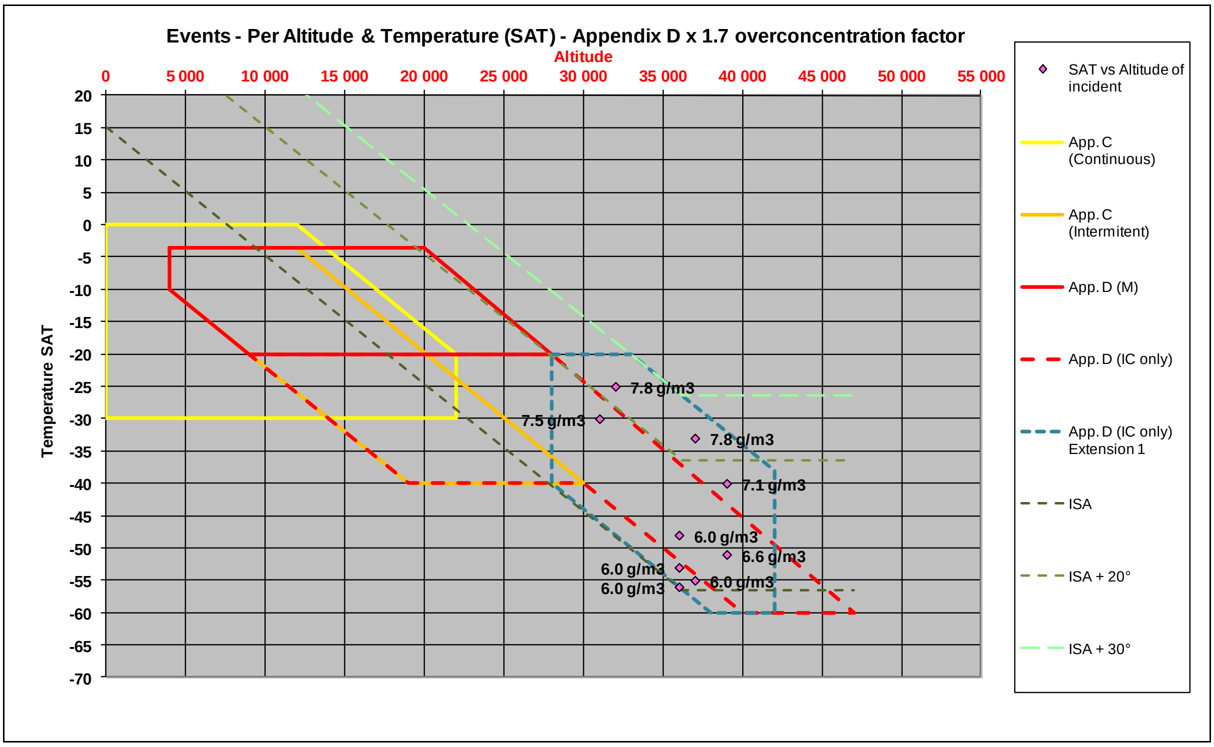

Figure IV-7: Airbus in-service experience in ice crystal conditions (3/4)

Airbus concluded from this analysis that the Appendix D TWC curves for a 17.4 Nm cloud are not relevant for Air Data Probes sizing.

On the contrary, if we use the Appendix peak values for the upstream concentrations, we have the following IWC upstream concentrations for each event:

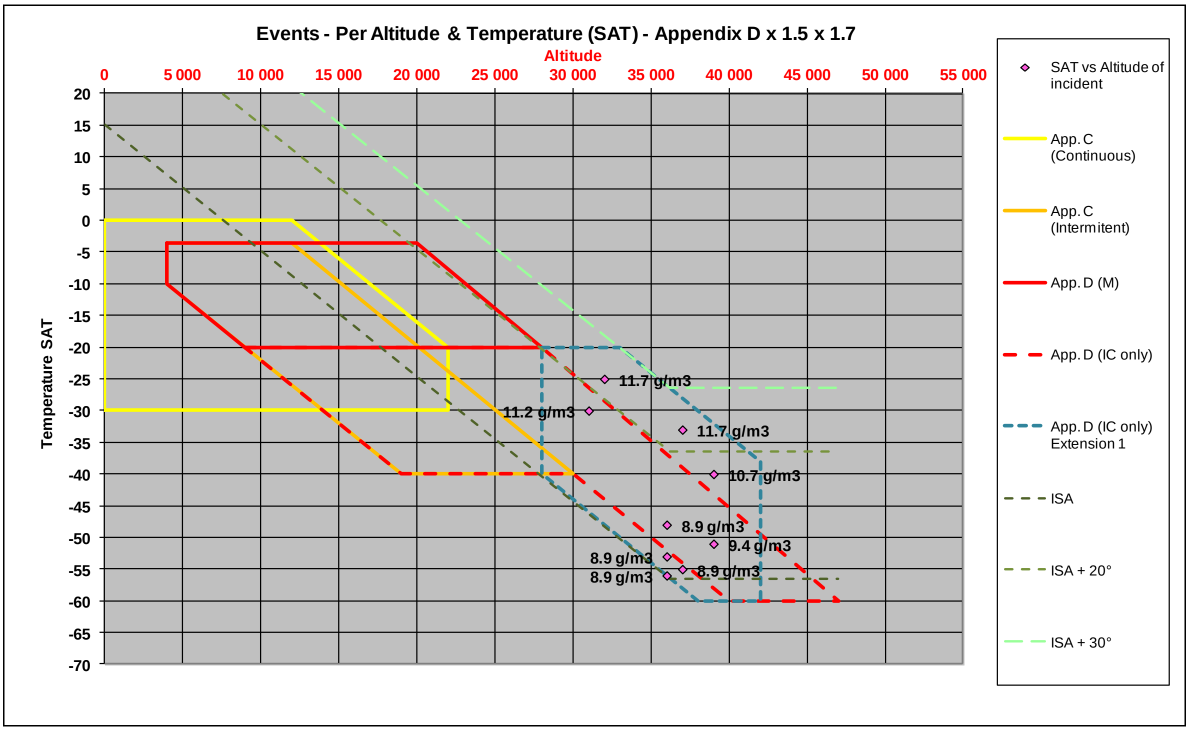

Figure IV-8: Airbus in-service experience in ice crystal conditions (4/4)

When applying the local overconcentration factor (F1) due to fuselage installation on IWC values given by Appendix D peak values, all cases are above the threshold of Pitot probes (determined thanks to icing wind tunnel tests for each plot), which is in accordance with the in-service events.

In conclusion, the Airbus in-service events of Pitot icing are fully consistent and confirm that the upstream concentrations encountered during the events are **fully consistent with the peak** concentration values and are **<u>not</u> consistent with the 17.4 NM scaled** concentration values. (cf. figures above).

Therefore, for sizing and qualification of air data probes, Airbus recommends the extension of proposed envelopes regarding mixed phase and glaciated icing conditions. Nevertheless, to perform a statistical approach of the analysis of proposed envelopes in terms of concentrations, additional results and measurements of the atmosphere are needed.
These results should be provided as part of the international field campaign.

IV.3. Dassault experience

Dassault experienced a Pitot icing event in Ice Crystals conditions that is significantly outside of the Appendix D domain in term of Altitude versus Temperature SAT. This event was in the region represented by the ellipse in blue dotted line. This event was at 45 000 ft, SAT -70°C, Mach 0.8.

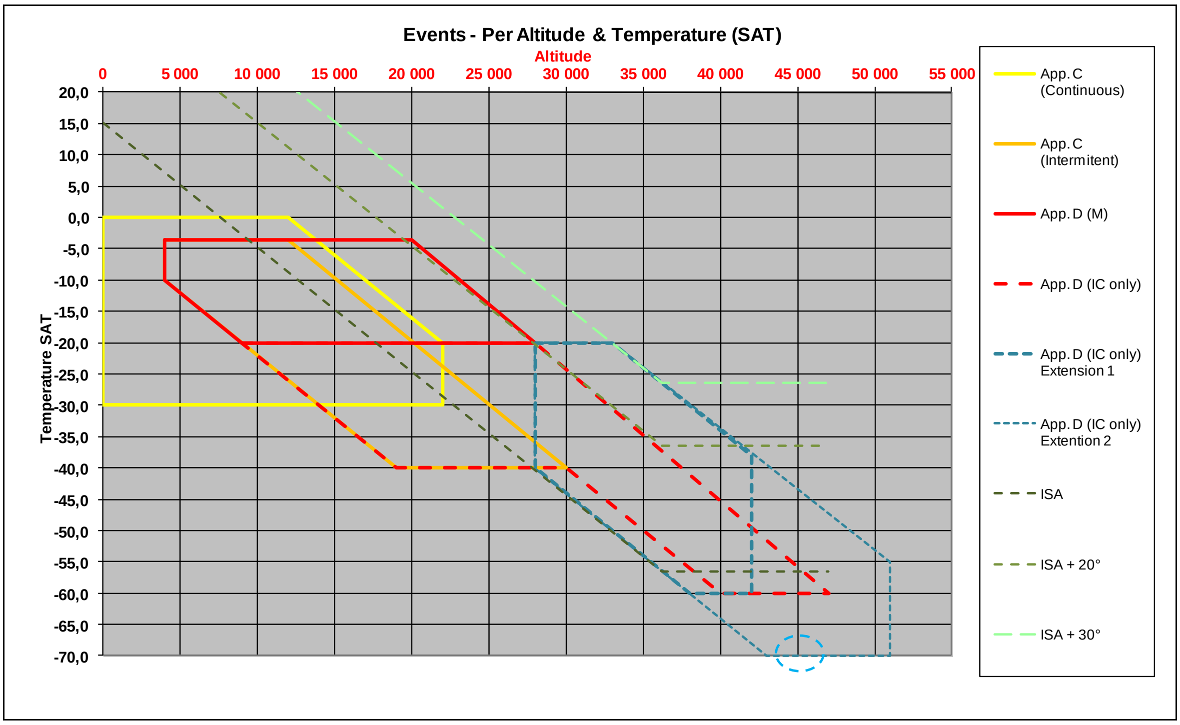

Figure IV-9: Dassault in-service experience in ice crystal conditions

Thus, in the frame of Eurocae WG89 activities, and based on its experience, Dassault proposes the following extension of the Appendix D Altitude vs Temperature domain for Pitot for ice crystals (blue dotted line):

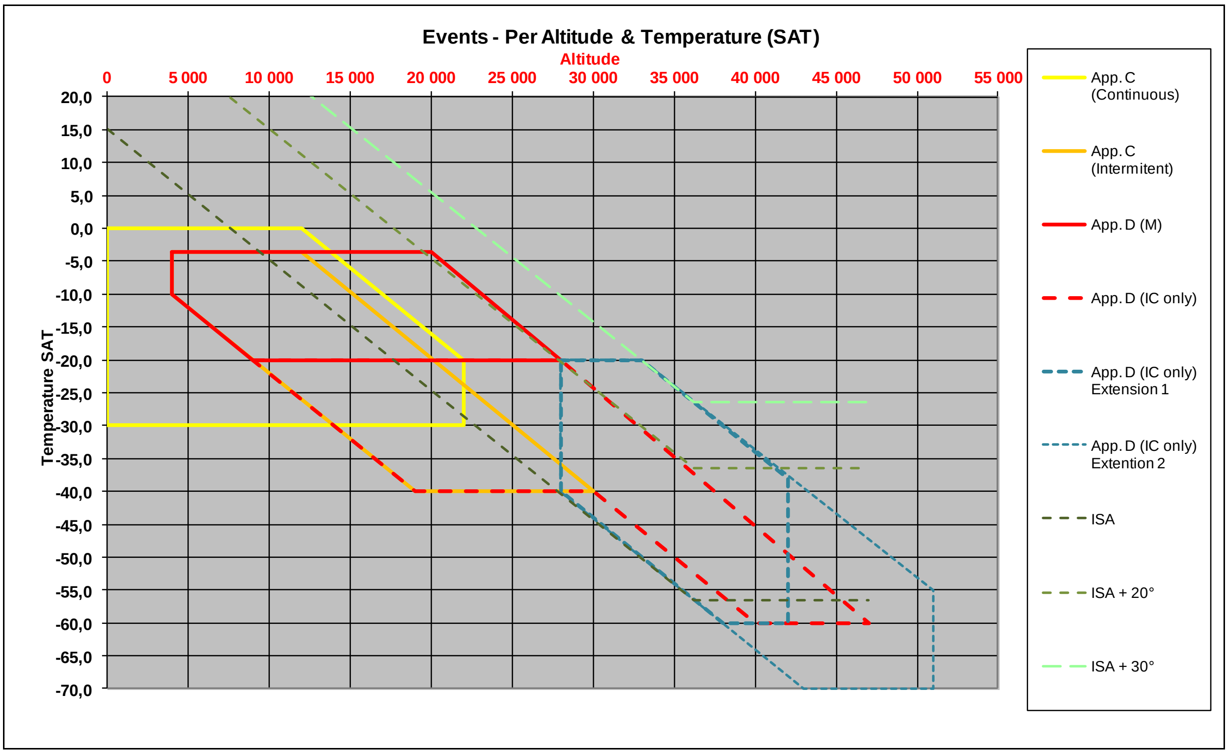

Figure IV-10: Dassault proposal for Alt. vs Temp. domain for ice crystals

IV.4. TWC peak values and encountered glaciated icing conditions during A340 Darwin and Cayenne and F-20 MT1 flights

The cloud non-homogeneity of convective cloud systems is demonstrated by much higher TWC values for much shorter spatial intervals or peak values (figure IV-11 for Airbus data from Darwin and Cayenne campaigns and IV-12 for MT1 data).

For MT1, data are presented intervals of approximately 1.0 Nm (10 s of Falcon 20 data).

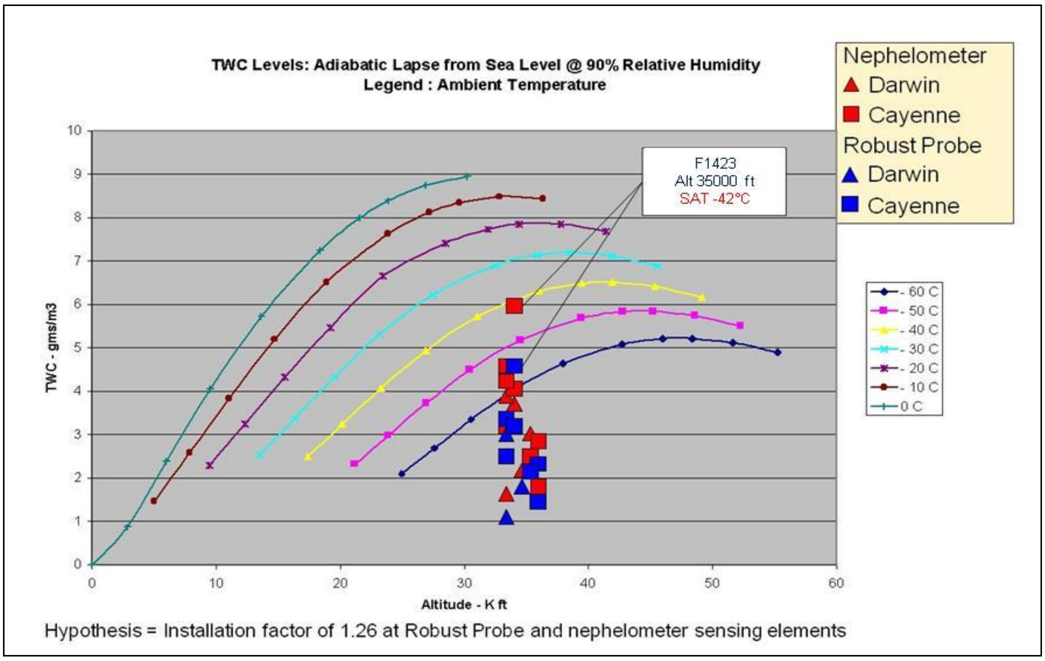

Figure IV-11: Airbus results (TWC peak values) versus proposed regulations envelope (altitude versus TWC).

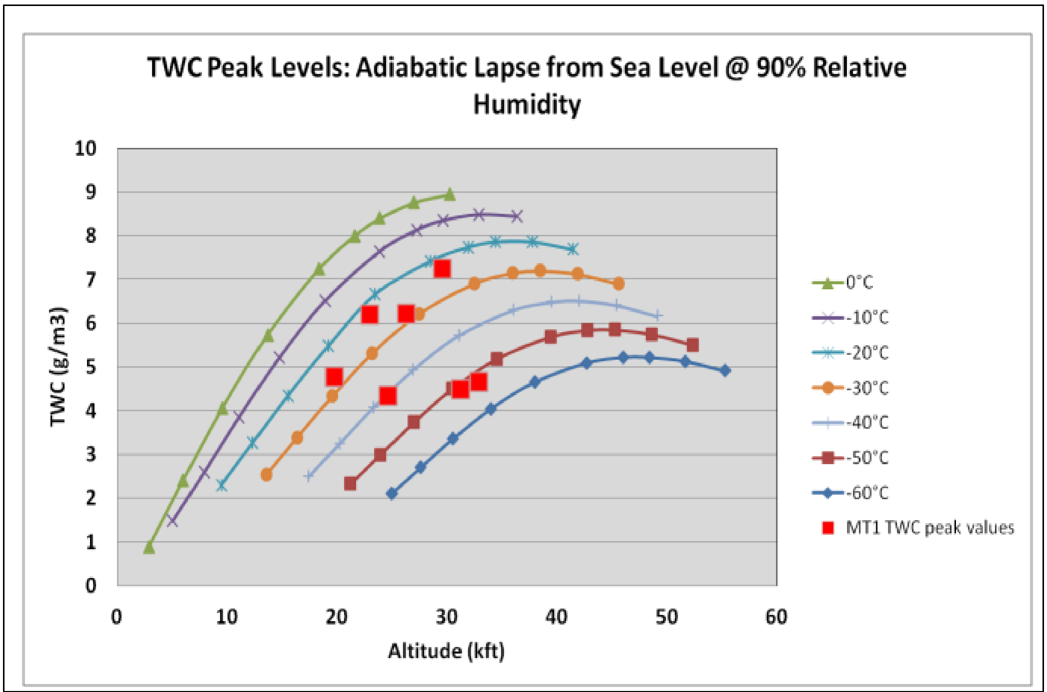

Figure IV-12: Megha-Tropiques results (TWC peak values) versus proposed regulations envelope (altitude versus TWC).

Arguments for presenting peak values (integrated over 10 s for Megha-Tropiques data for statistical reasons) instead of 17.4 Nm values in particular for Air Data probes have been discussed in this chapter and are confirmed by TWC peak values as compared to 17,4 nm average TWC values.

IV.5. Synthesis of comparison study between existing in-service events and proposed envelope

To be able to evaluate proposed envelopes, Airbus has reviewed existing in-service events.
Pending on the type of technology, the reported in-service events are not occurring in the same conditions and thus, two types of in-service events were considered.

IV.5.1. Engine in-service events

Analysis made by the EHWG of the international database of engine in-service events led to the recommendations at the basis of proposed envelope.
No engine in-service event had been reported outside of the proposed envelope (altitude – SAT envelope).
Due to lack of information available on the concentration of water during the in-service events, no evaluation of proposed envelope for TWC values can be made.

IV.5.2. Air Data Probes in-service events

For sizing and qualification of air data probes, Airbus recommends the extension of proposed envelopes regarding mixed phase and glaciated icing conditions:

- ➔ Extension of altitude-temperature envelope as proposed on figure IV-4
- ➔ Use of Peak values instead of 17.4Nm scaled values for TWC

Nevertheless, to perform a statistical approach for the analysis of proposed envelopes in terms of concentrations, additional results and measurements of the atmosphere are needed. International field campaign should fill this gap and provide the necessary data for rulemaking activities and evaluation of proposed envelopes.

V. Recommendation & development plan for research activities and Falcon 20 Flight Tests

Recall from proposal:
The objective of this task is to define preparatory actions for a comprehensive determination of the composition of cloud masses at high altitude (HighIWC) with the appropriate precision to complete and justify on the basis of scientific findings the amendment of the environment proposed in the NPA 2011-03 (Appendix P) defining mixed phase and glaciated icing conditions. In particular, the work focuses on the development of requirements and recommendations for research activities and further flight trial campaigns.
Airbus will coordinate at international level the collaboration between NASA international field campaign and European flight tests. BOM, as subcontractor of LAMP, together with LaMP produce a summary of findings using the Darwin and Cayenne data regarding the microphysical properties of HighIWC regions, and provide further recommendations for the scientific requirements of the Falcon 20 payload. BOM and LaMP provide recommendations for instruments to be used and where to be installed and finally define the Falcon 20 instrumental payload.

Ice crystals are various macroscopic crystalline formations, with a basic hexagonal symmetry, which depends on the conditions of temperature and vapour pressure. They are common in the atmosphere and particularly in high altitude clouds. Their creation is induced by the formation of a crystalline structure on microscopic nuclei or by the freezing of very small supercooled droplets. Ice particles may be in the form of individual ice crystals, aggregates of crystals such as snowflakes, or crystals that have collided with supercooled water droplets to form more dense and spherical particles such as graupel and hail. Ice particles can span a very large size range, from microns to centimetres.
The challenges for the High-IWC instrumental payload on the Falcon 20 are:

- To increase of maximum bulk IWC measurement capability far beyond 2-3 g/m^3 of current reference instruments (CVI & Nevzorov probes).
- To facilitate the most precise quantitative measurement of small ice particle properties (well below 100µm): size dependent crystal number and mass.
- To discriminate the phase of smaller cloud particles: crystals, supercooled droplets.
- To avoid possible small ice crystal contamination on spectrometer data due to ice particle shattering, thus using anti-shattering tips, inter-arrival time measurement & post processing.
- To select a series of instruments in order cover the entire range of expected cloud particle sizes and bulk TWC!

V.1. State of the art instruments for ice phase microphysics

The current state of the art instruments (figure V-1) for cloud glaciated particle size and shape determination as well as bulk TWC measurements are mainly based on the three principles of:

1. Optical spectrometers: Diffusion of light single particles (to determine the size of assumed spherical particles of known refractive index)
2. Particle imagers: Non-intrusive imaging (of a 2D cross section of a 3D particle) to derive concentrations in number and surface size distributions and to estimate volume and mass size distributions.
3. Bulk TWC & IWC devices: Phase change of particles (in order to measure the bulk mass of condensed water).

Numerous instruments are available within research laboratories (particularly CNRS-LaMP and also European partners within HAIC). Nevertheless, serious gaps associated with instrumental measurement uncertainties and limitations remain and need to be overcome. First, the total number of ice crystals can be overestimated due to ice crystal shattering on the inlets and arms of optical spectrometers (Korolev et al., 2005). Cloud lifetimes are sensitive to the sedimentation velocity of the ice crystals as are the rates of aggregation and riming that depend on the relative fall velocities (Heymsfield et al., 2003) of ice crystals and supercooled water droplets. The measurement of the size distribution of ice crystals is complicated by a number of factors, not the least of which is the lack of a universally accepted definition of size when referring to non-spherical particles. Number concentrations of particles smaller than at least 50 µm, derived from classical optical array probes OAPs (of often 25 µm of pixel size) are uncertain by factors of two or three, due to the operating principles, which limits the determination of sample volume using this imaging technique.

Although advances in high speed electronics have led to the development of higher resolved (10 µm pixel for 2D-S) OAPs like the 2D-S (Lawson et al., 2006) that can measure a more representative particle sample at high airspeeds, OAPs still suffer from contamination by fragments of ice crystals that shatter on the extended arms, or even on aircraft surfaces ahead of the probes depending on measurement location. The issue of ice shattering as a source of measurement contamination remains a major concern when interpreting measurements from any particle spectrometers mounted on aircraft. A strong general requirement then is to mount cloud probes rather on under wing stations than on the aircraft fuselage. The cloud droplet probe (CDP) has a design that greatly reduces the influence of ice shattering (Lance et al.,2010) and new tips have been designed for particle probes that also have been shown clearly to greatly reduce the production of ice fragments from shattering (Korolev et al., 2011) . Software techniques related to elimination of closely spaced particles, assumed to result from shattering, have also been proposed, although not yet rigorously evaluated.

Determination of glaciation rates and ice fractions in mixed phase clouds requires the means to identify liquid droplets separately from ice crystals. This can be accomplished using optical array probes when enough pixels are shadowed to determine the particle shape. Determining the phase of cloud particles smaller than about 100 µm, however, is more challenging and only recently has the introduction of the Small Ice Detector (SID) and Cloud Particle Spectrometer with Depolarization (CPSD) provided the possibility to separate liquid from ice particles, on an individual particle basis. The CPSD measures the amount by which a cloud particle rotates the polarization of incident light. Water droplets cause very little rotation whereas ice crystals will rotate the incident light proportional to the complexity of their morphology. Even nearly spherical frozen water droplets will depolarize the light more than water droplets.

To summarize, the main measurement challenges related to the HIWC-HAIC project are related to the capability of measuring small ice particle properties (<100µm), avoiding shattering (modified probe tips) and/or removing (filtering) shattered/splashed particles, discriminating phases of particles (solid/liquid), and enhancing total bulk IWC measurements of high IWC on aircraft and a better characterisation of the collection efficiency of probes. The quality of the images, and hence the accuracy of the data, significantly depend on the depth-of- field effect. Possible sources of error caused by the depth-of-field effect are related to the particle boundaries definition, particles that are out of focus, and the dependency of the depth-of-field on particle size. This effect is also known to bias the counting of the particles towards the larger size images. A variety of optical probes has been used to date and has served the scientific community well.

Emerging technologies may introduce new imaging instruments and measurement approaches, including improvements in holography, faster electronics, and depolarisation measurements that can separate water

from ice on an individual particle basis. In addition to imaging probes, the international project will characterise and use the phase change of particles probes (ice water content measurement).
Finally, the selected probes for the HAIC first flight tests campaign will also include highly sophisticated cloud radar, capable of measuring the Doppler velocity and reflectivity of small ice crystals. Beyond the state of the art, the performed work to produce the presented deliverable started to identify instrumental needs and improve the performances of existing/emerging technologies to allow the most appropriate instrument configuration to be chosen for flight tests measurements.

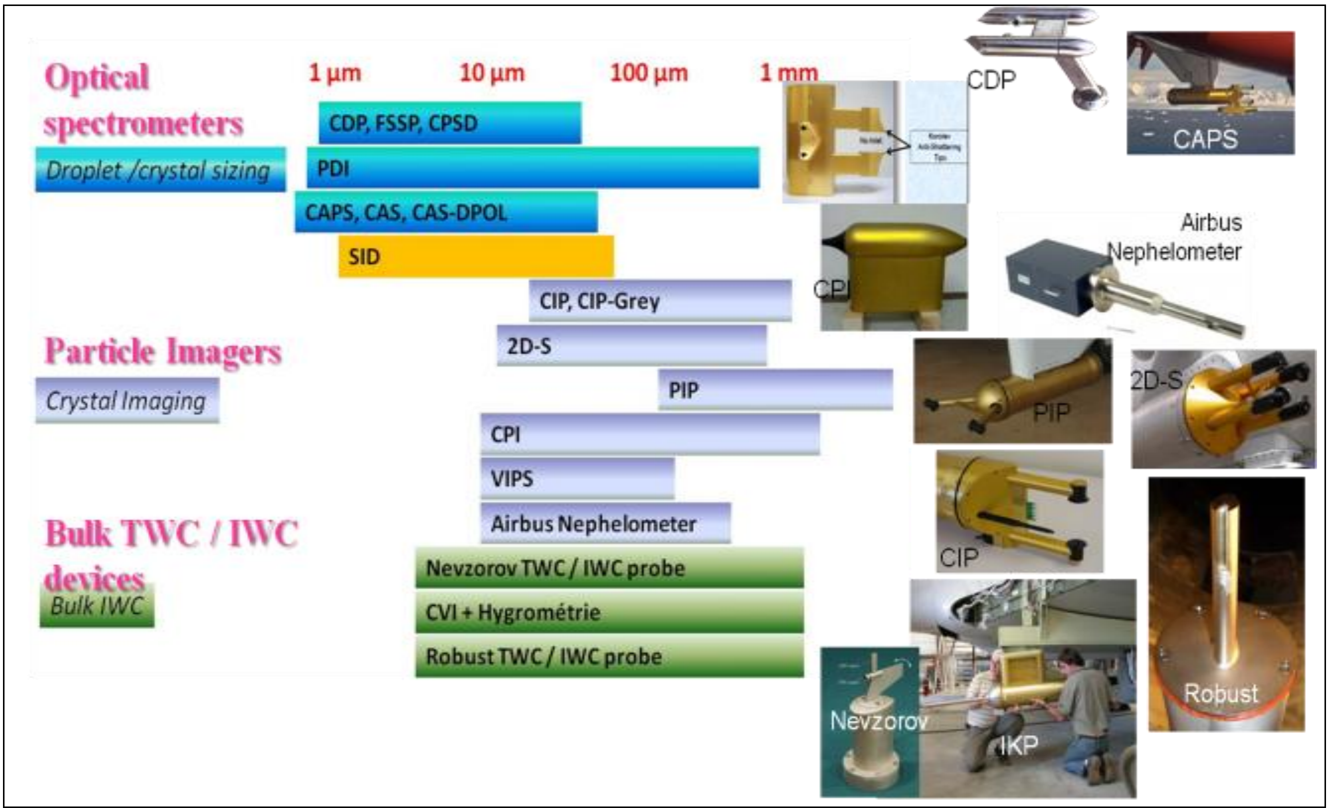

Figure V-1: Multiple instruments to cover complete range from 1µm to several mm. Task: Choose most reliable set of actual/future instruments combining "Optical spectrometers + 2D crystal imagers + bulk TWC/IWC devices" for multiple IWC retrievals using various methods!

V.2. G-II instrumentation as defined by NASA and partners for HIWC project

The European part of the High Ice Water Content project (HAIC + EASA HighIWC) contributes to a collaborative international research project, the HIWC Study, which aims at collecting a data set to characterise the microphysical properties of convective clouds. This project is led by NASA with the contribution of the Federal Aviation Authority (FAA), Transport Canada, the Boeing Company, Airbus and Environment Canada. An international field experiment out of Darwin is now planned in January-March 2014. The main HIWC aircraft, a Gulfstream G-II, will be highly instrumented for in situ cloud microphysics. Measurements will focus on the in situ characterisation of high HIWC regions and the provision of 99th percentile total water content statistics as a function of distance to the convective cores.
HAIC + HighIWC will join this international effort by bringing the French Falcon 20 research aircraft to Darwin equipped with (i) active remote sensing measurements (multi-beam 95GHz Doppler cloud radar and lidar), providing 3D high-resolution characterisation of the dynamical and microphysical properties of ice

clouds which surround the G-II in situ observations and (ii) a state-of-the-art in situ microphysics package while flying at an additional flight level to G-II one.
In particular, the EASA-HighIWC project contributes to the HIWC / HAIC study in securing the preparation of the most appropriate instrumental payload for the French Falcon 20.
In the past, ice particles were thought to have no impact on airframe and engine since they bounce off cold surfaces of aircraft or engines and do not result in any accretion. Information gathered since the 1990's on over 100 weather-related engine power loss events has permitted the Scientific and Regulatory community to conclude that aircraft flying in areas of high Ice Water Content (IWC) are subject to weather-induced incidents and to propose new regulations.
Ice particles are mainly encountered in high levels of atmosphere (above the freezing level estimated at ~20000 ft for a standard atmosphere), in deep convective complexes (anvils of thunderstorms, tropical storms, etc.). Convective weather is caused by deep lifting and condensation of air in an unstable atmosphere, resulting in one or more of the following: deep cloud and large anvil regions, areas of strong wind shear and turbulence, lightning, heavy precipitation and hail and high water contents. In high altitude (low temperature), these high TWC areas are made exclusively of ice (glaciated icing conditions). An extension of certification icing envelope (Appendix D and P) had been proposed to cover this icing threat, based on literature survey and calculations, as no accurate and reliable characterisation of these conditions is available.
The international field experiment HIWC-HAIC-EASA HighIWC project is dedicated to these particular icing conditions. In anticipation of regulation changes according to mixed phase and glaciated icing conditions, HAIC will provide Acceptable Means of Compliance (numerical and test capabilities) and appropriate ice particle detection/awareness technologies to the European Aeronautical industry for on-board use by commercial aircraft in order to enhance safety when the aircraft is flying in such weather conditions.
This HIWC-HAIC-EASA HighIWC experiment will provide the first modern extensive data set of the core areas of tropical oceanic deep convection and less vigorous tropical continental convection and as such will be a unique resource for fundamental research, new industrial developments of detection and/or awareness technologies and for the regulation makers to update the icing envelope for glaciated conditions (Appendix D and P).
The main HIWC aircraft (G-II) will particularly be instrumented with in-situ cloud microphysics instruments and focus on the in-situ characterization of high IWC regions (figure V-2).

In more detail the G-II will be equipped with the following under wing instruments:

(i) Meteorology: AIMMS-20
(ii) Aerosol: PCASP
(iii) Remote cloud sensing: Ka Band Radar
(iv) Bulk microphysics: Hot Wire Boom, Isokinetic Probe, Robust Probe, Rosemount Ice Detector
(v) Cloud in situ spectrometers: FSSP-100, CDP (N.B.: the CDP is the successor probe of the FSSP-100, thus probes are redundant)
(vi) Cloud particle imagers : 2D-S, CIP, 2D-C, CPI, 2D-P (N.B.: the CIP is the successor probe of the 2D-C probe, thus probes are redundant; 2D-S provides higher resolution measurements as compared to the CIP in the same particle size range; The 2D-P is an old probe version for imaging the super-millimetre hydrometeors.
(vii) Cloud optical properties: Extinction Probe

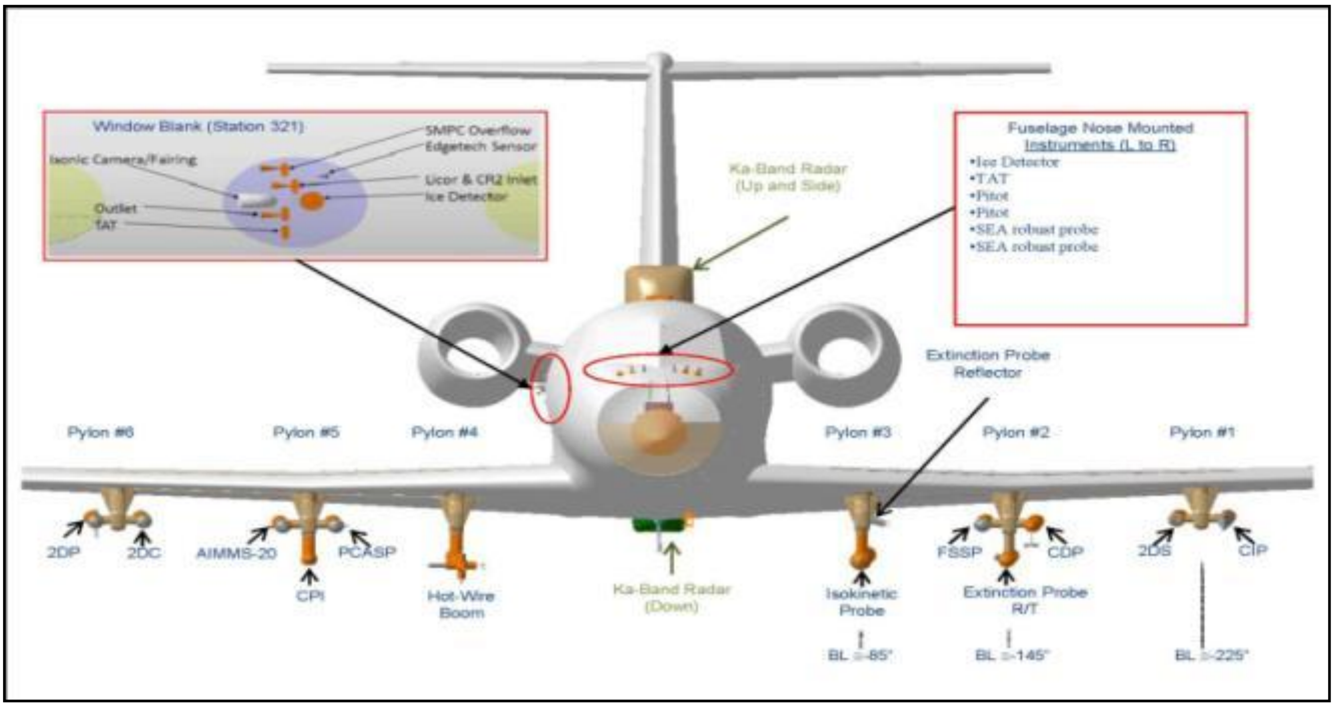

Figure V-2: Planned G-II instrumental payload for the Darwin campaign

V.3. Recommendations for F-20 microphysics instrumentation

The objective within this task is to provide recommendations in order to define the most adequate instrumental payload for the F-20 to fully meet the objectives of the HIWC / HAIC study with measurement campaign performed out of Darwin. It will be particularly challenging to choose the best instrumental configuration, knowing that the F-20 is limited to only 4 under wing stations for microphysical instrumentation.

The following recommendations are being discussed/evaluated as part of the HAIC project:

1. Use of one in situ probe measuring beyond crystal sizes of 1 mm. Up to 50% of ice crystal mass (average value) was found beyond 1 mm for continental tropical convection (Megha-Tropiques I, 2010 West Africa) and 60 % of ice crystal mass beyond 1 mm for oceanic convection (Megha-Tropiques II, 2011 Indian Ocean). The precipitation imaging probe **PIP** (CNRS) is capable of sizing crystals up to 6.4 mm (at 100 µm pixel resolution, twice the resolution of the legacy 2D-P probe), the **HSI** (high speed imager, under development) is sizing up to 2.5 mm, and the **AIRBUS nephelometer** probe up to roughly 2 mm. However, the more the ice particle is at the upper size limit of a corresponding probe the higher the probability of truncated images.
2. Use of highest resolution array probes such as the 2D-Stereo or **2D-S** probe (CNRS-LaMP) or the high speed imager **HSI** from the CIRA (Centro Italiano Ricerche Aerospaziali) laboratory, partner of the European HAIC project. The 2D-S has a pixel resolution of 10 µm as compared to standard pixel resolution of 25 µm for comparable cloud imaging probes **CIP** (new probe, SAFIRE) and **2D-C** (older CIP probe, CNRS-LaMP). An alternative probe is the high speed imaging probe HSI measuring up to 2.5 mm. First tests of the new probe are planned for autumn 2012 in the CIRA (Italy) icing wind tunnel.

3. The need for reliable high condensed TWC (particularly IWC) measurements on the Falcon 20 led to the acquisition of the **ROBUST probe**, measuring bulk condensed TWC up to 10 g/m^3. For best probe performance, a probe under the Falcon 20 wing is preferred, to avoid installation issues.
4. Discrimination of phases of particles (solid/liquid): **Nevzorov** probe, **RICE** (Rosemount Ice detector) probe, cloud particle spectrometer probe with depolarization **CPSD**.
5. Measurement of small ice particle properties (<100µm, if possible): **CPSD**, **CPI** (cloud particle imager), **2D-S** (2 dimensional stereo probe), **HSI** (high speed imager).
6. Avoidance of possible small ice crystals contamination on spectrometer data due to ice particle shattering. Reduction of the possible artefacts created by particle breakups and bouncing off surfaces ahead of the instrumentation sample volume: new 2D-S probe tips, CIP (cloud imaging probe) Korolev tips, CDP anti-shattering tips, CPSD equipped with **Korolev** tips**.**
7. Inter-arrival time analysis: precise arrival time measurements of individual particles performed by data acquisition systems of majority of probes CDP, CPSD, 2D-S, CIP, PIP, HSI, etc…
8. Enhancement of IWC measurements (Total amount!). Only 4 under-wing pods available for best instrumental configuration: Robust probe measures up to 10 g/m3 and even beyond since the ROBUST probe efficiency should be below 1.
9. No single instrument covers the range from 1µm to several mm. A selection of adequate instrumentation will be deployed to cover the range for ice crystals measurement: 1-50 µm: CDP, CPSD; 10-1500 µm: CPI, 2D-S, CIP, HSI; 500-6000 mm: PIP (precipitation imaging probe).
10. Swapping payload should be possible during the campaign: spare probes: SPP-100 for CDP, HSI for 2D-S, CPI for CPSD, additional available probes: FSSP-100, 2D-C, 2D-Grey, and 2D-P.
11. During the recent coordination meetings with NASA close collaborations have been established between Environment Canada and CNRS-LaMP, in order to optimize best probes in a simultaneous way (anti shattering, nitrate coating to minimize static charges leading to measurement noise, common data processing).

V.4. Decision of F-20 instruments to be used for first HAIC campaign

The **first** core instrument of the Falcon 20 to be deployed is the multi-beam 95 GHz Doppler cloud radar RASTA (RAdar SysTem Airborne, Protat et al. 2004), which allows for the three-dimensional (3D) wind and microphysical and radiative properties of clouds (IWC, visible extinction, particle size, terminal fall speed, concentration) to be retrieved in a vertical cross-section along the flight track in thick ice clouds (including precipitating ones). The RASTA radar in its current version includes 3 downward-looking beams (nadir, 28 degrees off-nadir and opposite the aircraft motion, and 20 degrees off-nadir perpendicular to the aircraft motion) and 3 upward-looking beams (zenith, 28 degrees off-nadir perpendicular to the aircraft motion, and 20 degrees off-zenith and opposite the aircraft motion). This unique configuration allows for the retrieval of the three-dimensional wind, a correction for 95 GHz attenuation by cloud particles, and an accurate correction of the navigation angles (using methods such as that proposed by Testud et al. 1995) which is mandatory for accurate 3D wind retrieval. Comparisons with in-situ measurements of the three wind components have also shown that three non-collinear views are mandatory for accurate wind retrievals. Calculations of gains and losses indicate that the downward-looking antennas will be of sensitivity -37 dBZ at 1 km range, while the upward-looking antennas should be at -32 dBZ at 1 km range (because they are smaller, 12 inch instead of 18, because the windows are smaller on the roof of the aircraft than on the belly). Such sensitivity is sufficient to document all stratiform and moderately-convective clouds down to the ground from 12 km height (despite severe attenuation), while allowing for the thin tropical cirrus clouds to be sampled near the aircraft altitude.

The **second** core instrumentation package is to be installed under the four wing stations of the Falcon 20. This package has to be a most sophisticated in-situ microphysical package allowing for state-of-the-art measurements of the ice particle mass deduced from direct measurement of the ice mass IWC (TWC respectively) and simultaneous spectrometry and imagery of hydrometeors in order to deduce crystal size distribution including phase discrimination in the range of few micrometers up to several millimetres. Whereas the Gulfstream-II will bring 12 under wing pods for microphysical instrumentation, the Falcon 20 will have only 4 under wing pods available. The in situ microphysical instrumental payload on the Falcon 20 then is defined via a combination of adequate probes as there are the Cloud Droplet Probe (CDP, diameter range : 3-50 µm), the 2D-Stereo cloud imaging probe (2D-S, diameter range : 10-1280 µm), and the precipitation size particle imaging probe PIP (diameter range: 100-6400 µm). An interesting feature of this combination is that there are overlapping diameter ranges, allowing for measurement consistency in hydrometeor dimensions (maximum diameter, surface equivalent diameter). Furthermore, the CPSD cloud probe for drop / ice discrimination for individual hydrometeors will help distinguishing small ice particles from supercooled droplets, which cannot be measured reliably with high resolution imagers. This package is complemented by measurements of the high resolution cloud particle imager CPI allowing for particle habit classification. An interesting alternative presents the HSI high speed imaging probe currently under construction at Atrium for the CIRA research laboratory.
The direct bulk measurements of condensed total water content TWC (=IWC+LWC) will be performed by using the Science Engineering Associates (SEA Inc.) ROBUST probe which has been mounted together with the CDP probe in one single PMS (Particle Measurement Systems) canister (work description see below).

The **third** instrumentation package is composed of two instruments installed under the Falcon 20 fuselage: In addition to the under wing probe package including the ROBUST probe which is currently mounted on the CDP canister, a second bulk TWC/IWC device, namely the Nevzorov probe (Korolev et al. 1998) will be installed under the fuselage. The Nevzorov probe has been already used during the 2011 Megha-Tropiques campaign on the Falcon 20. The Nevzorov is currently modified, lengthening the pylon in order to minimize fuselage effects on the sampling. The Nevzorov and ROBUST sensors will also be mounted on the HIWC aircraft, and their accuracy in a HighIWC environment at high aircraft speed will be fully characterized by statistical comparisons with the reference measurement of TWC (IWC+LWC), the so-called isokinetic probe, developed by Environment Canada and National Research Council (NRC). This characterization will in turn be used to correct/calibrate the Falcon 20 ROBUST and Nevzorov probe data. Finally, we acquired this year in view of HYMEX and High-IWC projects a newest version of the Rosemount Ice Detector, which is in fact a semi-quantitative instrument to detect and measure supercooled cloud water at negative temperatures.

The figure V-3 below shows the actual probe deployment on the Falcon 20 for the HYMEX measurement campaign (project dedicated to the intense precipitation events in southern France related to mid-latitude vigorous convection) deployed in Southern France during September –November 2012.

Figure V-3: Falcon 20 operating during HYMEX campaign (September-November 2012.

V.5. Intercomparison of chosen F-20 instrumental payload with G-II instrumentation

The following table 3.1 compares a very likely instrumental payload of the Falcon 20 (figure V.4 right) to the planned Gulfstream II (figure V.4 left) instrumental payload.

Figure V-4: Gulfstream-II (left) and Falcon 20 (right).

Whereas the Gulfstream-II disposes of roughly 12 under wing pods as mentioned above, the Falcon 20 is limited to only 4 microphysics probe stations.

For HAIC purposes the most relevant instrumentation for the HAIC project are cloud active remote sensing devices, bulk cloud microphysics instrumentation, and single cloud particle µ-physics instrumentation. Following conclusions can be drawn from currently selected F-20 instrumentation as compared to the planned G-II instrumentation (table V-1):

1. With respect to the cloud radar the Doppler cloud radar on the Falcon is superior to the G-II K band radar, since we have 6 non-collinear antennas and in addition to the reflectivity measurements the Doppler radar is capable to accurately measure the terminal fall speed of hydrometeors. It has been demonstrated that the combination of radar reflectivity and fall speed could provide constraints on the relationship between mass and maximum dimension of ice crystals, which is the main

assumption to be held for IWC calculations using radar data (Delanoë et al. 2007; Plana-Fattori et al. 2010).

2. Bulk cloud microphysics devices are comparable (Robust probe, modified Nevzorov, Rosemount Ice detector), except, of course the isokinetic evaporator reference probe (IKP) for IWC retrieval, which will be solely installed on the G-II. The strategy will consist in using the efficiency of collection of the robust probe that will be characterized from direct comparisons with the IKP to derive IWC estimates from the Falcon 20 Robust probe.

3. With respect to single cloud particle microphysics instrumentation, we have at least the most sophisticated instruments on the Falcon 20 concerning optical spectrometer, CCD camera technology, and intermediate and large particle optical array probes. The most evident drawback then is that with only 4 available instrument stations we cannot put redundant instrumentation on the Falcon, as is the case for the Gulfstream-II.

Measurement	Size range	Gulfstream-II	Falcon-20
Meteorology		AIMMS-20	p, T, humidity (LICOR, CR-2, WVSSII), v, pos.
Aerosol		PCASP	----------
Cloud optics		Extinction probe	----------
Cloud active remote sens.		Ka Band Radar	95 GHz Doppler cloud radar
Bulk cloud μ-phys		Hot wire boom/devices	Nevzorov probe
		Isokinetic probe	----------
		Robust probe	Robust probe
		Rosemount Ice Detector: RICE	RICE (new model 0871LM5)
Single cloud particle μ-phys	Opt. spectrometry: (1-50 μm)	FSSP-100 (old), CDP (new)	CDP (newest) or PDI (in PMS) CPSPD (depol.)
	CCD camera: (10-1000 μm)	CPI Imager (2.3μm pixel, 1000*1000 pixel)	CPI (2.3μm pixel) or HSI (5μm pixel, 500*500 pixel)
	2D-array probes: (100-1500 μm)	2D-S: 10μm pixel, 128 photodiodes CIP: 25μm pixel, 64 photodiodes 2D-C: 25μm pixel, 32 photodiodes	2D-S (10μm pixel),
	2D-array probes: (500-6000 μm)	2D-P (old)	PIP (new)

Table V-1: Instrumental payload intercomparison between G-II and Falcon 20 instrumentation.

V.6. Contingency Plan with Falcon 20 as primary Aircraft to be secured

In late spring 2012 NASA decided to delay the primary HIWC measurement campaign by one year to early 2014. This decision has been due to workmanship and quality assurance lapses at Flight test Associates (FTA; NASA contract for G-II modifications) that led to stoppage of ongoing work and investigation/corrective action planning. Work resumed at FTA in mid-July. HIWC Partners met in August 2012 to discuss impacts of delay. All agreed to support the 2014 Darwin Campaign with the G-II, but expressed strong desire for contingency plans.

This is when first versions of a Contingency Plan have been developed, in order to prepare solutions for different scenarios of G-II and F-20 deployments. The original contingency plan accounted for four basic scenarios presented in Table V-2 below:

Contingency Plan(s)			
Option A	Option B	Option C	Option D
			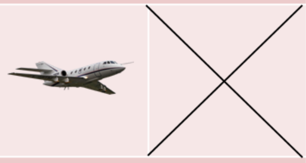
Description: Nominal plan ; both F20 and G-II on time and ready for 2014 Darwin primary field campaign	Description: Degraded plan ; F20 ready for 2014 F/T campaign ; **IKP on F20?** ; **Additional F/H?** ; delay in G-II preparation → trial campaign or/and limited payload	Description: Degraded plan ; F20 on time and ready for 2014 F/T campaign ; **IKP on F20** ; **Additional F/H?** ; **G-II not available**	Description: Worst scenario ; F20 on time and ready for 2014 F/T campaign ; **IKP can't be installed on F20**; **Additional F/H? G-II not available** ;
Assumption(s): •G-II is the primary A/C equiped with probes, **IKP**, Ka band radar, HWL RDR-4000 radar •F20 is the secondary A/C equiped with probes and RASTA radar (IKP, F/H option)	Assumption(s): • F20 Primary A/C equipped with probes, RASTA radar and **IKP IKP** ; **Additional F/H** •G-II secondary A/C equipped with probes, **IKP**, (Ka band radar), HWL RDR-4000 radar	Assumption(s): •F20 Primary A/C equipped with probes, RASTA radar and **IKP** ; **Additional F/H?**	Assumption(s): •F20 Primary A/C equipped with probes, RASTA radar ; **Additional F/H?**
Impact(s): NO	Impact(s): YES (limited)	Impact(s): YES (medium)	Impact(s): YES (high)

Table V-2: Contingency plans for F-20 probably as primary aircraft.

On September 18th NASA management, procurement and legal personnel visited FTA. They briefed NASA on FTA's financial capability as it relates to its ability to perform the contract. To reduce risk exposure to NASA and its partners all government (and partner) provided equipment were removed from FTA site to NASA DFRC (Dryden Flight Research Centre) for storage. Finally, on October 19th, 2012 NASA issued a

contract termination notice to Flight Test Associates. NASA and Environment Canada have secured all equipment on the aircraft including the instrument racks and associated avionics.
During the NASA/FAA Top Management meeting held on November 20th, 2012 it has been decided that no viable options for the G-II, or other NASA A/C, exists to support a 2014 field campaign. The only remaining option for a backup of the G-II contract aircraft is the Falcon 20 research aircraft deployed within the frame of the High Altitude Ice Crystal (HAIC) European project. Although the Falcon-20 will address many HIWC objectives, the G-II is also required to fulfil un-addressed or incompletely addressed objectives as defined in Engine Harmonization WG meetings and the HIWC Science Plan. Still, both Associate Administrators (FAA-Aviation Safety and NASA- Aeronautics) support the objectives of the HIWC flight research project and the continued development of an aircraft option (the G-II is the most likely candidate) for a full complement of instruments to conduct a field campaign in ice crystal environments, earliest in 2015, possibly later.
According to the NASA/FAA decision that the G-II aircraft will not be operational for the planned F-20 campaign in early 2014 flying out of Darwin, the contingency plan is now updated (Tab. V-2). Remaining options C and D of the above presented contingency plan (Table V-2) distinguish now between options C1 and C2, and D1 and D2, respectively (Table V-3), where options C1 and D1 are the most favourable ones (among the remaining scenarios).

Contingency Plan(s)

Option C.1	Option C.2	Option D.1	Option D.2
			
Description: Degraded plan ; F20 on time and ready for 2014 F/T campaign ; **IKP on F20** ; **Additional F/H?** ; **G-II not available**	Description: Degraded plan ; F20 on time and ready for 2014 F/T campaign ; **IKP on F20** ; **Additional F/H?** ; **G-II not available**	Description: Worst scenario ; **G-II not available** ; **IKP can't be installed on F20** ; reconcilliation IKP/Robust after the field campaign	Description: Catastrophic scenario ; **G-II not available** ; **IKP can't be installed on F20 ; No reconcilliation IKP/Robust**
Assumption(s): •IKP installation - Feasibility demonstrated: second IKP to be designed and manufactured for installation on F20 •**Additional F/H?**	Assumption(s): •IKP installation - Major change(s) requested wrt installation : strong support from HIWC requested in order to adapt IKP design (wiring, …) • **Additional F/H?**	Assumption(s): • To correlate IKP and ROBUST probe after the 2014 Darwin F/T campaign: dedicated campaign or 2016 HAIC F/T campaign • **Additional F/H?**	Assumption(s): •IKP can't be installed •No reconciliation robust/IKP possible •**Additional F/H?**
Impact(s): YES (medium)	Impact(s): YES (high)	Impact(s): YES (very high)	Impact(s): YES (campaign postponed)

Table V-3: Updated contingency plans for F-20, being the only A/C.

In order to go forward we need urgently confirmation from FAA/NASA to be willing to fund contingency costs for use of Falcon 20 aircraft for 2014 field campaign.

The most urgent tasks are now to:

- Complete the assessment of mini-IKP re-design to meet Falcon 20 pylon structural, drag, and electrical limits: NRC and SAFIRE confirmed that IKP re-design can meet Falcon 20 constraints for operation and certification.
- Determine if the schedule for developing and integrating the mini-IKP equipment on Falcon 20 can be aligned with Jan-Mar 2014 field campaign.
- Review HIWC versus HAIC flight mission requirements to confirm, if we can obtain acceptable level of HIWC project objectives.
- Develop (FAA and NASA) modifications to existing NASA Glenn contract and FAA Memorandum of Cooperation with NRC Canada to provide procurement funds to initiate new IKP.

V.7. Darwin campaign data exploitation: main challenges and expected progress

The scientific knowledge is very limited (or almost inexistent) about the frequency of occurrence, conditions of formation, and microphysical and dynamical processes involved in the HighIWC regions encountered by commercial aircraft during the reported in-service events.

The HAIC-EASA HighIWC project with measurement campaign in early 2014 primarily relies on the most precise estimation of TWC from different approaches. In addition, the update of the icing conditions in Appendix D requires a large number of measurements. Therefore our overall goal is to produce as many estimates of TWC from our instrumentation as possible and reconcile them through improvement of assumptions in retrieval techniques, careful analysis of measurements, joint use of different measurements, and closure analysis between measurements. In particular, we will estimate TWC from in-situ particle probe sizing, bulk microphysics, and airborne cloud radar retrievals as we'll have G-II in-situ, Falcon 20 in-situ, and Falcon 20 Doppler radar data.

- ⇨ The Falcon 20 in-situ bulk IWC probes (Robust, Nevzorov, and RICE) all have limitations (collection efficiency, saturation, etc …) but the IKP (isokinetic evaporation probe) onboard the G-II should be able to characterize the Falcon probes better. **3 IWC estimates** from IKP, Robust, and Nevzorov probes.
- ⇨ The Falcon 20 in-situ probes measuring the PSD also allow for another estimate of IWC given some assumptions about the m(D) relationship that can be constrained using 1) m(D) parameterizations, 2) the CPI images and / or 3) the airborne cloud radar reflectivity and Doppler. **3 additional IWC estimates** !
- ⇨ The Falcon 20 airborne Doppler cloud radar can estimate IWC from reflectivity + Doppler and assumptions about m(D), A(D) and the PSD characteristics over the whole vertical extent of the HighIWC regions. **1 IWC estimate** !
- ⇨ Closure analyses between these measurements should in principle **reconcile these 7 different estimates** of IWC in HighIWC regions.

VI. Work performed on F-20 payload and integration feasibility: combination probes, probe modifications, certification work

Recall from proposal:
The objective of this task is to define preparatory actions for a comprehensive determination of the composition of cloud masses at high altitude (HighIWC) with the appropriate precision to complete and justify on solid scientific grounds the amendment of the environment proposed in the NPA 2011-03 (Appendix P) defining mixed phase and glaciated icing conditions. In particular the work will consist in a feasibility study to demonstrate the capability to get the results from flight trial campaigns, by conducting demonstration flights of 4 hours with a ready to fly aircraft.
BOM, as subcontractor of LAMP, will contribute to the definition of the Falcon 20 payload for HighIWC, and will provide the airborne cloud radar data from the new Falcon 20 demonstration flights allowing for a validation of the Falcon 20 payload.
LAMP will lead the task 2.2 and will interact with the aircraft operator SAFIRE in order to implement the new in-situ microphysical payload for the Falcon, to be used during the HighIWC Study in 2013. LAMP will also participate to test flights after instrument certification to validate this new payload.

In the following some more details are presented concerning probe acquisitions and optimizations according to discussions led between CNRS-LaMP, BOM, and Environment Canada, in collaboration with DMT, SPEC, and SEA scientific instrumentation companies. The overall goal is to mount best performing probes (on both aircraft) that have been optimized for best measurement performances.
HAIC project probe optimization occurs in close collaboration with Walter Strapp (Environment Canada, NASA) and Alexei Korolev (Environment Canada, Transport Canada) both scientifically responsible for the Gulfstream-II instrumentation.

VI.1. Falcon 20 cloud Doppler radar 94 GHz

The multi-beam 95 GHz Doppler cloud radar RASTA (RAdar SysTem Airborne, Protat et al. 2004), allows for the three-dimensional (3D) wind and microphysical and radiative properties of clouds (IWC, visible extinction, particle size, terminal fall speed, concentration) to be retrieved in a vertical cross-section along the flight track in thick ice clouds (including precipitating ones).

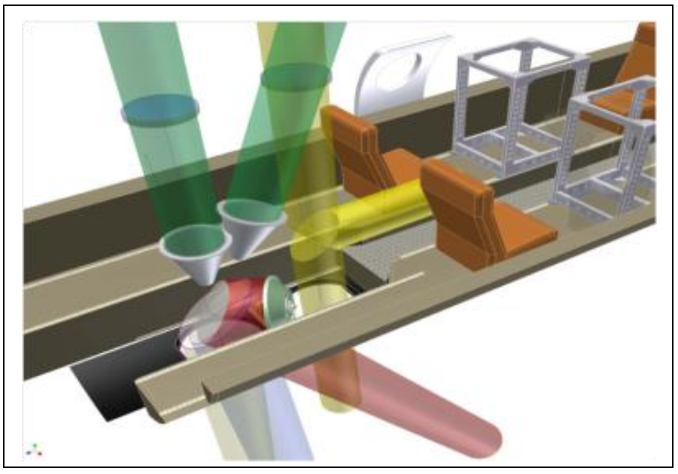

Figure VI-1: Cloud Doppler radar RASTA (6 antenna version) for the Falcon 20.

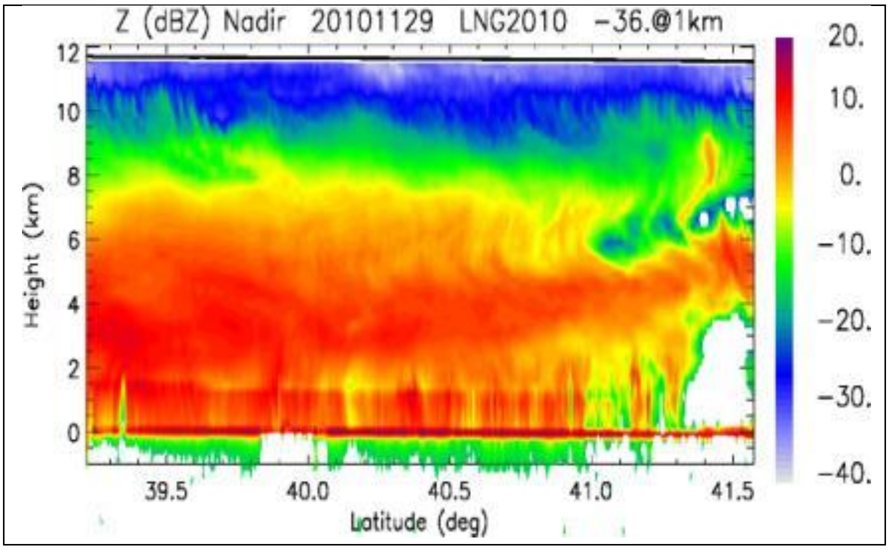

Figure VI-2: Example of nadir reflectivity along Falcon 20 flight track

The RASTA radar in its current version includes 3 downward-looking beams and 3 upward-looking beams. This unique configuration allows for the retrieval of the three-dimensional wind (Papazzoni 2010). Measured reflectivity and retrieved fall speed are used to estimate microphysical parameters, as there are IWC, extinction, effective radius, N_T (Delanoë et al. 2007).

VI.2. Falcon 20 in-situ instrumentation

VI.2.1. Nevrorov TWC (IWC) probe: pylon lengthening

CNRS-LaMP in collaboration with SAFIRE worked out the concept of lengthening the pylon of the Nevzorov Probe (figure VI-3). The overall goal hereby has been to find equilibrium between the scientific need to lengthen the pylon thus avoiding IWC enrichment due to ice bouncing off the fuselage and a geometry that can be certified without modifying the structure of the hard point of the Falcon 20, where the probe will be installed for the HAIC project. The blue interface represents the version of the additional pylon that will be fabricated and certified. The objective of installing the Nevzorov probe is to compare the measurements to those of the ROBUST probe on the Falcon 20 and with the Nevzorov probe on the Gulfstream-II. The Nevzorov probe performance will be compared to the ROBUST probe measurements on the Falcon 20 (HYMEX, HAIC).

Status of work: Aerodynamic profile of the pylon interface has been designed, thereby increasing the drag of the Nevzorov by a maximum of 50% acceptable for the corresponding Falcon 20 hard point of the Nevzorov mounting position. Fabrication and certification has been accomplished. The new probe had been mounted on the F-20 for HYMEX and worked properly.

Nevzorov probe on Falcon 20 (Megha-Tropiques 2011) 	Design pylon lengthening 	Nevzorov probe with new pylon on Falcon 20 : certified and operating during test flight and subsequent HYMEX campaign (September-November 2012) 

Figure VI-3: Nevzorov probe on Falcon 20

VI.2.2. Design & acquisition of ROBUST probe combined with CDP probe

The ROBUST probe in combination with the CDP probe was ordered in March 2012 in one single PMS canister. The ROBUST TWC probe will play a central role in the High-IWC measurements.
The ROBUST-CDP combination probe (figure VI-4) has been tested and successfully operated during the HYMEX campaign. The use of the ROBUST probe on F-20 during the first HAIC F/T campaign will:

(i) Retrieve in situ IWC on F-20 flight level (-50°C, -30°C, -10°C).

(ii) Validate the various TWC estimates from particle imagery and Doppler cloud radar estimates of IWC in HighIWC regions (retrieved from reflectivity and Doppler velocity) using G-II and Falcon 20 in situ data.

Discussion of ROBUST probe integration in PMS canister (December 2011) 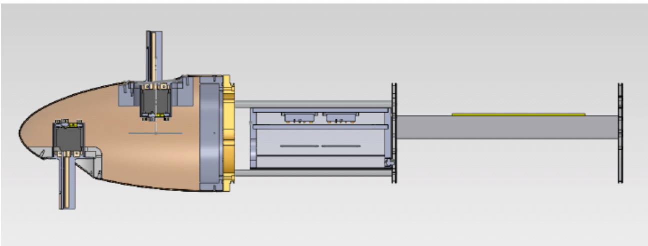	Chosen design of ROBUST-CDP probe by CNRS-LaMP & DMT & SEA (January 2012) 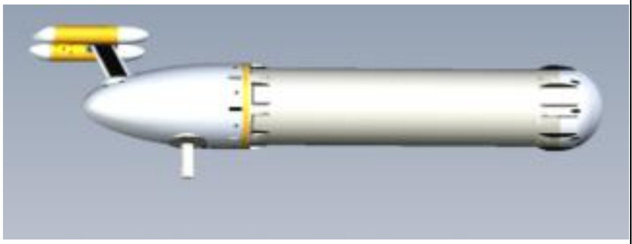
Probe fabricated and delivered to CNRS-LaMP (June 2012) 	Probe certified and mounted on Falcon 20 for HYMEX (September 2012) 

Figure VI-4: CDP-ROBUST combination probe on Falcon 20

Moreover, two single ROBUST probes will be installed on the Gulfstream-II besides the Isokinetic evaporator probe that is considered to be the TWC/IWC reference probe.

Status of work: CNRS-LaMP received the combination probe end of June 2012. Subsequently the probe has been certified by the French certification authority DGAC (Direction Générale de l'Aviation Civile). The ROBUST-CDP probe has been installed and tested on the F-20 in July 2012. The probe has been operated during the entire HYMEX campaign in September-November 2012.

VI.2.3. CPSD probe for drop / ice discrimination: F-20 design and certification issues.

In highly convective cloud systems the ice formation mechanisms and subsequent precipitation processes remain poorly understood, largely due to the lack of instruments that can distinguish liquid water from ice in the early stages of glaciation, i.e. when the droplets and crystals are less than 50 µm. Decision was made to acquire the Cloud Particle Spectrometer with Depolarization (CPSD) probe (figure VI-5) within the EASA High-IWC project and to operate this probe within the HAIC measurement campaign.

<table>
<tr>
<td>
CAS-DPOL depolarization detector:
> Probe subject to fragmentation…</td>
<td>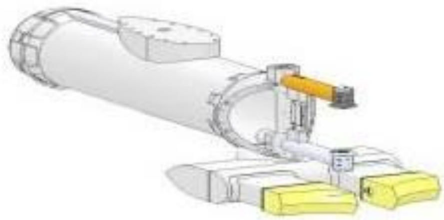
Successor probe: CPSD – original DMT version.
> Certification problem on Falcon 20…</td>
</tr>
<tr>
<td>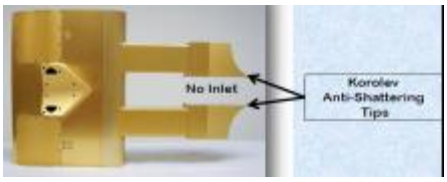
CPSD with anti-shattering tips: 3D simulations with cpsd.step file revealed severe certification issues on Falcon 20:
➔ drag and mass seem to exceed certification tolerance</td>
<td>Chosen design within EASA project of CPSD for Falcon 20.
High-IWC project: The CPSD has been certified for Falcon 20 (October 2012). Delivery in first half of 2013. Flight tests during TC2 project.
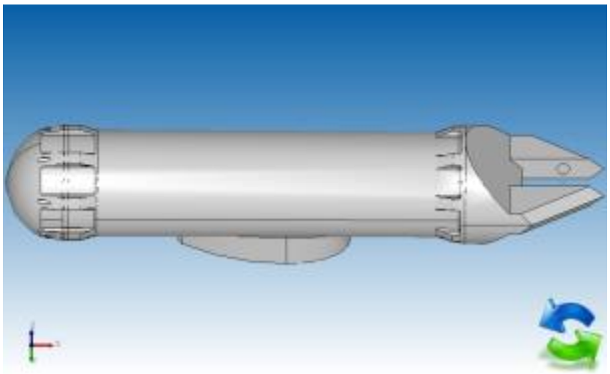</td>
</tr>
</table>

Figure VI-5: New design of CPSD: Designed for Falcon 20 within EASA High-IWC project

The CPSD probe equipped with anti-shattering tips is a modification of the Cloud Aerosol Spectrometer with Depolarization (CAS-DPOL) that currently uses bi-directional light scattering from individual particles to derive size and shape, adding an additional measurement of depolarization to separate ice particles from water droplets. As the commercialized CAS-DPOL might be subject to artificial fragmentation of large hydrometeors, and as CNRS-LaMP in collaboration with SAFIRE demonstrated that the initial CPSD version of DMT may not be certified on the French Falcon 20 aircraft (3D calculations performed by the SAFIRE certification engineer yielded drag forces that may not allow its certification on the Falcon-20 without modifications of the wing structural parts), CNRS-LaMP has been working with the DMT company on the modification of their CPSD version. The result of that collaboration is presented in the below figures. The new design developed for the F-20 aircraft (and certainly other aircraft) is presented below. Probe fabrication is underway. The probe will be delivered in the first half of 2013. The CPSD is an ideal step forward when complementing the existing in situ instrumentation (CDP, high resolution imager CPI, 2D-Stereo Probe, PIP) for cloud microphysical measurements in the lower particle diameter range up to some 50 m.

The resulting measurement data are cloud particle spectra colour coded by depolarization intensity (or ice fraction) for single particles. The following figures VI-6 and VI-7 show very recent measurements of the CPSD probe that is currently integrated in the PMS tube adapted for use on the Falcon-20. This CPSD version will be delivered in the first half of the year 2013 to CNRS-LaMP for subsequent integration and flight tests on the Falcon 20.

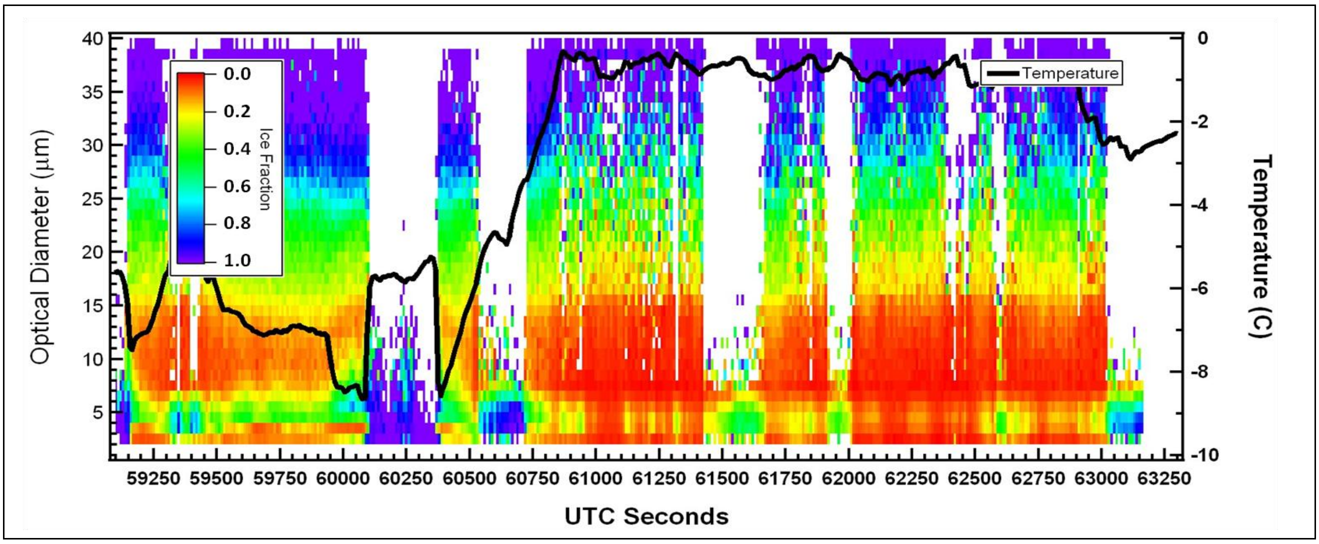

Figure VI-6: Time series of the ice fraction as a function of optical diameter and time illustrating the way that mixed phased clouds shift the distribution of fraction with size, even within clouds with the same temperature.

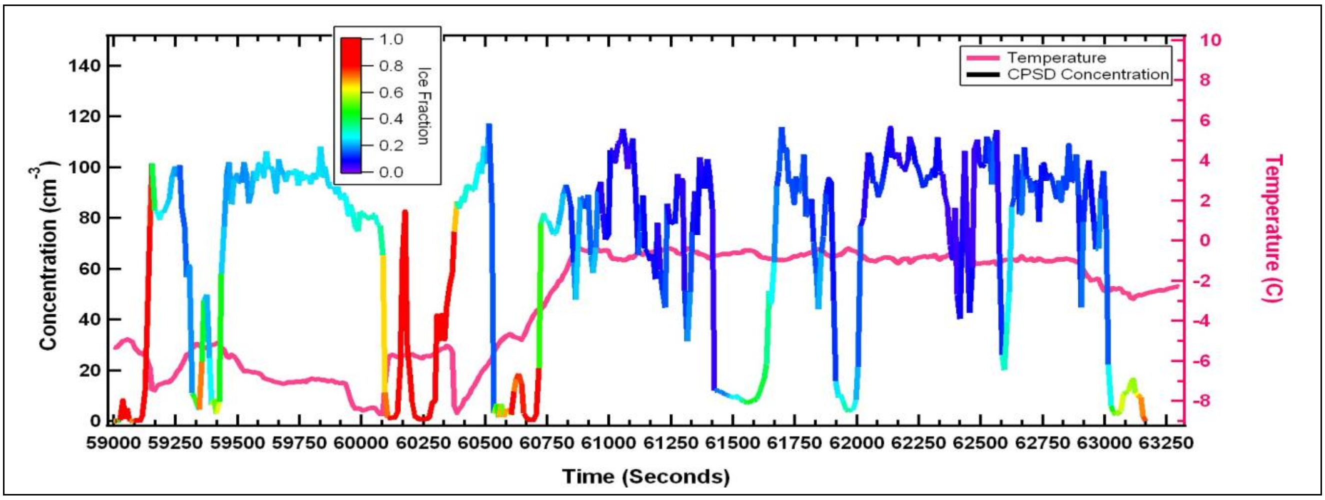

Figure VI-7: Time series of CPSD concentration, colour coded with ice fraction, showing the inhomogeneity of mixtures of water and ice, and this within cloud sequences of the same temperature. Especially at cloud edges (red circles) there are mostly ice crystals while within the cloud the fraction varies from one edge to the other (green circle).

Status of work: CPSD instrument exists in its former (original) version exists at DMT. CNRS-LaMP and SAFIRE performed 3D simulations (3D file in *.step format) of drag in view of the CPSD certification on the French Falcon 20 for the HAIC project. The 3D simulations for the original CPSD version of DMT yielded drag forces that were higher by a factor of 2 to 2.5 as compared to drag forces of already certified probes on the Falcon 20, as for example 2D-S, PIP, CIP, SPP-100, etc… Therefore CNRS-LaMP instructed DMT to work on a lighter version of the CPSD probe with improved aerodynamic characteristics. The result is presented in the figure above. The new CPSD probe has been ordered in August 2012 and is under construction at DMT (Droplet Measurement Technologies) for the Falcon 20. The French certification authority DGAC accepted the certification document prepared from SAFIRE without test flights, the new CPSD probe is now certified (October 2012). The probe wiring of the CPSD is compatible with the standard PMS canister wiring. The probe will be plugged as all the other probes (2D-S, CDP-ROBUST, PIP) that we integrated on the Falcon 20 during the past years. At least one or two test flights are foreseen after CPSD probe receipt in 2013.

VI.2.4. 2D-S: probe improvement with newest anti-shattering tips.

<table>
<tr><td></td><td>Left: 2D-S probe version at CNRS-LaMP (with standard circular sharp probe tips) used during Megha-Tropiques campaigns in 2010 and 2011 on the French Falcon-20</td></tr>
<tr><td>
Manufactured adapter test probe tips fitted to the standard probe tips</td><td>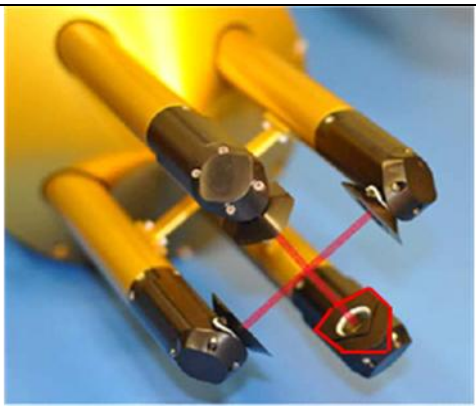
Manufactured metallic non-circular sharp probe tips for the 2D-S version operated at CNRS-LaMP.</td></tr>
</table>

Figure VI-8: Upgrade of 2D-S probe tips.

In order to improve further the already well performing 2D-S probe (operated during two Megha-Tropiques campaigns in 2010 and 2011 on the French Falcon 20 and several other international field experiments), we decided to spend additional money on even better probe tips, newly designed in collaboration at SPEC. The

2D-S Probe has been sent to SPEC and will return with newest tips by the end of July 2012. The probe will be operated on the Falcon 20 during HYMEX this fall. No additional certification issue. A presentation of the excellent probe performance including inter-arrival time analysis and processing of possible fragmentation has been given CNRS-LaMP at the International Conference of Clouds and Precipitation (ICCP conference) in Leipzig July 30 to August 03, 2012 (Dupuy et al., ICCP 2012).

Status of work: The 2D-S from CNRS-LaMP has been sent to SPEC Inc. for probe tip upgrade (the new non-circular sharp probe tips). The probe will return end of July 2012 to France. Installation and test flight end of August 2012 to be ready for the HYMEX campaign in September-November 2012. The probe gives very good results during HYMEX flights.

VI.2.5. Rosemount Ice Detector new model 0871LM5

The improved, semi-quantitative version 0871LM5 of the Rosemount Icing Detector (RICE) has been acquired in order to improve the detection of supercooled cloud water. The instrument has been **installed recently (May 2012) on the fuselage of the Falcon 20** close to the Nevzorov probe position and will be operated on the French Falcon during HYMEX (mid-latitude convection) in September/October 2012 and subsequently during the High-IWC campaign.

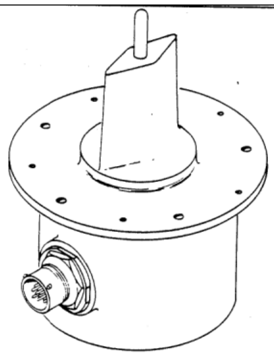	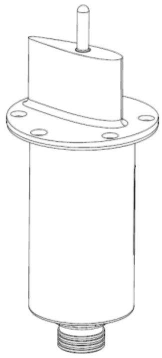
Old RICE model : 0871*LH1*	New RICE model : 0871***<u>LM5</u>***

Figure VI-9: Rosemount Ice Detector probe upgrade

The new RICE model is better profiled as compared to the old one. The principal advantages are :

A more powerful de-icing to get rid of the accumulated ice much more rapidly, implicating less sampling dead time.

The communication of digital data via the serial port, as compared to analogue data for the old RICE version will allow minimizing considerably the noise level on the signal.

The new electronics yield improved probe characteristics and probe control.

Status of work: The 0871LM5 version has been delivered in April 2012. Installation and ground tests were successful. In flight tests have been combined with test flights for ROBUST/CDP probe in July and August 2012. The probe works properly during HYMEX.

VII. Management & Reporting

Recall from proposal:

The objective of this task is to monitor the timely performance of the project and perform administrative tasks with the EASA.

Meeting activities performed in the frame of this task

- Kick-off meeting support and preparation (held on the 30th of January),
- Proposal and dissemination of project templates,
- WebEx progress discussion meeting: 17th of April 2012 ,
- WebEx progress discussion meeting: 13th of July 2012,
- Face to face progress meeting between EASA and Consortium in September 3-4, 2012 in Toulouse,

Monthly Reports

- February report (delivered on the 8th of March 2012)
- March report (delivered on the 16th of April 2012)
- April & May report (sent on 19th of June 2012)
- June report (sent 24th of July)
- July and August report (sent on 10th of September)
- September and October report (sent on 5th of November)

Distribution of deliverables to EASA

- First interim report distributed 17th of April 2012
- Second interim report 11th of July 2012
- Final report (this report)

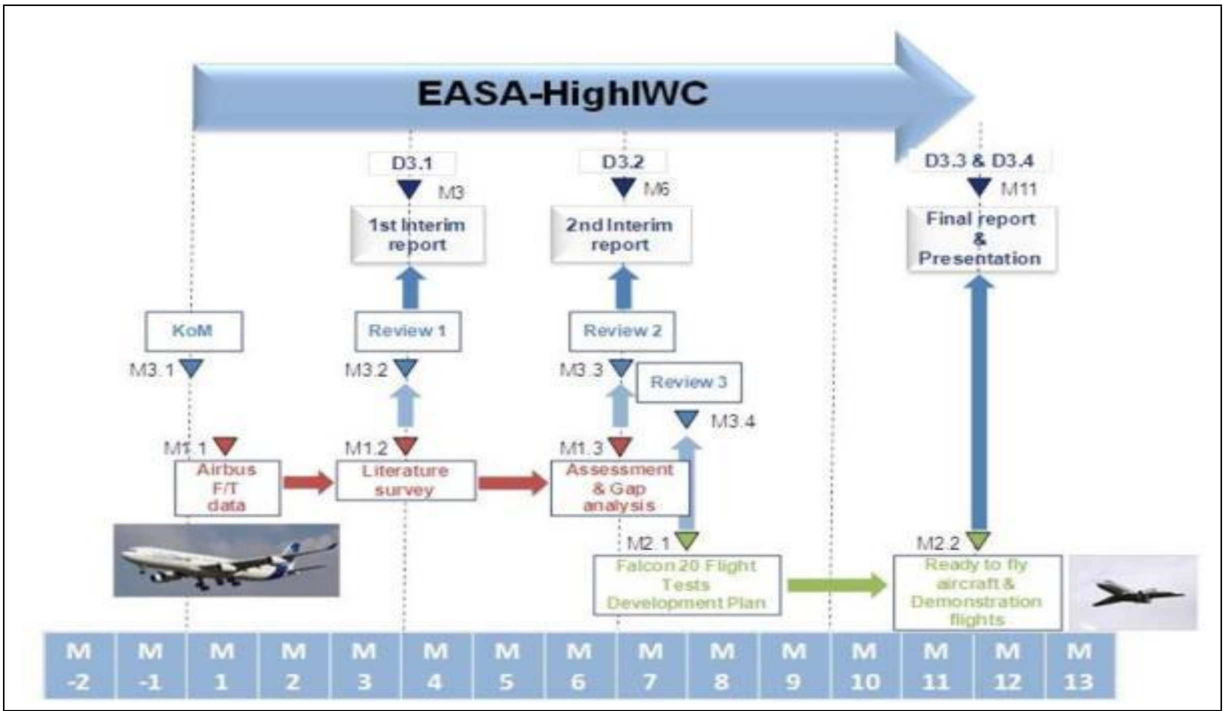

Figure VII-1: Sequencing of EASA-HighIWC Milestones & Deliverables recalled from proposal

Recommendations

Recall from proposal:

The objective of this task is to provide recommendations and to highlight open issues regarding the validation of the environment proposed in the NPA 2011-03 (Appendix P) defining mixed phase and glaciated icing conditions and the necessary steps to achieve a more comprehensive determination of the cloud characteristics at high altitude with the appropriate precision.

Convective weather is caused by deep lifting and condensation of air in an unstable atmosphere, resulting in deep cloud and large anvil regions, areas of strong wind shear and turbulence, lightning, heavy precipitation and hail and high total water contents. In high altitude (low temperature), these high TWC areas are made exclusively of ice (glaciated icing conditions). An extension of the certification icing envelope (Appendix D and P) had been proposed to cover the icing threat in these regions, based on literature survey and calculations, as no accurate and reliable characterisation of these conditions is available.

The international field experiment HIWC-HAIC-EASA HighIWC project is dedicated to these particular icing conditions. The HIWC-HAIC-EASA HighIWC experiment will provide the first modern extensive data set of the core areas of tropical oceanic deep convection and less vigorous tropical continental convection and as such will be a unique resource for fundamental research, new industrial developments of detection and/or awareness technologies and for the regulation makers to update the icing envelope for glaciated conditions (Appendix D and P).

A) Recommendations regarding the validation of the proposed rulemaking envelopes defining mixed phase and glaciated icing conditions.

1. **Need of reliable IWC measurements as a function of the distance to the convective core:** The scientific community does not have sufficient evidence to determine specifically where relative to a core updraft area power loss events are likely to occur. Some events have occurred in anvils, others have occurred while diverting around high reflectivity regions at altitude, and may therefore be closer to cores. Therefore the flight strategy employed during HIWC/HAIC will consist in flying through updraft cores (at least for oceanic convection) of convective cells and progressively fly out of these cores to document the variation of IWC as a function of distance to the convective cores (probably up to 50 km away from the cores).
2. **Consequences of cloud inhomogeneity within 17.4 Nm:** MT and A340 data sets produced lots of evidence that within 17.4 nautical miles (Appendix D charts) the convective cloud systems are not at all homogeneous. Retrieved IWC values averaged over 17.4Nm have been found to be inside the envelope specified by future proposed regulations. The cloud non-homogeneity is demonstrated by much higher IWC values for much shorter spatial intervals. Arguments for presenting peak values instead of 17.4 Nm values in particular for Air Data probes have to be considered.
3. **Retrieval of IWC during A340 flights and MT data:** The IWC values estimated using microphysical characteristics constrained by the in-situ observations (see further explanations later) seem to reach several times 5-6 g/m3 (10 s measurement) particularly during the 2010 campaign over West Africa, and 10.1 g/m3 (1 s measurement) for A340 data, respectively. Peak

values in TWC are capable to exceed the proposed TWC envelope, while 17.4 Nm values do not, at least for all gathered 340 and MT data.

4. **No evaluation possible of proposed envelope (regarding mixed phase and glaciated icing conditions) for TWC related to in service events (engines):** No engine in-service event had been reported outside of the proposed envelope (altitude – SAT envelope). Due to lack of information on the concentration of TWC during the in-service events, no evaluation of proposed envelope for TWC values can be made. The international field campaign should help to fill this gap and provide the necessary data for rulemaking activities and evaluation of proposed envelopes.
5. **Evaluation of proposed envelope (regarding mixed phase and glaciated icing conditions) for TWC related to air data probes**: Airbus has observed 6 in-service events of Pitot icing in ice crystals conditions that were outside of the altitude versus temperature SAT domain (see Appendix D). Based on air data probe observations, Airbus proposes an extension of the Appendix D altitude versus temperature domain for Air Data Probes as well as an extension of the Appendix D TWC concentration for ice crystals for Air Data Probes. Actually the Appendix D provides TWC concentration values scaled for a 17.4 NM cloud. The extension in TWC for air data probes, however, should correspond to the maximum or peak TWC concentration values that can be encountered in clouds, since Airbus results presented in this report demonstrates that these 17.4 Nm scaled values are not adequate for Air Data Probes qualification. Due to its size, a probe has a low reaction time and rapidly freezes (in less than 10 seconds) as soon as the IWC concentration exceeds values above the threshold limit of the probe (no inertia phenomenon). Due to its size, a probe has a low reaction time and rapidly freezes (in less than 10 seconds) as soon as the IWC concentration reaches exceeds value above the threshold limit of the probe (no inertia phenomenon). On the contrary, an engine needs a certain exposure time (corresponding to a distance in icing conditions i.e. cloud size) before being affected as there is a minimum size for accreted ice block that can lead to engine adverse issues.
6. **Enlarge dataset for statistical evaluation of proposed envelopes:** In order to perform a statistical approach for the analysis of proposed envelopes in terms of mass concentrations, additional results and measurements of the atmosphere are needed. The international field campaign should fill this gap and provide the necessary data for rulemaking activities and evaluation of proposed envelopes.

B) Recommendations in order to achieve a most comprehensive and exact determination of the cloud characteristics at high altitude with the appropriate precision.

1. **Mass-diameter relationship m(D) to be used for best guess of ice density in HIWC regions:** Use of a single mass-size relationship such as that of Brown and Francis (1994) used for the A340 data could not represent accurately the dependence of the mass-size relationship as a function of particle mean diameter and temperature. Our study demonstrates that the mass-diameter relationship is significantly influenced by the temperature. This result is fully consistent with the observation in Heymsfield et al. (2010) that the use of a single mass-size relationship is not appropriate to represent the variability of ice mass as a function of temperature. More studies need to be performed in order to understand how the area-diameter law varies in natural

clouds, and what are the most significant physical parameters controlling the calculation of the area-diameter law. In general, the mean density of the cloud particles is larger in continental MCS (MT1) than in oceanic MCS (MT2). Whereas it is not possible to clearly classify the particle shapes in the continental MCS (shapes somewhere between graupel and aggregates), in the oceanic MCS much more pristine (rosettes, columns, sideplanes, etc…) ice can be found. An important conclusion is that for observed oceanic convection the growth of the cloud particles is much more dominated by vapour diffusion, as compared to the more violent continental convection. Thus, cloud particle aggregation that leads to very large particles in the continental convection is for some reason limited in oceanic convection.

2. **Confirmation of high IWC and small crystal diameter relation:** We know that simultaneous occurrence of high IWC and relatively low radar reflectivity implies that the ice particles are smaller than usual (to produce relatively small radar reflectivity) but in very high concentration (to produce significant ice water content). The aircraft TAT probe anomaly is very frequently observed, and is known to occur when high mass concentrations of ice crystals are present.
3. **Derive full information from 2D images for further refinements of IWC estimates for A340 data.** A study is actually performed to derive more parameters from each single Airbus nephelometer image, so that we can really apply other relationships (as performed for MT data) and estimate the variability of TWC estimates as a function of different mass-size relationships, as has been performed for imaging probes used during MT.
4. **Need of a true TWC reference measurement:** This bulk measurement will be provided by the ROBUST probe and in particular the isokinetic evaporator probe (IKP) during the HIWC / HAIC project. The ROBUST probe is still lacking accurate calibration and has to be calibrated absolutely by the use the isokinetic evaporator probe (IKP).
5. **Reconcile IWC measurements/estimations/retrievals from different techniques:** The HAIC-EASA HighIWC project with measurement campaign in early 2014 primarily relies on the most precise estimation of TWC from different approaches. Therefore our overall goal is to produce as many estimates of TWC as possible from our instrumentation and reconcile them through improvement of assumptions in retrieval techniques, careful analysis of measurements, joint use of different measurements, and closure analysis between measurements. In particular, we will estimate TWC from in-situ particle probe sizing, bulk microphysics, and airborne cloud radar retrievals as we'll have G-II in-situ, Falcon 20 in-situ, and Falcon 20 Doppler radar data. Closure analyses between these measurements should in principle reconcile the estimates of IWC in HighIWC regions.

Conclusions

The presented study investigated TWC estimates from two available datasets sampled in deep convective clouds. Both the studies, of the A340 and also the Megha-Tropiques data sets are particularly based on measurement of particle imagery, from which we try to estimate the total water content TWC. These TWC estimations are subject to assumptions (partly constrained) of mass-diameter relationships m(D) to be used for best guess of ice density in HIWC regions. We illustrated that the use of a single mass-size relationship cannot represent the variability of the ice mass as a function of temperature and growth regime (vapour diffusion plus aggregation and/or riming). Concerning the A340 datasets, TWC derived from Airbus nephelometer imagery and ROBUST probe direct TWC measurements are correlated, however, the ROBUST probe efficiency is not yet calibrated and an uncertainty in solely using the crystal surfaces of Airbus nephelometer data for TWC mass calculations remains . A current work is extracting more parameters from each single Airbus nephelometer image, so that we can apply refined m(D) relationships and estimate the variability of TWC estimates as a function of different mass-size relationships, as has been performed for imaging probes used during Megha-Tropiques. Concerning the Megha-Tropiques data, the TWC calculations from crystal imagery have been more constrained by additional geometric parameters derived from images, and mainly by the radar reflectivities measured simultaneously on the aircraft trajectory. During a recent measurement project (HYMEX) in mid-latitude deep convection, bulk TWC measurements have been provided for the first time by the ROBUST probe in addition to particle imagery and radar reflectivity. Within this recently collected dataset we will try a very preliminary characterization of the ROBUST probe performance for flight conditions on the Falcon 20.

The TWC values estimated using microphysical characteristics constrained by the in-situ observations (see further explanations later) seem to reach several times 6-7 g/m3 (10 s measurement) particularly during the 2010 campaign over West Africa, and 10.1 g/m3 (1 s measurement) for A340 data, respectively. Peak values in TWC are capable to exceed the proposed TWC envelope, while 17.4 Nm values do not, at least for all gathered 340 and Megha-Tropiques data.

Analysis made by the EHWG of the international database of engine in-service events led to the recommendations at the basis of proposed envelope. With respect to engines, no engine in-service event had been reported outside of the proposed envelope (altitude – SAT envelope). Due to lack of information available on the concentration of water during the in-service events, no evaluation of proposed envelope for TWC values can be made. With respect to air data probes, Airbus recommends the extension of the altitude-temperature envelope as proposed in chapter III. In addition, we propose peak values of measured TWC instead of 17.4Nm scaled values for TWC. In order to perform a most reliable statistical approach for the analysis of proposed envelopes in terms of mass concentrations, additional results and measurements of the atmosphere are needed. The HAIC international field campaign should fill this gap and provide the necessary data for rulemaking activities and evaluation of proposed envelopes.

The work performed in order to define the most adequate instrumental payload for the F-20 focused on the in-situ and active remote sensing characterization of high IWC regions. The strategy in the HAIC project is to validate the Doppler cloud radar IWC estimates of HighIWC regions (reflectivity and Doppler velocity) using the detailed state-of-the-art in-situ microphysical measurements on the flight trajectory. The validated radar estimates then will be used to retrieve good estimates of the vertical distribution of IWC.

Overall, very good progress has been achieved in the definition, selection, preparation and certification of the F20 instrumental payload for the 2014 Darwin F/T campaign.
Related to the very recent NASA/FAA decision (November 2012) that the G-II aircraft will not be operational for the planned F-20 campaign in early 2014 flying out of Darwin, a contingency plan is proposed here. To proceed, we now need urgent confirmation that and to what extent FAA/NASA are willing to fund contingency costs for use of Falcon 20 aircraft for 2014 field campaign. Contingency costs concern in particular a re-design of the mini-IKP to be mounted on the Falcon 20. In addition, we have to review HIWC versus HAIC flight mission requirements to evaluate, if we can obtain an acceptable level of HIWC project objectives, when carrying out intensive flight missions during Darwin 2014, thereby only using the remaining Falcon 20 research aircraft.

In case that the mini-IKP can be installed on the Falcon 20 for Darwin 2014, the instrumentation is very competitive with formerly planned G-II instrumentation regarding coverage of particles sizes and distributions. For sure we don't have redundant probes operated simultaneously on the F-20, since only 4 probes can be mounted on F-20 under wing stations, as compared to the 12 instrument stations originally planned on the G-II.

EUROPEAN AVIATION SAFETY AGENCY
AGENCE EUROPÉENNE DE LA SÉCURITÉ AÉRIENNE
EUROPÄISCHE AGENTUR FÜR FLUGSICHERHEIT

Postal address
Postfach 101253
50452 Cologne
Germany

Visiting address
Ottoplatz 1
50679 Cologne
Germany

Tel +49_221_89990-000
Fax +49_221_89990-999
Mail info@easa.europa.eu
Web easa.europa.eu